Response of the Indonesian Seas and its Potential Feedback to the Madden Julian Oscillation

Asmi Marintan Napitu

Submitted in partial fulfillment of the
requirements for the degree of
Doctor of Philosophy
in the Graduate School of Arts and Sciences

COLUMBIA UNIVERSITY

2017

ABSTRACT

Response of the Indonesian Seas and its Potential Feedback to the Madden Julian Oscillation

Asmi Marintan Napitu

The impact of the Madden Julian Oscillation (MJO), a major source of intraseasonal variability in the tropical atmosphere, on the Indonesia Seas is investigated using satellite-derived, reanalysis and mooring data. The MJO footprint on the Indonesian Seas is evident from the surface layer into the pycnocline. In the surface, MJO air-sea heat fluxes govern the intraseasonal sea surface temperature (SST) variations. Within the pycnocline, the MJO reduces the transfer of the Pacific water to the Indian Ocean, the Indonesian Throughflow (ITF). In addition to the ocean's response, the oceanic feedback to the MJO is also examined. Warmer SST in the Indonesian Seas during the suppressed phase of the MJO promotes the MJO convective phase to propagate eastward over the maritime continent (MC).

Intraseasonal SST variation accounts for 55 - 60% of the total non-seasonal SST variance across the Indonesian Seas. It is most energetic in Banda and Timor Seas, with its standard deviation varying between 0.4 – 0.5°C. Coupled to the MJO surface fluxes, the intraseasonal SST exhibits stronger variation in boreal winter than in summer. A slab ocean model indicates that MJO surface heat fluxes account for 69-78% of the intraseasonal SST variability. The SST increases by 1.1° - 2°C, on average, in response to

intense surface heating and weak winds over the suppressed (dry) MJO phase, and then decreases by 1.8° - 2.1°C over the course of the ensuing MJO active phase that is characterized by enhanced convective cooling and westerly wind bursts. Intraseasonal variability is also significant in the Sulawesi Sea SST, but it is mostly derived from eddies and local winds.

Over the period 1980 - 2012, we observe 86 significant MJO (Real-time Multi variate MJO index > 1) events occurring in the Indian Ocean, of which 51 events achieve eastward propagation (EP) over the MC, while 35 events attentuate in the eastern Indian Ocean, or show no propagation (NP) over the MC. Eastward propagation (EP) MJO events occur more frequently during La Niña years than during El Niño years. Analyses of SST across the Indonesian Seas during the suppressed phase of the MJO events indicate that the SST in Java, Banda, and Timor Seas attributed to the EP MJO events is warmer by 0.5^{o}C that associated with the NP MJO events. The warmer SST corresponds with enhanced surface latent heat flux, sensible heat flux, and low-level moisture in the atmospheric boundary layer, driven by diurnal activity. The EP MJO events are more frequent during La Niña, as the SST response to MJO events is influenced by the thermocline depth: shallower thermocline during El Niño enables cooler subsurface water under the MJO forcing to reduce SST that then attenuates MJO activity, with deeper thermocline of La Niña having the opposite outcome.

Moored velocity data in Makassar Strait between 2004 – August 2011 and August 2013 – August 2015 document substantial direct impacts of the MJO on the ITF, particularly with the surface layer (< 80 m). A composite of the along-strait velocity within the surface layer for 10 MJO events observed during the observational period

exhibits strong northward velocity within days, following the peak of MJO wind stress. The MJO forces both northward along-strait pressure gradient and the resultant of northward wind stress and turbulent stress at the base of the surface layer that, together with the seasonal forcing, maintain the reduction or even reversal of the ITF southward transport on timescales of 1-3 months during boreal winter.

Table of Contents

List of Figures

List of Tables

Acknowledgments

I would like to express my gratitude to my advisor, Arnold L. Gordon, for his advice, patient and tremendous support all the time. My gratitude also extends to my committee members, Xiaojun Yuan and Christopher Zappa for their assistances and suggestions.

I would also like to extend my thanks to all grants that support my study: NOAA-OCO, GSAS-Columbia University and Schlumberger foundation Faculty For the Future. My Indonesian mentors: Aryo Hanggono, Berny Subki and Ngurah Wiadyana from Kementerian Kelautan dan Perikanan, who keep reminding me that my study would be useful for my society.

Special thanks to all my DEES and OCP friends: Sophia Brumer and Ramon Perez, Winnie Chu, Angel Munoz, Julius Busecke, Catherine Pomposi, Sage lee and Claudia Giulivi. My field trip mentors: Bruce Huber and Phil Mele.

My graduate study life is easier with a lot of helps from DEES and OCP admins: Carol Mountain, Sally Odland, Mia Leo, Missy Pinckert, Laura Litchblau, and Jean Economos.

Most of all, I would like to thanks to my family: 1) Siantar family that inspires me to begin and finish my PhD journey. My big and little brothers, Janhotman and Berlin to set the bar to begin with, sisters Ernita and Raskita, in laws Polin and Santi for their patience and supports, Inangtua, Mamak Haloho and Bapak Napitu for all prayers, supports and reasons to start this journey. 2) My Bandung family: Hj. Elis Pudjaastuti who keeps me in her prayer, my in-laws and Mamam. Last but not least to 3) My little family: Albany to maintain my stress level normal and my lovely husband, Kandaga

Pujiana, who is always there during my ups and downs and has to experience a double PhD life. I believe without his compass, I would never see the finish line.

in dedication to my late father Bapak Kostan Napitu and Mamak Minaria Haloho

Chapter 1

Introduction

1.1. Madden-Julian Oscillation

The MJO is the most pronounced tropical convective system recurring on timescales of 1-3 months, mostly originates in the Indian Ocean and traverses eastward over the Maritime Continent and the rest of the tropics at a speed between 3-9 ms^{-1}. (Zhang, 2013; Yoneyama et al., 2013; DeMott et al., 2015). It is characterized by alternating zonal wind anomalies within the troposphere, where deep (suppressed) convection corresponds with surface convergence (divergence) and upper troposphere divergence (convergence) (Fig.1.1; Moum et al., 2014; De Szoeke et al., 2015). The reduced rainfall phase (MJO suppressed phase) precedes the convective phase (MJO active phase) (Gottschalck et al., 2013).

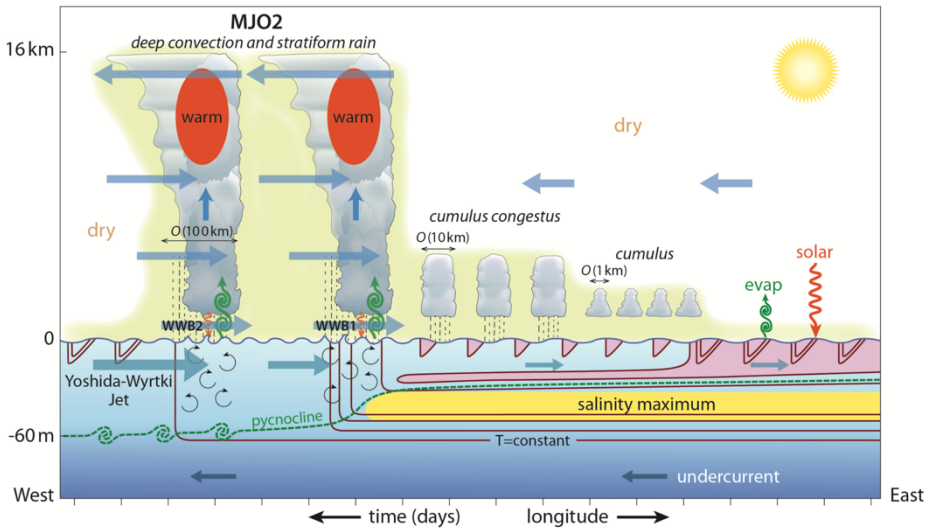

Figure 1.1. Schematic illustrating atmospheric and oceanic processes marking the transition from the MJO suppressed phase to the MJO convective or active phase inferred from comprehensive measurements at 0 80°E in the Indian Ocean in November 2011 (From Moum et al., 2014). Dry or shallow convection conditions characterizes the troposphere during the suppressed phase, while deep convection prevails in the troposphere during the active phase.

Along its path, MJO events impact global weather and climate from affecting the Indonesia-Australia monsoon to triggering the El Niño in the Pacific. Wheeler and McBride (2005) suggested that the MJO is an important component defining the Indo-Australian monsoon characteristics extending from the monsoon's sudden onset to its break. In addition to governing the beginning and cessation of the monsoon, the MJO also modulates the level of rainfall during the monsoon. The average rainfall over Indonesia is increased by 60-70% when the MJO wet phase prevails over the region (Hidayat and Kizu, 2009). The effects are not only felt within the tropics but they extend

to mid latitudes. Increased rainfall and number of flood events by 40-50% are reported over the states of Oregon and Washington when low level westerlies attributable to the MJO wet phase occur over Indonesia (Bond and Vecchi, 2003).

Despite its importance, the MJO genesis and evolution are still not fully understood. DeMott et al. (2015) argue that many modeling experiments, involving either Atmospheric-only General Circulation Model [AGCM] or coupled GCM [CGCM], have demonstrated poor prediction skills to improve the representation of the MJO. They attribute two common threads to the low quality of GCM experiments in simulating the MJO: poor simulation of the upper ocean's response to the MJO and large systematic errors in tropical sea surface temperature [SST]. CGCM experiments with better representation of the upper ocean response generally demonstrate improved MJO simulations (e.g. Ham et al., 2014; Seo et al., 2014). This suggests that the MJO is a coupled atmosphere-ocean process, and hence air-sea interactions are considered to play a fundamental role to initiate and regulate the evolution and propagation of a MJO pulse.

MJO air-sea interactions generally consist of three components: (1) MJO forcing to the ocean, (2) ocean's response to MJO forcing, (3) ocean feedbacks to the MJO (DeMott et al., 2015). Of these three components, the last two components have been the least developed. Earlier study generally classifies oceanic responses to the MJO into three categories: (1) heat response, (2) freshwater response, and (3) dynamic response. Since the MJO initiation is thought to be closely linked to the heat content of the upper ocean, the focus of the previous study has been on the upper ocean heat content to the MJO. Surface forcing has been considered as the dominant heat source that dictates surface mixed layer temperature under MJO convective systems (Duvel et al., 2004; Duvel and

Vialard, 2007; Jayakumar et al., 2011; Drushka et al., 2012). For example, Drushka et al. (2012), using Argo profiling float data, suggest that surface heat flux controls mixed layer temperature variations during the MJO period over the Indo-Pacific warm pool.

Recent observations during the Dynamics of the Madden-Julian Oscillation [DYNAMO] experiment in the central equatorial Indian Ocean (Yoneyama et al., 2013; Moum et al., 2013), however, provide new insights into the role of subsurface turbulence in governing the ocean's response to the MJO (Pujiana et al., 2015; Moum et al., 2016; Pujiana et al., 2017). Detailed measurements of surface heat flux, mixed layer temperature, and subsurface turbulent heat flux during the experiment indicate that upward surface heat flux and downward subsurface turbulent heat flux are equally important to account for the surface mixed layer heat loss during the MJO active phase in the equatorial Indian Ocean (Pujiana et al., 2017). Subsurface turbulence transfers less heat from the surface to deeper depth during a weak MJO event, resulting in larger heat content, a favorable precondition for a subsequently stronger MJO event (Moum et al., 2016). The strength of downward turbulent heat flux is sensitive to the barrier layer thickness, that is stronger (weaker) when the barrier layer is thin (thick) (Chi et al., 2014).

Ocean feedback has been the least understood component and the most controversial subject of air-sea interactions of the MJO. The ocean communicates to the atmosphere through surface flux that is partially controlled by SST. Hence ocean feedbacks to the MJO are dependent upon physical processes dictating the upper layer heat content of the ocean. Baranowski et al. (2016) report plausible connection between diurnal SST-controlled precipitation and the evolution of the convectively coupled Kelvin Wave [CCKW]. They argue that a phase locking between diurnal precipitation and a

CCKW pulse is favorable for the convective envelope of the MJO to propagate eastward over the Indian Ocean. Analyzing two successive MJO events, each separated by less than two months, Moum et al. (2016) demonstrate that a weak (strong) event tends to be followed by stronger (weaker) event. They argue that large ocean heat capacity (4 x that of atmospheric heat capacity) introduces a memory effect into the MJO such that a MJO event is dictated in part by the previous MJO event.

1.2. Dynamics of the Indonesian Seas

The Indonesian Seas are governed by complex bathymetry with multiple narrow straits, large and deep basins, and the dynamics of the seas involve physical processes exposed to influences on a broad frequency band from the surrounding major basins, the South China Sea (SCS) and the Pacific and Indian Oceans (Fig. 1.2). The straits funnel water and associated temperature and salinity properties from the Pacific Ocean to the Indian Ocean, constituting the Indonesian throughflow (ITF), the only low-latitude interocean exchange of the global thermohaline circulation (Gordon et al., 2001, 2005; Murtugudde et al., 1998). The primary inflow passage for the ITF is Makassar Strait that routes ~80% of the ITF transport (Fig. 1.2; Gordon et al., 1999, 2008, 2010). The North Pacific subtropical water primarily supplies the ITF within the thermocline, while the South Pacific subtropical water is the primary source of the ITF within the lower thermocline and deeper water (Sprintall, et al., 2014). Strong tidal mixing in the Indonesian Seas transforms the subtropical water mass characteristics of the ITF (Ffield and Gordon, 1992; Koch-Larrouy et al., 2008)

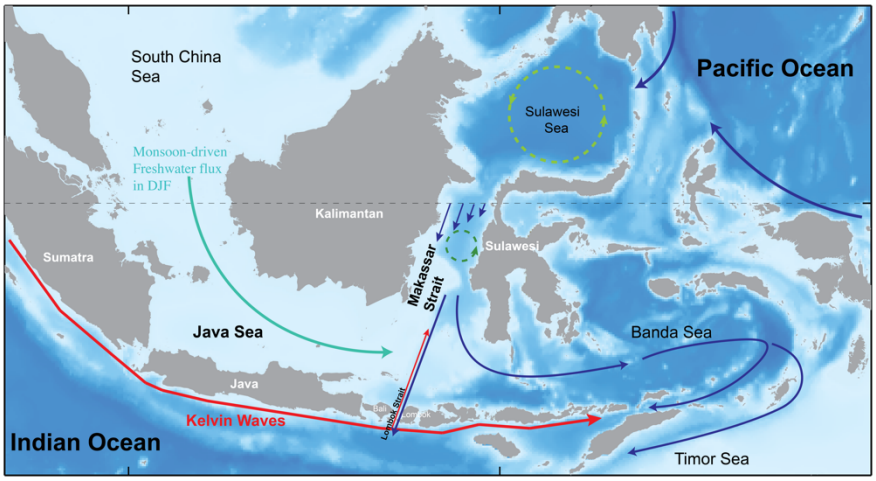

Figure 1.2 Schematic illustrating pathways of the ITF (blue), Kelvin waves (red), monsoon-driven buoyancy flux (teal) through major basins and straits constituting the Indonesian Seas. Dashed green circle in the Sulawesi Sea and Makassar Strait denotes cyclonic eddies. The ITF pathway is adapted from Gordon et al. (2005).

The ITF variation demonstrates a broad-spectrum, encompassing timescales from intraseasonal to interannual (Gordon et al., 2003, 2012; Pujiana et al., 2009; Susanto et al. 2012; Sprintall and Revelard, 2014). On seasonal timescale, The ITF is sensitive to the influence of the Indo-Australia monsoon. Northwesterly monsoon winds are dominant during the boreal winter monsoon months of December-February and drive buoyant SCS surface layer water into the Indonesia Seas, acting as a 'freshwater', buoyant plug of the ITF transport within the upper 100 m of the water column (Gordon et al., 2012). The opposite southeasterly winds prevailing over the course of the boreal summer monsoon (June-August), by contrast, remove the plug. This seasonal variation of the ITF is influenced by long-term, background conditions of regional climate such as El Niño Southern Oscillation (ENSO) (Tillinger and Gordon, 2010). More buoyant SCS water is

flushed into the Indonesian Seas, strengthening the buoyant plug that further weakens the ITF, under an El Niño condition (Gordon et al., 2012).

In addition to seasonal variability, the ITF exhibits significant intraseasonal (<90 days) variability. A planetary waveguide extending along the equatorial Indian Ocean to the southern coasts of the Indonesian archipelago entering Makassar Strait, via Lombok Strait, spreads the equatorial Indian Ocean wind energy on intraseasonal timescales of 2-3 months into the Indonesian Seas (Fig.1.2, Pujiana et al., 2009; Schiller et al., 2010 Drushka et al., 2012; Pujiana et al., 2013). On shorter timescales, shear-instability at the ITF core depth in the pycnocline, perturbed by planetary waves originating from the Western Pacific warm pool, generates the 1-month variability observed in Makassar Strait (Pujiana et al., 2012).

Analyses of the temperature time series inferred from expandable bathythermograph (XBT) sections between Java and Australia indicate that the wave pathway can also facilitate penetration of the equatorial Indian Ocean planetary waves with timescales longer than 1-3 months into the Indonesian Seas (Wijffels and Meyers, 2004). Semiannual coastally trapped Kelvin waves generated via an equatorial Kelvin wave impinging upon the west Sumatra coast propagate along the waveguide and force the northward geostrophic flow in Lombok and Makassar Straits during the transition months from the northwest monsoon to southeast monsoon (Sprintall et al., 2000).

1.3. Madden-Julian Oscillation imprints on the Indonesian Seas

The MJO dynamics over the Maritime Continent (MC) are even less known than over the Indian and Pacific Oceans. A performance review of many GCMs experiments indicated low quality skills of these experiments to simulate MJO properties over the MC such that the continent has been considered as a MJO propagation barrier (Innes and Slingo, 2006; DeMott et al., 2015). Peatman et al. (2014) suggested that the MJO nature of smooth eastward propagation of a large-scale precipitation envelope, as observed in the Indian and Pacific Oceans, no longer holds through the MC. We suspect that poor model simulations of the MJO through the MC, as is the case for the Indian Ocean, also stem from the lack of accurate representation of oceanic processes governing air-sea interactions on intraeasonal timescales in the simulations.

Interactions between physical process in the Indonesian Seas and the MJO aloft are not understood. The objective of my research is to identify primary characteristics of the MJO over the MC, their impacts on the Indonesian Seas dynamics, to explore the role of the underlying ocean processes to influence behaviors of the MJO over the MC, and to describe the surface and subsurface expressions of the MJO within the Indonesian Seas. The MJO expressions in a semi enclosed basin such as the Indonesian Seas may be distinctively different from those learned from the open ocean such the Indian and Pacific Oceans. This makes this study unique. The research results are documented in three main chapters organized as follows:

- Chapter 2 discusses the MJO over the MC and its impact on sea surface temperature across the Indonesian Seas[1]. Primary characteristics of the MJO over the MC are investigated from a suite of satellite-derived data ranging from wind stress to outgoing longwave radiation [OLR]. Reanalysis product of surface heat flux data are also utilized to identify the MJO characteristics. The influences of MJO surface heat flux on SST across the Indonesian Seas are then quantified using coherence analyses and a slab ocean model. The MJO significantly accounts for intraseasonal variability of OLR, wind stress, rainfall, and surface heat fluxes over the MC. Substantially reduced OLR, upward surface heat flux, and westerly wind bursts characterize the MJO active phase, while a net downward heating and weak winds mark the suppressed phase. It demonstrates seasonal variation, more energetic during boreal winter (December-February) and weaker during boreal summer (June-August). Moreover, MJO surface heat flux is significantly coherent with SST on intraseasonal timescales in Banda and Timor Sea, two major basins constituting the Indonesian Seas, and to a lesser degree in Java Sea. Intraseasonal SST variability in Sulawesi Sea is independent from the MJO and derives from locally generated eddies. The slab ocean model confirms the coherence between MJO surface heat flux and intraseasonal SST variability and demonstrates that the heat flux accounts for on average about 70-80% of intraseasonal SST variability, and the amount of intraseasonal SST variances explained by the heat flux is larger during boreal winter months than boreal summer months. Increased influence of ocean processes, due to shallower thermocline, compete against MJO surface heat flux to regulate intraseasonal SST variability in Banda and Timor Seas.

[1] Napitu, A. M., A.L. Gordon, K. Pujiana (2015) Intraseasonal Sea Surface Temperature Variability Across the Indonesian Sea, *Journal of Climate*., Vol. 28, No. 22: 8710-8727.

- Chapter 3 explores the likely oceanic feedback to the eastward propagation of the MJO and discusses the role of oceanic process to control the MJO-SST on ENSO timescale[2]. Over the period of 1980 – 2012, 86 MJO events are generated over the western-central Indian Ocean, of which 51 events traverse over the MC into the western Pacific, while 35 events discontinue over the eastern Indian Ocean. It appears that the MJO events propagating over the MC are preceded by high SST across the Indonesian Seas. The SST during the suppressed phase of the 51 MJO events is warmer by 0.5 °C than that associated with the MJO events that do not propagate over the MC. The warmer SST condition, likely governed by increased diurnal SST activity, enhances latent and sensible heat fluxes and low-level moisture content. This condition over the Indonesian Seas serves as a favorable precondition for the MJO convection to propagate across the MC. During the MJO active phase, the SST-MJO coupling at El Niño Southern Oscillation [ENSO] timescale in the Indonesian Seas is sensitive to the thermocline depth and demonstrates stronger coupling during La Niña than El Niño.
- Chapter 4 attempts to elucidate subsurface expressions of the MJO in the ITF[3]. The emphasis here is to examine the role of MJO to relax the ITF transport in its most important inflow passage, the Makassar Strait, funneling about 80% of the ITF transport. Analyses of current velocities across depths extending from the surface to 750 m during 2004 – August 2011 and August 2013 – August 2015 indicate that the ITF relaxation in Makassar Strait can be classified into three groups of water column: 1) the surface layer

[2] Napitu, A. M., A.L. Gordon, K. Pujiana (2017), "Oceanic Responses and Feedbacks to the Eastward Propagation of the Madden-Julian Oscillation in the Maritime Continent", to be submitted to *Geophysical Research Letters*.

[3] Napitu, A. M., K. Pujiana, A.L. Gordon (2017), "Intraseasonal relaxation of the Indonesian Throughflow", submitted to *Journal of Physical Oceanography*.

[0 - 80 m], 2) the main pycnocline layer [80 - 200 m], and the deep or lower pycnocline layer [>200 m], where each layer exhibits unique properties of the relaxation. Of these three layers, I focus on examining the surface layer. Within the surface layer, the MJO affects to amplify seasonal relaxation of the ITF in Makassar Strait during boreal winter. The MJO induces northward acceleration, against the typical boreal summer southward directed ITF, through northward along-strait pressure gradient and wind stress. Increased shear instability during the MJO forces subsurface turbulence to transfer momentum downward to decelerate the northward MJO-driven ITF. The northward along-strait pressure gradient during the MJO contrasts the southward along-strait pressure gradient observed during boreal winter and summer. The southward along-strait pressure gradient during boreal winter is smaller than during boreal summer, driven primarily from buoyancy input from less saline Java Sea water flux into the southern Makassar Strait.

- In Chapter 5 provides a summary and discussion on possible future research to further advance our understanding on the dynamics of the intraseasonal variability in the MC region.

Chapter 2

Intraseasonal Sea Surface Temperature Variability Across the Indonesian Seas

Published as: Napitu, A. M., Gordon, A. L., and Pujiana, K. 2015. Intraseasonal Sea Surface Temperature Variability Across the Indonesian Seas, Journal Of Climate, 28 (22), 8710–8727.

Abstract Sea surface temperature (SST) variability at intraseasonal timescales across the Indonesian Seas during January 1998-mid 2012 is examined. The intraseasonal variability is most energetic in the Banda and Timor Seas with a standard deviation of 0.4-0.5^{o}C, representing 55-60% of total non-seasonal SST variance. A slab ocean model demonstrates that intraseasonal air-sea heat flux variability, largely attributed to the Madden-Julian Oscillations [MJOs], accounts for 69-78% intraseasonal SST variability in the Banda and Timor Seas. While the slab ocean model accurately reproduces the observed intraseasonal SST variations during the northern winter months, it underestimates the summer variability. We posit that this is a consequence of more vigorous cooling effect induced by ocean processes during the summer. Two strong MJO cycles occurred in late 2007-early 2008, and their imprints were clearly evident in the SST of the Banda and Timor Seas. The passive phase of the MJOs (enhanced outgoing longwave radiation [OLR] and weak zonal wind stress) projects on SST as a warming period, while the active phase (suppressed OLR and westerly wind bursts) projects on SST as a cooling phase. SST also displays significant intraseasonal variations in the

Sulawesi Sea but these differ in characteristics from those of the Banda and Timor Seas, and are attributed to ocean eddies and atmospheric processes independent from the MJO.

2.1 Introduction

Various processes, both local and remote, govern sea surface temperature (SST) variability across the Indonesian Seas, often referred to as the maritime continent. Local processes include intense tidal mixing, Ekman dynamics and air-sea heat fluxes (Gordon 2005; Sprintall et al. 2014). The Indonesian Seas SST is also sensitive to the large-scale climate of the Indo-Pacific region, such as El Niño-Southern Oscillation (ENSO), the Indian Ocean Dipole (IOD) (McBride et al. 2003) as well as the seasonal forcing of the Asian-Australian monsoon, which is the largest contributor to SST variability within the Indonesian Seas (Qu et al. 2005; Kida and Richards 2009; Halkides et al. 2011). Furthermore the maritime continent falls along the pathway of the Madden-Julian Oscillation (MJO), an intraseasonal tropical atmospheric phenomenon consisting of convective and subsidence cells propagating eastward from the Indian Ocean to the Pacific Ocean affecting weather across the tropics and mid-latitude. (Waliser et al. 1999; Madden and Julian 1994; Zhang 2005).

The Indonesian Seas are characterized by warmer SST over their southern hemisphere region during the boreal winter months of December-January-February (DJF). The months of DJF are also marked with increased precipitation over the Indonesian maritime continent (Tanaka 1994). Colder SST characterizes the Indonesian Seas during the boreal summer months, June-July-August (JJA) during which time the climate is somewhat drier, particularly its southern hemisphere region, as the Intertropical Convergence Zone shifts to the north of the equator (Meehl 1987).

By applying an Empirical Orthogonal Function (EOF) to a~15-year SST data set (see section 2), extending from January 1998 to mid 2012, we find that seasonal variability

explains about 52% of SST variability over the Indonesian Seas. At shorter timescales, variability at semi-annual timescales accounts for about 18% of SST in the Indonesian seas. This semi annual component occurs during the monsoon transition period, during which solar insolation is increased and wind is weaker, that results in warmer SST (Halkides et al. 2011).

The combined seasonal and semi-annual variability can explain about 70% of total SST variances in the Indonesian Seas. The remaining 30% of the SST variability is attributed to intraseasonal and interannual variations. As for intraseasonal SST variability, previous studies suggested that SST perturbation with periods less than 120 days over the Indo-Pacific region is dictated by the MJO (Duvel and Vialard (2007); Drushka et al. (2012)). Drushka et al. (2012) argued that surface heat flux attributed to the MJO dominates mixed layer heat budget variability in the region. The MJO activity over the western Pacific warm pool is suggested to be linked and interact with ENSO. Waliser et al. (1999) and Kessler (2001) showed that MJO signature increases over the warm pool during the development of the ENSO warm phase, and the increased MJO activity shifts further east as El Niño is fully developed.

The MJO-ocean interaction is likely not confined to atmospheric impact on a passive ocean as MJO induced intraseasonal SST variability potentially feedbacks to the atmosphere through modifying the surface flux, which in turns affects the MJO evolution if the subsurface cooler waters enter into the surface layer (Shinoda et al. 1998a). The most active period for MJO activity, indicated by strong signature of eastward propagation from the Indian Ocean to the Pacific Ocean, takes place between late fall-early spring during which the warm pool has its greatest east-west extent (Salby and

Hendon 1994).

Given the MJO influence on ENSO and the potential feedback that intraseasonal SST may provide to the atmosphere over the maritime continent, with potential impact on MJO behavior enroute from the tropical Indian Ocean to the West Pacific Ocean warm pool, we examine intraseasonal SST variability of the Indonesian Seas, specifically the SST response to strong MJO events, which we argue is one of the primary drivers for SST variability at intraseasonal timescales in large expanses of the Indonesian Seas. Other factor that might influence intraseasonal SST variability include eddies and planetary waves (Qiu et al. 1999; Wijffels and Meyers 2004). Drushka et al. (2010) suggested that the intraseasonal Kelvin waves originating in the equatorial Indian Ocean propagate along the southern coasts of the Indonesian archipelago. These waves manage to squeeze through several narrow straits into the internal Indonesian Seas and affect the thermocline and SST variability along their paths (Pujiana et al. 2013). Intraseasonal eddies are also abundant in the Indonesian Seas and might perturb SST (Qiu et al. 1999).

This study which focuses on the Indonesian region of themaritime continent complement similar studies investigating intraseasonal SST variability in the neighboring and broader Indo-Pacific region (Duvel et al. 2004; Vialard et al. 2013). We begin with describing the data and method in section 2. Section 3 presents general characteristics and generation mechanisms of intraseasonal SST in the Indonesian Seas. This section is aimed to elucidating key intraseasonal SST features and their genesis, which include the role of MJO surface heat flux in governing intraseasonal SST variability in the Indonesian Seas. The intraseasonal SST responses to strong MJO events across the Indonesian Seas are presented in section 4. We conclude the paper with summary and

discussion in section 5.

2.2. Data and methods

2.2.1 Dataset

The main data used in this study are the SST data from the Tropical Rainfall Measuring Mission (TRMM) Microwave Imager (TMI) satellite acquired during January 1998-June 2012. The gridded satellite-derived SST data have a spatial resolution of 0.25^{o} x 0.25^{o} and a sampling interval (Δt) of 7 days, and the region of interest is within longitudes of 90^{o}-140^{o} E and latitudes of 10^{o}N-15^{o} S. Previous studies, e.g. Kida and Richards (2009), found that the TMI data are better than radiometric satellite data because the TMI data contain fewer gaps due to the ability of the TMI satellite to penetrate cloud cover (Wentz et al. 2000). In addition to SST, we also analyze the precipitation data from the TMI product.

The outgoing long wave radiation (OLR) is examined to relate intraseasonal variability within the atmosphere to SST variability as the OLR is commonly used as a good indicator to study convective activity. The OLR data have a spatial resolution of 2.5^{o} x 2.5^{o} and are sampled daily (Liebmann 1996). The data used for this study extend from January 1998 to June 2012. Wind data, from the level 3.5A gridded cross-calibrated multiple platform (CCMP) product, 1998 to 2011, have a spatial resolution of 0.25^{o} x 0.25^{o} (Ardizzone et al. 2009). The OLR, precipitation, and wind data encompass the same region as that of the SST data.

For surface heat flux analyses, we utilize reanalysis TropFlux products (Praveen Kumar et al. 2012) consisting of shortwave, latent, longwave, sensible heat fluxes from

1978 to mid 2012 with daily time resolution and a spatial resolution of 1^o x 1^o, showing a good agreement with the surface heat flux data observed from equatorial moorings in the Indian and Pacific Ocean. We find that he TropFlux reanalysis data are useful for our analysis as they consistently exhibit intraseasonal features over the Indonesian maritime continent which reasonably agree with that from satellite derived data.

The mixed layer depth information is important to estimate the influence of surface heat flux on SST. In our study, we use the mixed layer depth data from a climatological dataset with a spatial resolution of 2^o x 2^o from de Boyer Montegut et al. (2004).

In addition to the above main datasets, we analyze the gridded sea level anomaly (SLA) product from Archiving, Validation, and Interpretation of Satellite Oceanographic Data (AVISO) (Ducet et al. 2000). The satellite-derived SLA has a horizontal resolution of 0.25^o x 0.25^o and temporal resolution of 7 days.

2.2.2 Methods

To extract the main characteristics of intraseasonal variability from the data, we employ statistical methods and a slab ocean model. The details of the statistical methods and the model are explained below.

2.2.2.1 Statistical method

- The monthly climatological mean is removed.
- The intraseasonal variability is obtained through applying a band passed filter with cut-off periods of 21 days and 119 days, resulting in the filtered data with oscillations varying between 21-119 days.

- Dominant periods characterizing intraseasonal variability of the data are identified by applying spectral analyses. The confidence interval for the spectrum estimate, *P(f)* is defined as $[(v-1)s^2(f)/\mathcal{X}^2_{1-\alpha/2,v}]$ <P(f)< $[(v-1)s^2(f)/\mathcal{X}^2_{\alpha/2,v}]$,

where *v* denotes the degrees of freedom, $S^2(f)$ is the observed standard deviation, $\mathcal{X}^2$is the cumulative Chi-square distribution value, and α is the level of significance.

- The degree of correlation in frequency domain between two time series is examined using a coherence or cross wavelet transform method. The confidence level for the squared coherence $\lambda^2_{(1-\alpha)}$ is given as $\lambda^2_{(1-\alpha)} = 1-\alpha^{[2/(v-2)]}$. The significance level of the cross wavelet transform is approximated using a Monte-Carlo method (Grinsted et al. 2004).
- The time variability of the dominant oscillations is investigated using a wavelet method. The confidence level of the wavelet transform Wn(s) is defined as $\mathrm{W_n(s)}\chi^2_2$, where χ^2_2 is the cumulative chi-square distribution value with 2ν (Torrence and Compo 1998).

2.2.2.2 Slab ocean model

The rate of SST change is governed by heat fluxes due to air-sea interaction, ocean advection and turbulence, which can be expressed as the following simplified surface mixed layer heat budget equation (Wang and McPhaden 1999):

$$\rho c_p h \frac{\partial T}{\partial t} = Q_o - \rho c_p h u.\nabla T - \frac{K_T}{h}\frac{\partial T}{\partial Z} + R \qquad 2.1$$

where *T* is the average surface mixed layer temperature, Q_o the net surface heat flux, ρ

the sea water density, c_p the heat capacity, h the surface mixed layer depth, u the velocity, and K_T thermal diffusivity. The terms in the right hand side of (1) represent, from left to right, the net surface heat flux, the ocean advective heat flux, the turbulent heat flux across the base of the surface mixed layer, and the residual flux which accounts for horizontal divergence of eddy heat flux within the mixed layer and errors attributed to other terms in (1). The net heat flux is the sum of shortwave radiation minus the penetrative component at the base of the surface mixed layer, latent heat flux, sensible heat flux, and longwave radiation as follows:

$$Q_o = Q_{SW}(1 - 0.45e^{-0.04h}) + Q_L + Q_S + Q_{LW} \quad 2.2$$

We can then classify the primary drivers for SST change into atmospheric and oceanic components. Since observations of heat fluxes due to ocean processes within the Indonesian Seas are not available and previous relevant studies demonstrated that surface heat fluxes contribute substantially to force surface mixed layer heat budget in the Indo-Pacific region (e.g. Vialard et al. (2013)), we here consider only the atmospheric component to investigate the generation mechanisms of SST variability across the Indonesian Seas. Thus (1) can be further simplified into

$$\rho c_p h \frac{\partial T}{\partial t} = Q_o + R \quad 2.3$$

where R now includes the advective and turbulent heat fluxes. Temporal integration of (3) results in estimated SST forced by surface heat flux. We use (3), named as a slab

ocean model, to quantify the contribution of surface heat flux to control intraseasonal SST in the Indonesian Seas. We use Q_o and the monthly climatology of h from the Tropflux product (Praveen Kumar et al. 2012) and de BoyerMontegut et al. (2004) respectively. Since the surface mixed layer depth data are monthly climatologies, the slab model derived SST does not take into account the mixed layer sub monthly variability for our calculation. This model has been used by other similar studies in other regions (Vialard et al. 2013).

2.3. Intraseasonal SST variability across the Indonesian Seas

2.3.1 General characteristics

The contribution of intraseasonal variability to total SST variances is estimated from the ratio between the sum of the SST variance at intraseasonal timescales (21-119 days) to total SST variances at periods longer than 14 days, whose formula is given as

$$\text{ratio} = \frac{\int_{\omega=1/21\ day^{-1}}^{\omega=1/119\ day^{-1}} P_{SST}(\omega)d\omega}{\int_{\omega=1/14\ day^{-1}}^{\omega=1/7n\ day^{-1}} P_{SST}(\omega)d\omega} \qquad 2.4$$

where n is the number of SST data at each gridpoint, ω is frequency, and P_{SST} is amplitude of SST spectral estimate. The ratio (Fig.2.2.1a) reveals that the largest contribution of intraseasonal SST variance to total SST variance across the deep basins of the Indonesian Seas occurs within the Banda Sea, Timor Sea, and Sulawesi Sea, with a ratio between 55-60%. Other basins such as Java Sea have intraseasonal variability that

explains 25-40% of the SST variation. The average of intraseasonal SST standard deviation across the study area is generally between 0.3 and 0.5^{o}C (Fig.2.1b). The mean standard deviations in the Banda and Timor Seas vary between 0.45 and 0.5^{o}C, while the Sulawesi has a standard deviation of 0.3^{o}C.

As mentioned above, seasonal variability accounts for 70% of SST variability. Therefore, the ratio suggests that 55-60% of the remaining 30% can be explained by intraseasonal variability, (i.e. this intraseasonal variability accounts for 16-18% of the total SST variability). We henceforth will not discuss the characteristics of intraseasonal variability over area with a ratio of less than 40%.

The dominant oscillations characterizing the significant intraseasonal SST across the Indonesian Seas are observed at periods of 30-70 days (Fig.2.2). For the Banda and Timor Seas the intraseasonal SST signal is marked with a spectral peak of 28-42 days centered at 35-days, whose magnitude is statistically different from a background red spectrum with a confidence level of 80% (Figs.2.2a,b). The Sulawesi Sea intraseasonal SST is however characterized by a significant spectral peak centered at 56 days (Fig.2.2c). In addition to the dominant 56-day period, intraseasonal SST in the Sulawesi Sea also shows another significant period of oscillation at 25-day although with smaller spectral energy (Fig.2.2c). These dominant oscillations explain more than half of the total variances attributed to intraseasonal SST in the Sulawesi Sea.

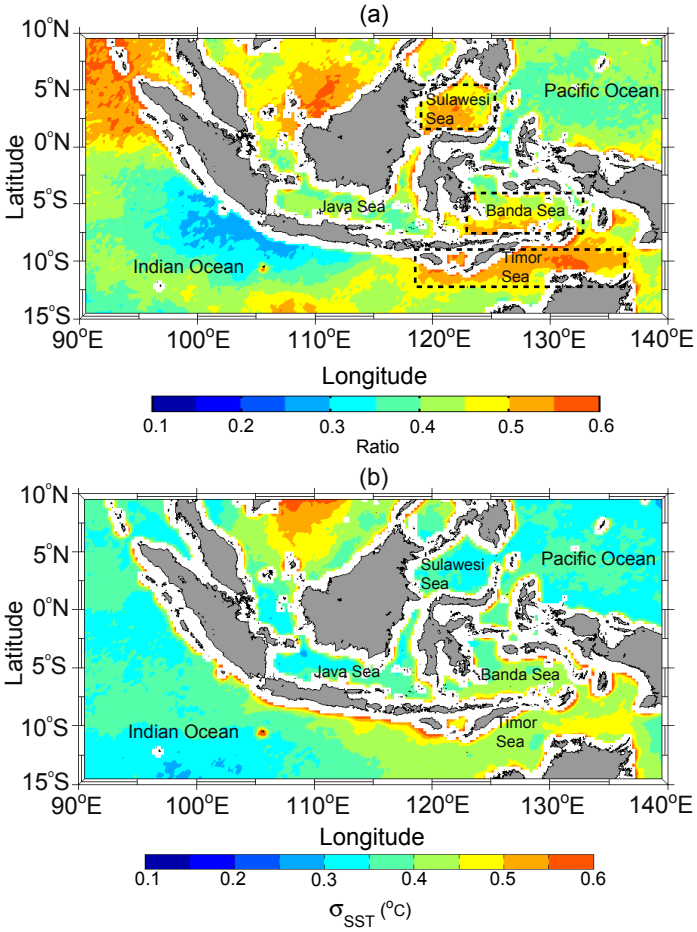

Figure 2.1. (a) The significance of intraseasonal SST variability across the Indonesian Seas. The significance is inferred from the ratio between the sum of SST variances on intraseasonal timescales (21 days<period<119 days) and the sum of SST variances with periods longer than 14 days. Dashed boxes illustrate regions with significant intraseasonal SST variability. (b) Standard deviation of intraseasonal SST across the Indonesian Seas.

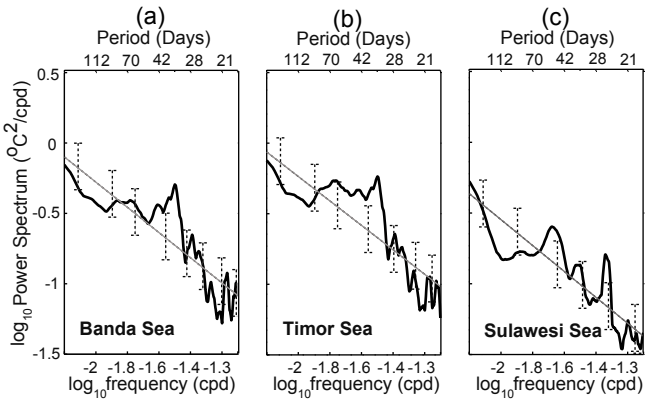

Figure 2.2. Power spectrum estimates of SST (black line) in (a) Banda Sea, (b) Timor Sea, and in (c) Sulawesi Sea. Each spectrum estimate is an average over a region bounded by the dashed box shown in Figure 1a. Gray line and error bars denote the red noise and 80% significance level respectively

The variance of intraseasonal SST displays its strongest magnitude during DJF period and is diminished during JJA (Fig.2.3). Figure 2.3 shows that standard deviation of intraseasonal SST in the Banda and Timor Seas reaches up to 0.6-0.7^{o}C during DJF winter, whereas the standard deviation reduces to 0.2-0.3^{o}C during JJA. This agrees with that reported by Duvel and Vialard (2007), who found that intraseasonal SST across the maritime continent shows seasonal variability although their standard deviation is 0.1^{o}C smaller than our finding. The difference likely arises from the shorter extent of the time series they analyzed. To examine the time variability of the dominant intraseasonal SST oscillations in the Banda, Timor and Sulawesi Seas, we apply a wavelet analysis of SST time series at each sea. The SST time series at each sea is obtained by spatially averaging SST time series for all grids within the boxes defined in Figure 2.1a.

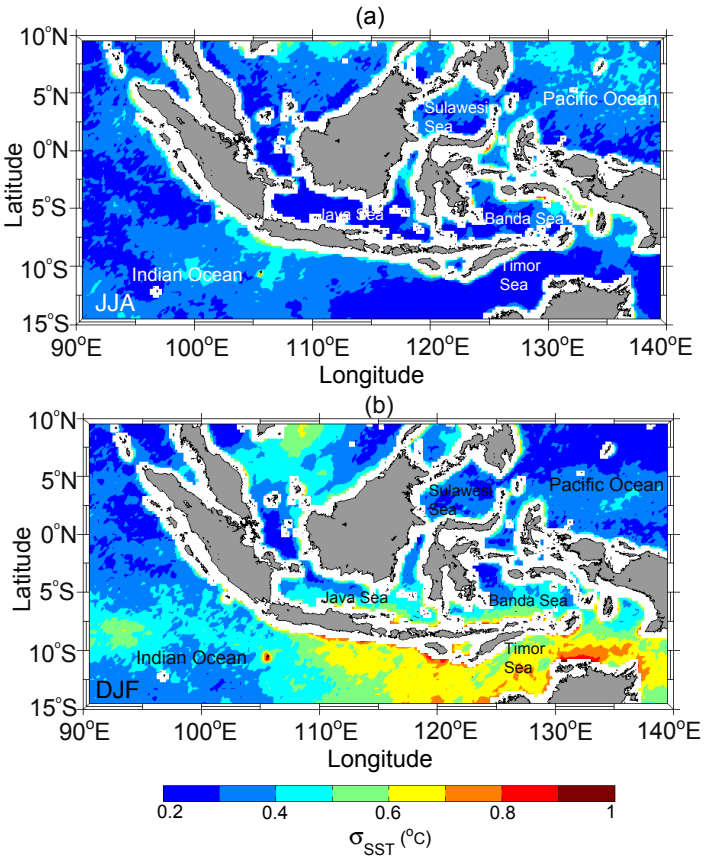

Figure 2.3. Standard deviation of intraseasonal SST across the Indonesian Seas averaged over (a) June-July-August [JJA] and (b) December-January-February [DJF].

A wavelet analysis of SST in the Banda and Timor Seas confirms that the magnitude of intraseasonal SST variance shows seasonal modulation, amplified during boreal winter and weak during boreal summer (Fig.2.4). The analysis also suggests that the signature of amplified intraseasonal SST during boreal winter varies year by year. Unlike in the Banda and Timor Seas, the Sulawesi Sea intraseasonal SST does not reveal seasonal nor interannual variability and is likely governed by processes that differ from that of the Banda and Timor Seas.

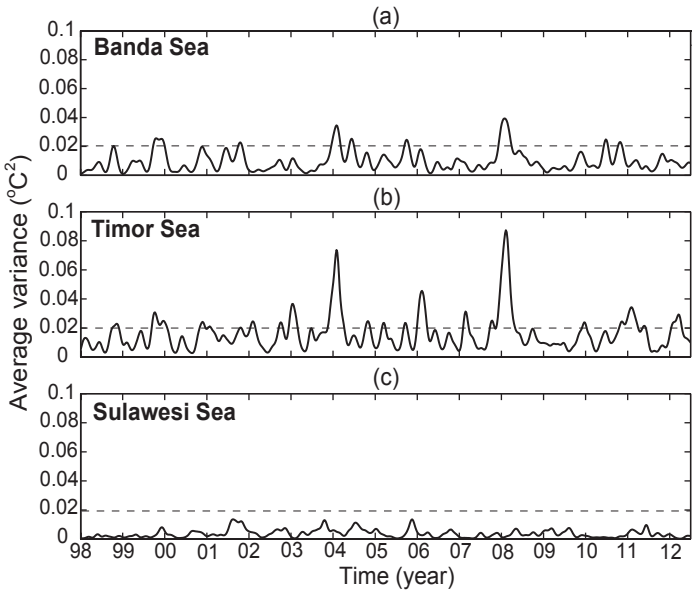

Figure 2.4. Time series of SST variances varying at periods of 28-56 days in (a) Banda Sea, (b) Timor Sea, and in (c) Sulawesi Sea. Each time series is obtained from a wavelet analysis to spatially averaged SST data within the dashed box shown in Figure 2.1a. Dashed horizontal line denotes the 95% significance level.

2.3.2 Generation Mechanism

2.3.2.1 Banda and Timor Seas

We have demonstrated that SST in the Banda and Timor Seas at intraseasonal timescales shows similar characteristics in their spectral peaks and seasonal patterns (Figs.2.2,3). A coherence analysis between the basin averaged SST timeseries in the Banda Sea and that in Timor Sea shows that their intraseasonal variations are strongly coherent with $r^2 = 0.85$. Moreover the coherent intraseasonal SSTs in the Banda and Timor Seas are also in phase, indicative of shared forcing mechanism for the intraseasonal SST variability. Duvel and Vialard (2007) suggested that the mechanism that controls intraseasonal variation over the Indo-Pacific region is related to eastward

propagating tropical convection originating from the Indian Ocean. We suspect that surface heat flux variation attributed to the MJO explains a substantial amount of intraseasonal SST variances in the Banda and Timor Seas.

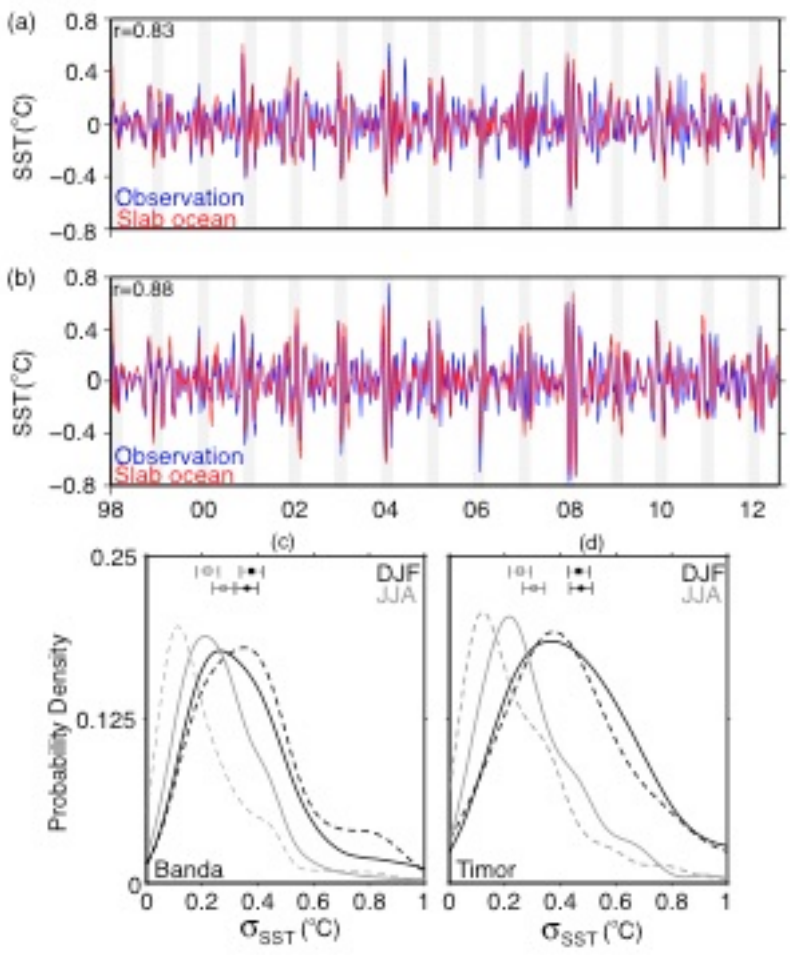

Figure 2.5. Time series of the observed (blue) and slab ocean model (red) intraseasonal SST in (a) Banda Sea and (b) Timor Sea. Gray bars mark the DJF period. Probability density functions of the observed (solid curves) and model (dashed curves) standard deviation of intraseasonal SST in Banda Sea (c) and Timor Sea (d). Black (gray) curve indicates the distribution for the DJF (JJA) period. Colored circle (rectangular) denotes the mean of the observed (model) standard deviation of intraseasonal SST.

A simple slab model, expressed as (3), quantitatively shows that intraseasonal SST variations in the Banda and Timor Seas are largely forced by surface heat flux. The model SST explains about 69% (r = 0.83) of the observed SST variability at intraseasonal timescales in the Banda Sea, while the model can predict almost 78% (r = 0.88) of the observed intraseasonal SST variation in the Timor Sea (Figs.2.5a,b). The model results suggest that surface heat flux may account for about three quarter of the total surface mixed layer heat budget variability at intraseasonal time scales in the Banda and Timor Seas.

Probability distributions of the model SST standard deviation during DJF closely resemble that of the observations, whereas the distributions for the JJA period indicate that the model underestimate the intraseasonal SST amplitude (Figs.2.5c,d). Figures 2.5c,d also show that distributions of the model intraseasonal SST in the Banda and Timor Seas reveal larger amplitude during DJF than JJA, consistent with observations. Shallower mixed layer depth during DJF likely explains the increased amplitude of intraseasonal SST during that period in the Banda and Timor Seas. Figure 2.6 demonstrates that intraseasonal SST variations do not solely follow that of surface heat flux but are also controlled by mixed layer depth. For example, the model intraseasonal SST variability exhibits continuously decreasing trend from January to June although the amplitude of intraseasonal surface net heat flux increases from April to June (Figs.2.6a,b). The sustained attenuation of intraseasonal SST variability from April to June is partly controlled by the mixed layer depth, which gets deeper over the same period (Fig.2.6c). Deeper thermocline, which potentially dampens the role of ocean process in modulating the mixed layer heat content, might also contribute to stronger

surface flux impact on SST during DJF in the Banda and Timor Seas. Gordon and Susanto (2001) suggested that less energetics upwelling explains deeper thermocline during DJF in the Banda Sea.

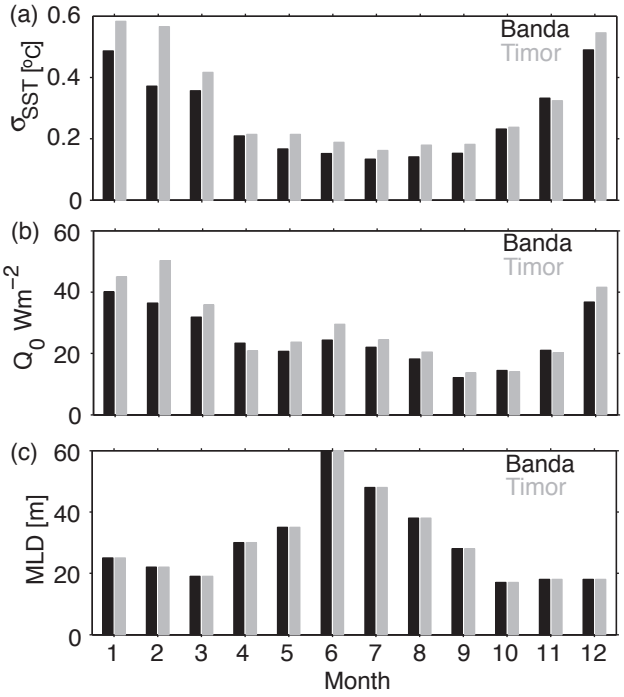

Figure 2.6. Seasonal variation of (a) the slab ocean model intraseasonal SST standard deviation, (b) the shortwave radiation flux standard deviation, and (c) the mixed layer depth in Banda (black) and Timor (gray) Seas.

Our slab ocean model results for the Timor Sea are similar to those of Vialard et al. (2013), who investigated intraseasonal SST variability in the North Western Australian basin (NWAB), which is to the Southwest of our Timor Sea domain. Nevertheless their slab ocean model overestimates the intraseasonal SST amplitude during JJA, while our model underestimates the observation during JJA in the Timor Sea

(Figs.2.5d).

We have shown that surface heat flux is the primary driver of intraseasonal SST variability in the Banda and Timor Seas. Some studies suggested that the intraseasonal surface flux variability over the Indo-Pacific region is associated with the MJO (Duvel and Vialard 2007; Drushka et al. 2012). To further illustrate the relationship between intraseasonal SST features and the MJO over the Banda and Timor Seas, we investigate both precipitation and OLR variability which may reflect atmospheric tropical convection variability associated with the MJO.

The significance of intraseasonal precipitation and OLR is obtained through computing a ratio of intraseasonal signal to other signals using (1), and the ratio demonstrates that intraseasonal precipitation and OLR variability is significant over the Banda and Timor Seas. Intraseasonal variability explains about 20-40% and 40-50% of OLR and precipitation total variances, respectively (not shown). The average standard deviation of intraseasonal OLR and precipitation over the Banda and Timor Seas varies between 16-20 W/m^{-2} and 0.15 and 0.22 mm h^{-1} respectively (not shown).

Oscillations at periods of 35-42 characterize OLR in the Banda and Timor Seas and precipitation over the Timor Sea (Figs.2.7a,b,d). Meanwhile a broader spectral peak with periods of 35-49 days characterizes the precipitation over the Banda Sea (Fig.2.7c). Moreover intraseasonal OLR variability over the the Banda and Timor Seas demonstrates seasonality that is larger OLR variance (18-25 W/m^{-2}) during DJF than that during JJA (6-10 W/m^{-2}) (Fig.2.8a). Similar to OLR, the average precipitation during DJF, varying between 0.28 and 0.31 mm h^{-1}, is larger than that during JJA, varying between 0.2-0.28 mm/h^{-1} (Fig.2.8b). This is consistent with the result of Zhang and Dong (2004) for

broader Indo-Pacific region, suggesting that MJO activity is stronger during DJF than JJA.

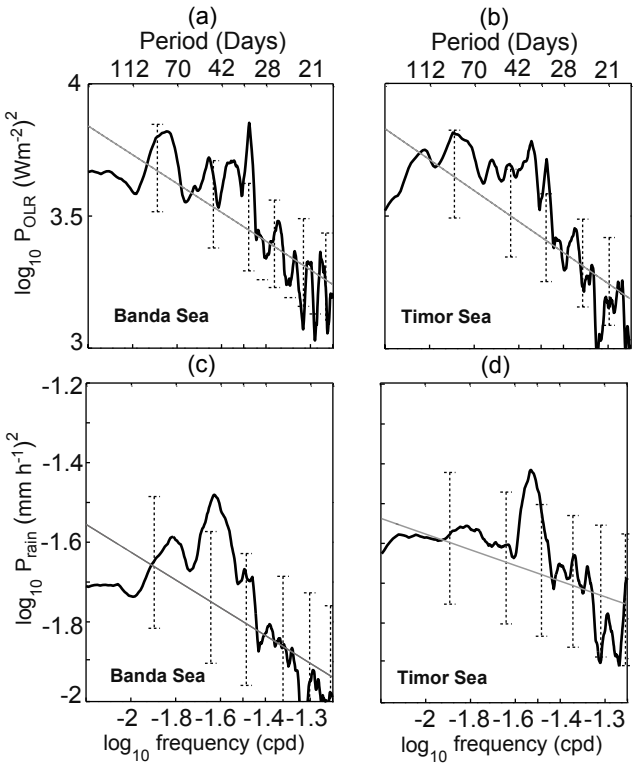

Figure 2.7. Power spectrum estimates of OLR (a, b) and precipitation (c, d) over Banda Sea and Timor Sea. Each spectrum estimate is an average over a region bounded by the dashed box shown in Figure 2.1a. Gray line and error bars denote the red noise and 80% significance level respectively.

Furthermore, intraseasonal OLR and precipitation signals over the Indonesian Seas exhibit eastward propagation along the equator with a phase speed of 5-8 m s^{-1}, which is another documented MJO characteristic across the tropics (Zhang 2005). We conclude that strong intraseasonal activities across the Indonesian Seas are consistently observed in SST, OLR, and precipitation with similar characteristics.

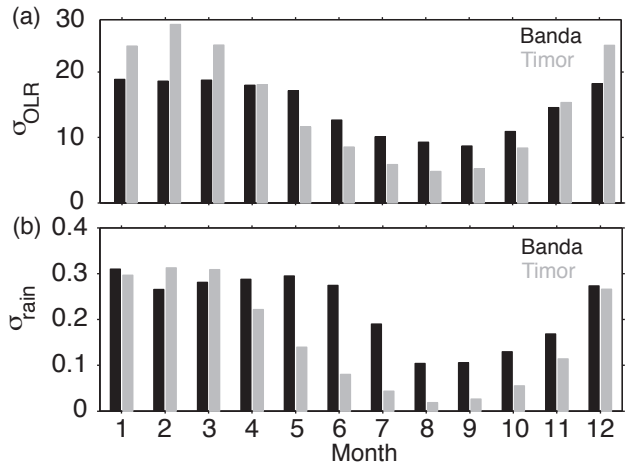

Figure 2.8. Seasonal variation of the intraseasonal (a) OLR and (b) precipitation standard deviation in Banda Sea (black) and Timor Sea (gray). The seasonal variation at each sea is an average over a region bounded by the dashed box shown in Figure 2.1a.

To quantify the relationship between SST and both OLR and precipitation at intraseasonal timescales, we apply a coherence method. The coherence analysis shows that the dominant intraseasonal SST, OLR, and precipitation in the Banda and Timor Sea are coherent with r^2 varying between 0.5 and 0.7 (Figs.2.9a,c). Furthermore the phase lag of the coherent signals suggest that both OLR and precipitation lead SST by 7-14 days (Figs.2.9b,d), which implies that atmosphere process is important to control the Banda and Timor Seas intraseasonal SST.

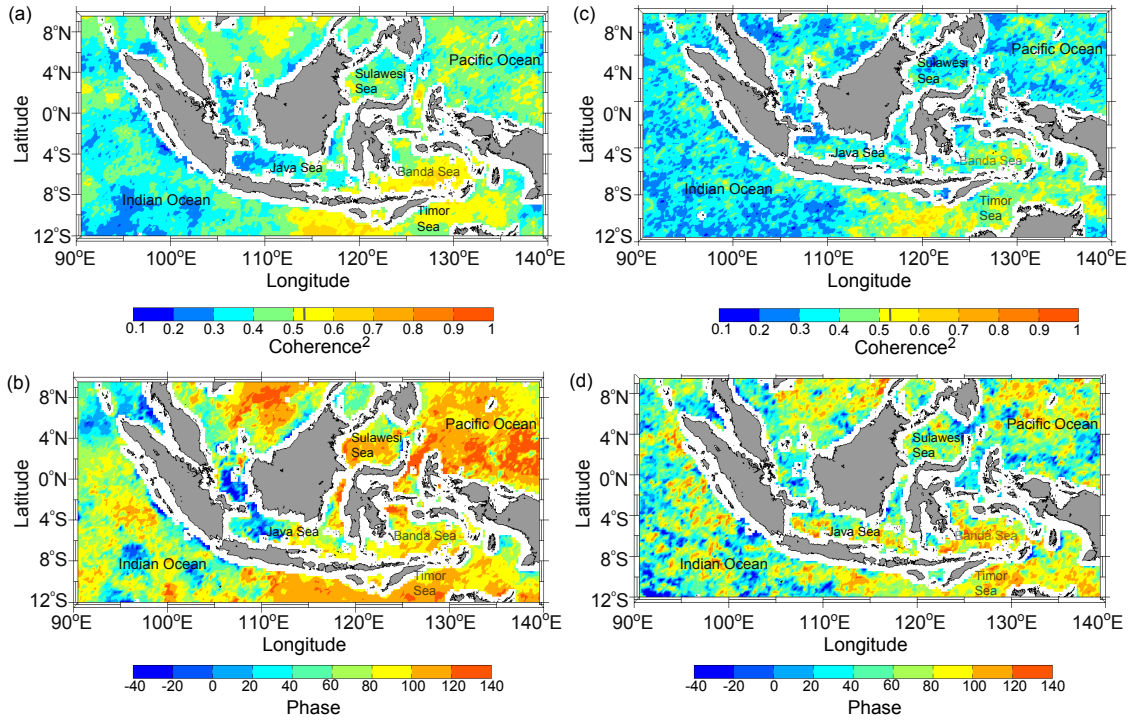

Figure 2.9. Coherence between SST and OLR (a,b) and between SST and precipitation (c,d) at intraseasonal timescales across the Indonesian Seas. Squared coherence amplitude (a,c) and phase difference (b,d), averaged across period of 28-56 days. A positive phase difference value indicates that OLR/precipitation leads SST. Vertical grey line on the squared coherence color bar marks the 95% significance level.

2.3.2.2 Sulawesi Seas

As discussed in section 2.3.1, Sulawesi Sea SST exhibits strong intraseasonal variations with different characteristic observed from the Banda and Timor Seas. The slab-model-derived SST indicates that surface heat flux predicts less than 40% (r = 0.6) of the observed intraseasonal SST variability in the Sulawesi Sea (Fig.2.10a). The amplitude of the model intraseasonal SST variability appears smaller than that of the

observed intraseasonal SST variability (Fig.2.10b).

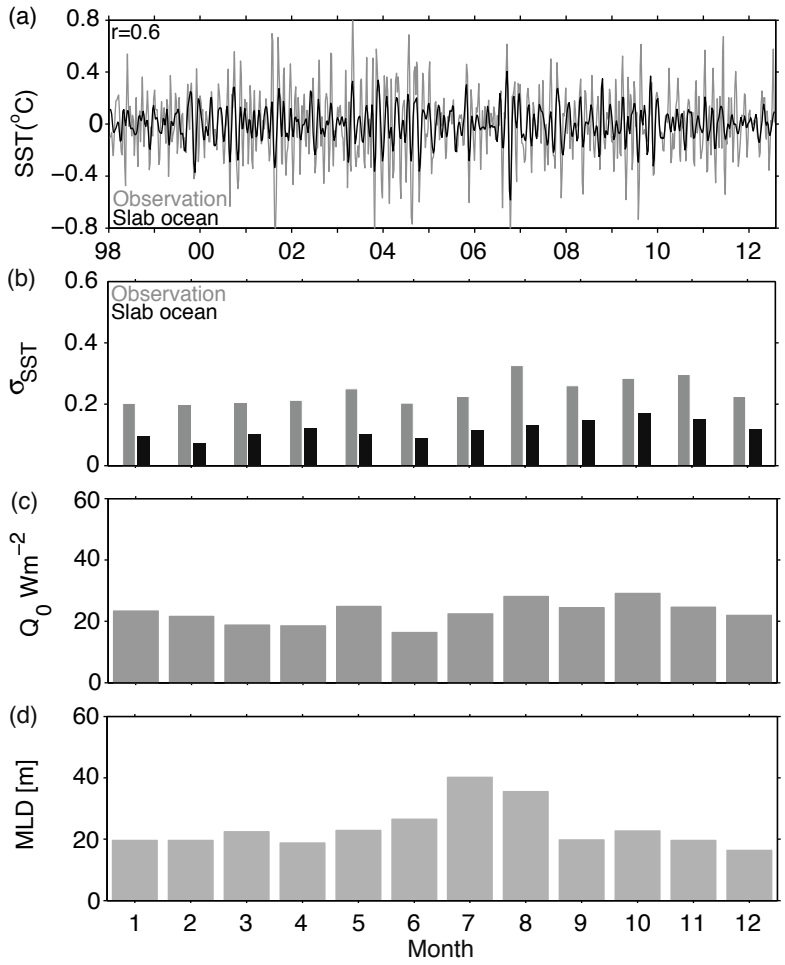

Figure 2.10. (a) Time series of the observed (gray) and slab ocean (black) model intraseasonal SST in Sulawesi Sea. Seasonal variation of the standard deviation of intraseasonal (b) SST and (c) shortwave radiation flux in Sulawesi Sea. (d) Seasonal variation of the basin averaged mixed layer depth in Sulawesi Sea. The data shown in (a), (b), (c), and (d) are basin averaged within the dash box shown in Figure 2.1a.

The model shows that the surface heat flux forced intraseasonal SST does not show seasonality, neither does the surface net heat flux (Figs.2.10b,c). Moreover the

model intraseasonal SST fluctuation follows the surface net heat flux variation, exemplifying the absence of seasonality in the mixed layer depth (Figs.2.10b-d). Because the model and observed intraseasonal SST show a rather weak correlation and non-seasonal nature, we argue that intrasesonal SST variability in the Sulawesi Sea is derived from ocean process and/or atmospheric process unrelated to the MJO. To identify other factors other than surface heat flux that might force intraseasonal SST anomalies in the Sulawesi Sea, we examine intraseasonal variation in winds and SLA.

The first Complex Empirical Orthogonal Function (CEOF) mode of average 2^{o}-4^{o}N intraseasonal wind stress along 117^{o}-125^{o}E over January 1998-mid-2012 reveals that the 20-30-day and 50-60-day variations characterize intraseasonal wind stress anomalies in the Sulawesi Sea. The reconstructed zonal wind stress data using the leading mode, containing about 80% of intraseasonal wind stress anomalies, clearly show that oscillations at 20-30 days and 50-60 days dominate intraseasonal zonal wind stress variability (Fig.2.11a). The data also indicate that intraseasonal zonal wind stress does not show eastward propagation over the Sulawesi Sea, which rules out the link between wind stress in the Sulawesi Sea and the MJO. We show only the zonal component of wind stress anomalies because the dominant oscillation's signature is weak in the meridional component.

We test a plausible relationship between SST and winds in the Sulawesi Sea by applying a coherence method to the data. Coherence analysis between SST and zonal wind stress time series, basin averaged over the Sulawesi Sea, indicate that both SST and zonal wind stress are coherent across the periods of 20-30 days with the squared coherence of 0.5, significant above the 95% significance level (Fig.2.11b). The phase lag

of the coherent oscillations indicates that zonal wind stress leads SST by about 3-days (Fig.2.11c). We thus suggest that the zonal wind stress oscillations at 20-30 days might induce a fraction of the total intraseasonal SST variances in the Sulawesi Sea.

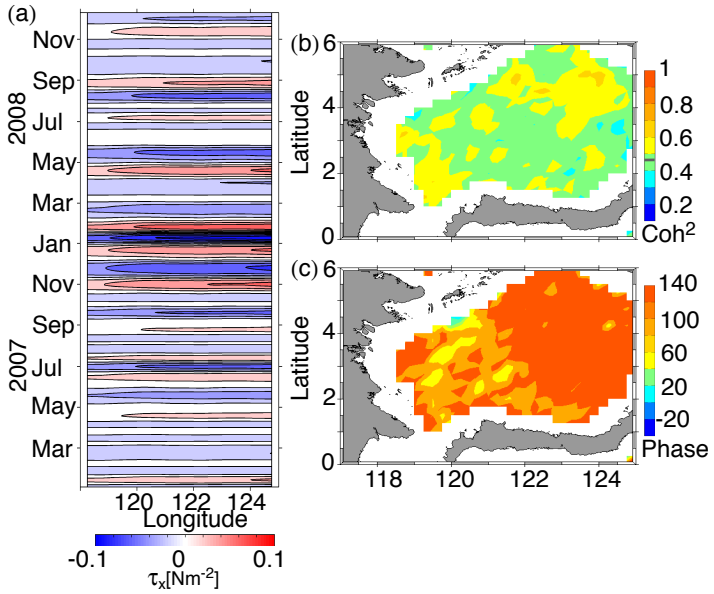

Figure 2.11. (a) Time and longitude plot of the reconstructed intraseasonal zonal wind stress over Sulawesi Sea. The leading CEOF mode of the zonal wind stress data along longitude between 118_E-125_E and at latitude averaged between 2_N-4_N observed during January 1998-mid 2012 is used to obtain the reconstructed data. The data during 2007-2008 is arbitrarily selected. Coherence between zonal wind stress and SST in Sulawesi Sea. (b) Squared coherence and (c) phase lag averaged across a period band of 20-30 days. Horizontal black line on the squared coherence color bar marks the 95% significance level.

Eddies dominate ocean processes at intraseasonal timescales in the Sulawesi Sea (Qiu et al. 1999; Masumoto et al. 2001; Pujiana et al. 2009). Using a numerical model, Qiu et al. (1999) and Masumoto et al. (2001) proposed that barotropic instability-generated vertical motions in the southern Mindanao Island largely contribute to intraseasonal variability in the Sulawesi Sea. Pujiana et al. (2009) argued that the eddies oscillate at around 50-60-day and propagate westward with a speed of a first baroclinic mode of Rossby wave. The eddies's signatures are evident across the upper thermocline in the Makassar Strait, to the southwest of the Sulawesi Sea (Pujiana et al. 2012). Eddy motions therefore potentially induce intraseasonal SST variability in the Sulawesi Sea.

To gauge the likelihood of eddies in generating SST in the Sulawesi Sea, we will show the correlation between eddies induced SLA and SST, which has not been addressed in previous studies. A CEOF analysis to the intraseasonal SLA along longitude between 118^{o}E-125^{o}E (averaged across latitude between 2^{o}N-5^{o}N) reveals that the first CEOF mode accounting for 60% of the SLA variability signifies an eddy characteristic, which is westward propagation. The reconstructed intraseasonal SLA attributed to the first CEOF mode clearly demonstrates westward propagating SLA at a speed of 0.2-0.4 m s^{-1} (Fig.2.12a), which is within the speed range for a baroclinic Rossby wave and consistent with the findings of Qiu et al. (1999), suggesting that eddies in the Sulawesi Sea are constrained by the baroclinic Rossby wave dynamics. A snapshot of intraseasonal SLA in 17 October 2007 in the Sulawesi Sea reveals a sea surface low and high likely attributed to cyclonic and anticyclonic eddies, respectively, propagating westward (Fig.2.12b). The propagating feature in SLA appears periodically at 50-60-day time scales (Fig.2.12a). The 50-60 day signal also characterizes the first CEOF mode of

intraseasonal SST at the same location, for which the CEOF mode accounts for 73% of the total intraseasonal SST variability. Unlike the SLA, the 60-day SST signal does not appear to propagate westward at a speed range of 0.2-0.4 m s^{-1}. The signal occurs almost instantaneously across the longitudes in the Sulawesi Sea. Although the dominant intraseasonal SST and SLA variability do not demonstrate a westward propagating feature consistently at the same speed, they are statistically coherent (Fig.2.12c). The basin averaged phase lag of the coherent oscillations indicates that SLA leads SST by about 8-days (Fig.2.12d). We thus suggest that the eddy motions at 50-60 days might induce a fraction of the total intraseasonal SST variances in the Sulawesi Sea.

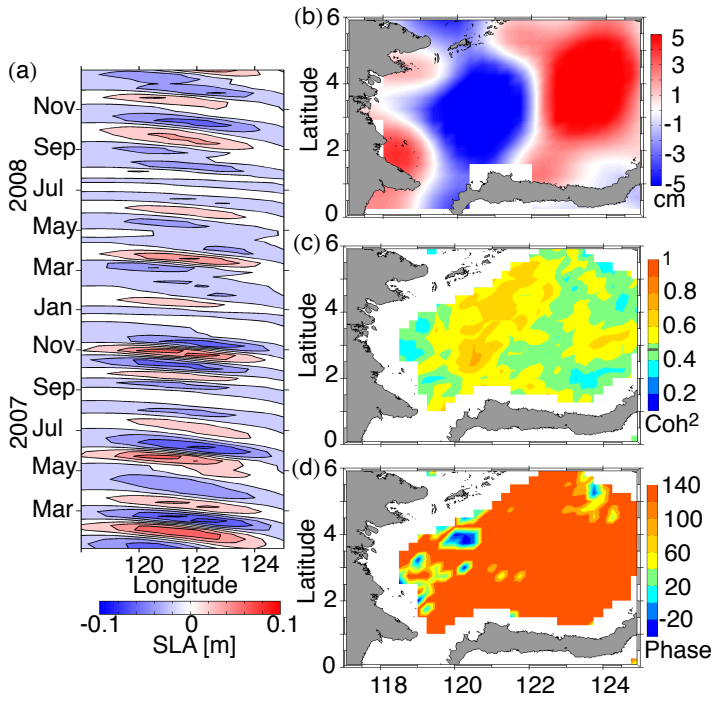

Figure 2.12. (a) Time and longitude plot of the reconstructed intraseasonal SLA in Sulawesi Sea. The leading CEOF mode of the SLA data along longitude between 118°E-125°E and at latitude averaged between 2°N-4°N observed during January 1998-mid 2012 is used to obtain the reconstructed data. The data during 2007-2008 is arbitrarily selected. (b) A snapshot of intraseasonal SLA over the Sulawesi Sea in 17 October 2007. Coherence between SLA and SST in Sulawesi Sea. (c) Squared coherence and (d) phase lag averaged across a period band of 20-30 days. Horizontal grey line on the squared coherence color bar marks the 95% significance level.

2.4. The Banda Sea SST response to 2007-2008 MJO events

We have shown that the dominant SST variations at intraseasonal timescales in the Banda and Timor Seas share distinct characteristics attributed to the MJO. The MJO surface heat flux contribute substantially to force intraseasonal SST in the Banda and

Timor Seas, where the MJO induced intraseasonal SST explains about 69-78 % of the total observed intraseasonal SST variability as inferred from the slab ocean model results (Figs.2.5a,b). The contribution of the MJO surface heat flux to force the mixed layer heat budget variability varies as a function of time. A cross wavelet transform of the slab ocean model derived SST and observed SST at intraseasonal timescales in the Banda Sea shows that the SST response to surface net heat flux varies with time: stronger during DJF and weaker during JJA (Fig.2.13b). This indicates that intraseasonal SST variability is dominated by surface flux variations in DJF, but other processes come into play in JJA. In addition to seasonal variation, the impact of surface heat flux on intraseasonal SST in the Banda Sea also exhibits interannual variations. Intraseasonal surface heat flux-forced SST is statistically correlated to the Niño 3.4 index (Fig.2.13a), with r = -0.47, indicating a significant correlation between the MJO-forced SST and the ENSO state. The impact of intraseasonal surface flux on intraseasonal SST appears stronger during neutral and La Niña years (e.g. 2004, fall 2007-spring 2008), while it is weaker during El Niño phases (e.g. late 2006) (Fig.2.13). Over the period of January 1998-mid 2012, the correlation between the model and observed SST is strongest during November 2007-February 2008 (henceforth is ND07/JF08) period (Fig.2.13b). Furthermore the time series of intraseasonal the Banda Sea SST variances between January 1998-mid 2012 is observed largest during ND07/JF08 (Fig.2.4). A more detailed discussion on how the MJO surface flux project its signature on SST over the Banda during ND07/JF08 is now investigated. We here solely focus our analysis in the Banda Sea, not in Timor Sea, because intraseasonal variability features observed in both the Banda and Timor Seas are strongly correlated.

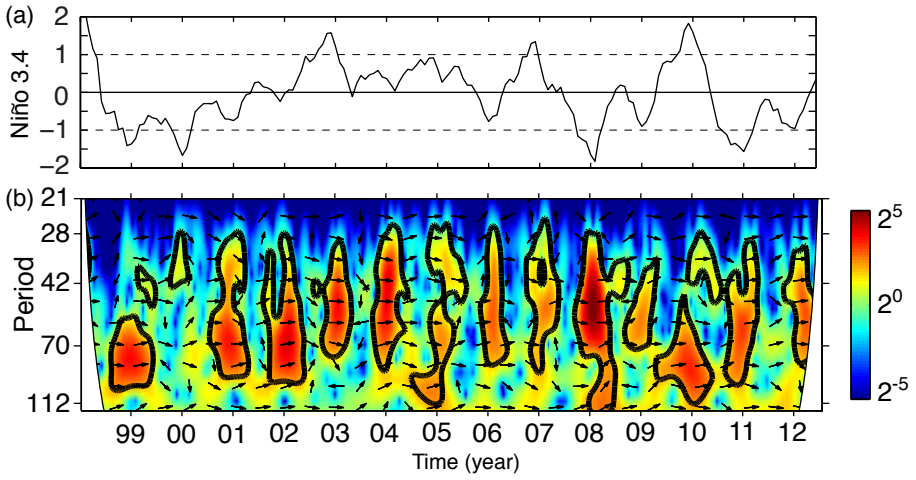

Figure 2.13. (a) Time series of the Niño 3.4 index. (b) Cross-wavelet transform between the observed and slab ocean model derived intraseasonal SST in Banda Sea. The SST data are basin averaged values within the dashed box shown in Figure 2.1a. Solid thick lines denote the 95% significance level. Arrows pointing right indicate that the observed and model SST are in phase.

To understand the MJO-SST coupling across the Banda Sea, the relationship between surface heat flux attributable to MJO life cycle and SST needs to be examined. Some studies suggest that surface heat flux attributed to MJO is the primary driver for SST variability (Shinoda et al.1998b; Duvel et al. 2004; Vialard et al. 2013). A MJO life cycle involves an active phase preceded by a suppressed phase. Reduced shortwave radiation due to strong convection and intense evaporative cooling driven by westerly wind bursts mark the MJO active phase (Shinoda et al.1998b).

Analyses of SST response to MJO are focused on two strong MJO events during ND07/JF08. We extend our analysis from the Indonesian maritime continent to a broader

region including the tropical Indian Ocean in order to examine the MJO evolution from the Indian Ocean to Pacific Ocean (Fig.2.14a). Vialard et al. (2008), using data from a mooring located in the Seychelles-Chagos Thermocline Ridge (SCTR), examined the impact of the ND07/JF08 MJO on SST in the tropical Indian Ocean. They showed that strong SST variability in the SCTR region during the ND07/JF08 period was correlated with the MJO, whose air-sea heat flux dominated the upper ocean heat budget.

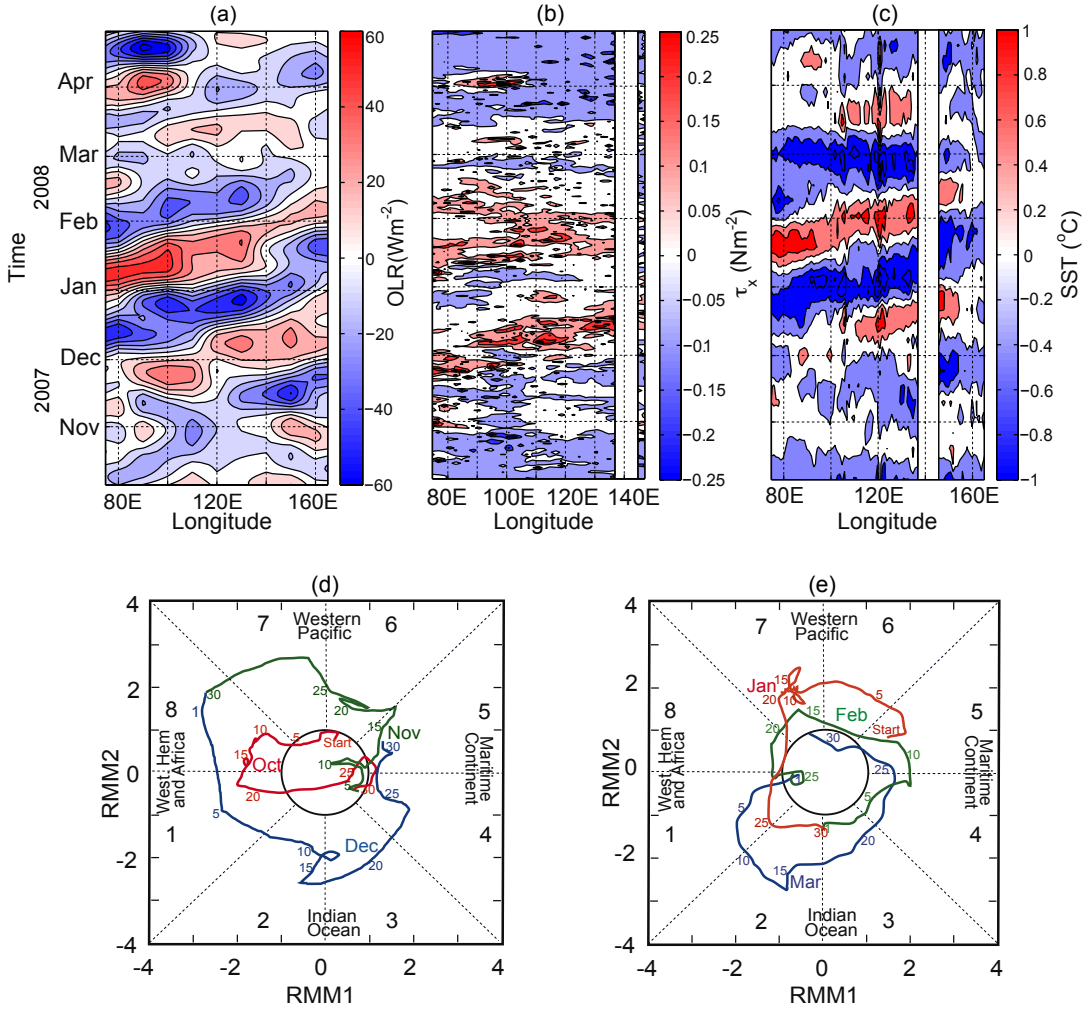

Figure 2.14. Time-longitude plots of intraseasonal (a) OLR, (b) zonal wind stress, and (c) SST during late fall 2007-spring 2008, averaged across latitude between 4°S-7.5°S. Real-time Multivariate MJO index during (d) October-December 2007 and during (e) January-

March 2008.

Our analyses indicate that a series of MJO events propagating eastward at a phase speed varying between 4-9 m/s is evident in OLR and zonal wind stress data during ND07/JF08 (Figs.2.14a,b). Each MJO event appears in OLR as a pair of positive and negative OLR phases respectively, where a positive phase indicates larger OLR or less atmospheric convection, while a negative phase implies colder cloud tops, more atmospheric convection (Fig.2.14a). The positive OLR (MJO suppressed phase) precedes the negative OLR (MJO active phase), and it takes about a month for each pair of propagating OLR to complete a cycle of positive and negative phases. Eastward propagation of MJO convective clouds along its path across the tropics also manifests in the wind variation. For the ND07/JF08MJO sequence, the suppressed MJO phase was characterized by calm winds while the active MJO phase was marked with westerly wind bursts (Fig.2.14b).

The eastward propagating feature during ND07/JF08 was consistently observed from the tropics of the central Indian Ocean to that of the Western Pacific Ocean (2.14a,b). The Wheeler and Hendon (2004) real-time multivariate MJO (RMM index during this particular period links the pairs of eastward propagating OLR and wind stress to two MJO events (Figs.2.14d,e). The index, OLR, wind stress are in agreement that the first MJO active phase (negative OLR and strong wind stress) occurred and propagated across the Indonesian maritime continent from mid-December 2007 to early January 2008, while the second MJO active event followed up and prevailed across the region in early February 2008 (Figs.2.14a,b,d,e). Each of the MJO active phases during the period

of ND07/JF08 was preceded by a suppressed MJO phase marked by positive OLR (reduced atmospheric convection) and calm winds prevailing across the maritime continent. Comparing the time evolution of OLR and RMM index, we find that the two MJO events observed during the period of ND07/JF08 differ in strength, with the first MJO displaying a stronger signature (Figs.2.14a,d,e).

The MJO passages propagating from the Indian Ocean to the Pacific Ocean across the maritime continent as indicated by OLR and wind stress data are projected in the intraseasonal SST warming and cooling episodes. The Banda Sea responds to passages of positive (negative) OLR and calm (westerly) during the ND07/JF08 MJO events by warming and cooling the SST, respectively (Fig.2.14c). Moreover the eastward propagation observed in OLR and wind stress associated with MJO is also evident in SST with a phase speed of 4-5 m/s.

Since OLR, wind stress, and SST reveal similar features, one of which is the eastward propagation, we conclude that intraseasonal SST fluctuations within the Banda Sea (and Timor Sea) are related to the MJO. The evolution of the first MJO propagating across the maritime continent during ND07/JF08 and how the SST responds to that event in the Banda Sea can be seen in Figures 2.15a-c. The onset of the first weak convective, passive phase was marked by positive OLR reaching the Banda Sea in late November 2007 and then followed by weak easterlies around a week after the positive OLR passed the Banda Sea. The sea surface responds to the passive phase by warming the temperature by about 1^{o}C. After the positive OLR completely passes across the Banda Sea, the propagation of deep convection within the atmosphere marking the active MJO phase reaches the Banda Sea. The convection that we can identify from the negative OLR

event is followed by a strong westerly wind burst. The Banda Sea responds to the reduced solar radiation, due to the deep convection, by cooling its SST by about 2°C (Fig.2.15d-f).

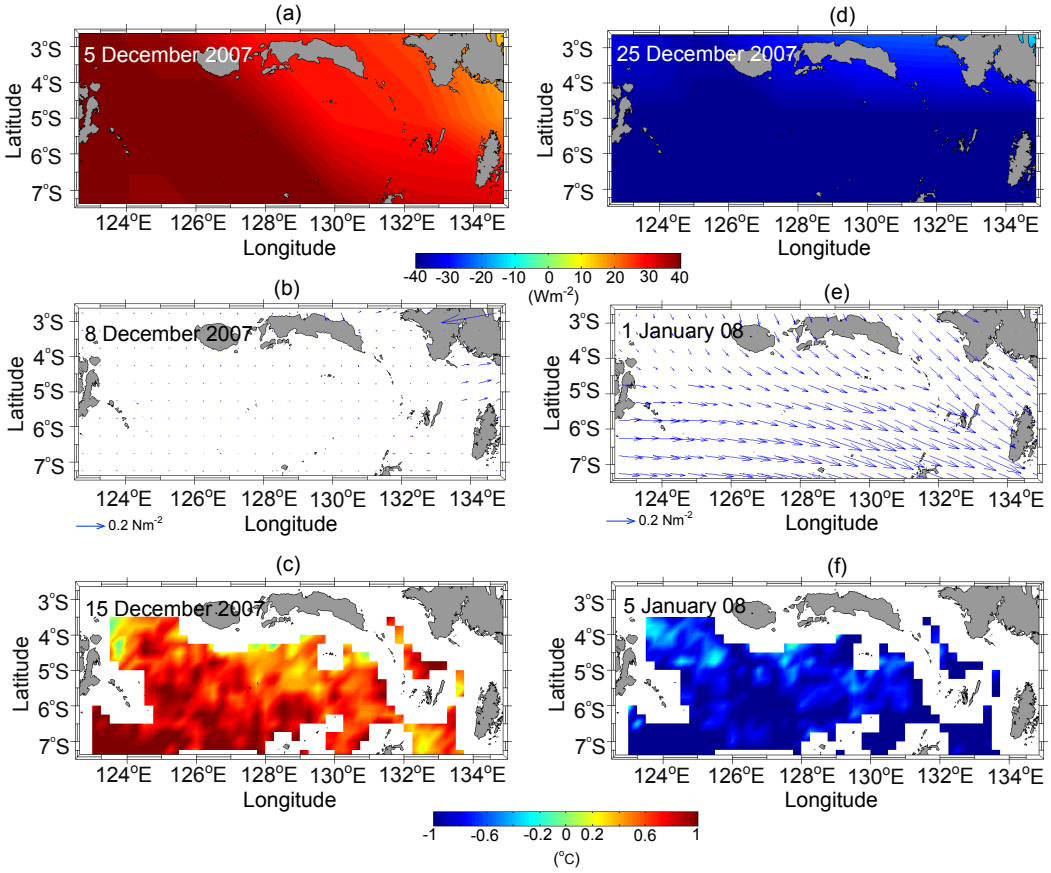

Figure 2.15. Snapshots of intraseasonal OLR, wind stress, and SST over Banda Sea attributed to (a-c) a passive MJO phase during early-mid December 2007 and (d-f) an active MJO phase during late December 2007-early January 2008. The dates are selected to represent the period of maximum (minimum) OLR and SST and of weakest (strongest) wind during the MJO suppressed (active) phase.

The slab model derived SST variability shows a good agreement with the observed SST variability at intraseasonal timescales in the Banda Sea over January 1998-mid 2012 (Fig.2.5a). The correlation between the model and observed SST variability improves during ND07/JF08 with the former explains about 90% of the later (Fig.2.16a). Moreover Figure 2.14 displays a strong correspondence between SST, OLR, and wind stress during the MJO phases of ND07/JF08. We thus propose that air-sea heat flux driven by atmospheric forcing associated with the MJO phases is more dominant than ocean mixed layer processes in governing intraseasonal SST variation during ND07/JF08.

The reanalysis data indicate that the net surface heat flux during ND07/JF08 was mostly controlled by solar radiation and latent heat flux (Figs.2.16b,c). Intraseasonal shortwave and latent heat flux combined contributes about 98% of intraseasonal surface net heat flux variability (Fig.2.16c). A combination of suppressed evaporative cooling due to calm winds and shortwave radiation during the first passive MJO phase from mid-November to mid-December 2007 resulted in an accumulated net heat flux of 758 Wm^{-2} which warmed SST up by $+1.1^{o}C$ (Figs.2.16a,b). The ensuing active MJO phase characterized by attenuated shortwave radiation and amplified latent heat flux to the atmosphere driven by strong westerly wind burst reaching its maximum strength in early January 2008 resulted in an accumulated net heat flux into the atmosphere of 1424 Wm^{-2}, which cooled SST by $-2.1^{o}C$ (Figs.2.16a,b). The overall cooling effect registered during the first MJO event is controlled by larger heat flux into the atmosphere during the MJO

active phase than that accumulated by the ocean during the MJO passive phase. By contrast, the second MJO induced intraseasonal SST warming of 0.2°C as the amount of heat flux into the ocean registered during the MJO passive phase through early-late January 2008 was slightly larger than the heat flux released to the atmosphere during the MJO active phase in February 2008 (Figs.2.16a,b). The ocean gained about 1534 Wm^{-2} of net heat flux, which increased intraseasonal SST by 2°C, over the MJO passive phase period. Moreover, the ocean lost about 1402 Wm^{-2}, cooling intraseasonal SST by 1.8°C, during the MJO active phase period.

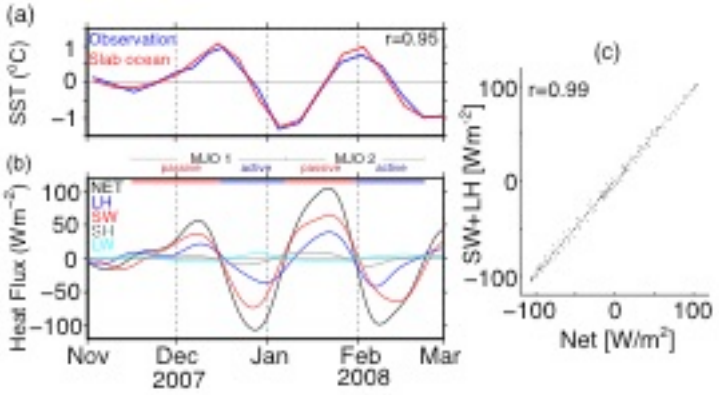

Figure 2.16. (a) Time series of intraseasonal SST from observation (blue) and slab ocean model (red) in Banda Sea. (b) Time series of intraseasonal net (black), shortwave radiation (red), latent (blue), sensible (gray), and longwave (cyan) heat fluxes over Banda Sea. Positive value indicates heat flux into the ocean. (c) Scattered plot of net heat flux and sum of shortwave and latent heat fluxes in Banda Sea. Dashed line denotes a line fit with a slope of 0.99. Horizontal red and blue bars indicate the active and passive phase respectively attributed to the MJO-1 and MJO-2 passages. Time series in (a), (b), and (c) are basin averaged values in Banda Sea within the box indicated in Figure 2.1a.

2.5. Summary and Discussion

2.5.1. Summary

Satellite-derived SST data, which extend from 1998 to mid 2012, reveal that intraseasonal variability explains about 18% of SST total variances over the Indonesian Seas. The largest intraseasonal contribution to the total non-seasonal SST variances are observed in the Banda, Timor, and Sulawesi Seas, with energy peaks centered at 35 days in the Banda and Timor Seas and at 25 and 56 days in the Sulawesi Sea.

The intraseasonal SST signals in the Banda and Timor Seas exhibit larger seasonal variation during the northern winter months (DJF) relative to the summer months (JJA). The standard deviation of intraseasonal SST anomalies varies between 0.6^{o} - 0.7^{o}C during DJF and 0.2^{o} - 0.3^{o}C during JJA. MJO surface heat flux accounts for significant variance of the coherent intraseasonal SST in the Banda and Timor Seas. The slab ocean model derived SST variation quantitatively demonstrates that surface net heat flux may explain 78% of intraseasonal SST variability within the Timor Sea, while it accounts for 69% of intraseasonal SST in the Banda Sea. The MJO-forced intraseasonal SST in the Banda and Timor Seas also shows variations on interannual timescales.

Over the period of January 1998-mid 2012, the magnitudes of intraseasonal SST variability in the Banda and Timor Seas are strongest between November 2007-February 2008, during which two strong MJO events were recorded. During those MJO passages, intraseasonal SST in the Banda Sea responds to MJO suppressed and active phases by warming and cooling respectively. The SST warms during the suppressed MJO phase (positive OLR) as a result of weaker winds and more shortwave radiation, with increased net surface heat flux into the ocean. More convective clouds (negative OLR), stronger

westerly winds, reduced shortwave radiation and increased evaporative lead to more heat transferred to the atmosphere, cooling the SST during the MJO active phase. The dominance of surface heat flux associated with the MJO in forcing intraseasonal SST is evident from observed eastward propagation in SST.

The intraseasonal SST variability in the Sulawesi Sea is characterized by dominant oscillations of 50-60 and 20-30 days, and it does not demonstrate significant correlation with intraseasonal SST in the Banda and Timor Seas. The slab ocean model predicts less than 40% of intraseasonal SST variability in the Sulawesi Sea. Unlike in the Banda and Timor Seas, intraseasonal SST and surface heat flux in the Sulawesi Sea do not exhibit seasonal fluctuations, a characteristic that couples MJO surface heat flux to intraseasonal SST variability. In addition to surface flux, a combination of eddy and wind induced SST may contribute to a considerable fraction of intraseasonal SST variance in the Sulawesi Sea. Eddy motion, signifying westward propagation at a baroclinic Rossby wave speed of 0.2-0.4 ms^{-1} in intraseasonal SLA variability, is coherent with the dominant intraseasonal SST variability with r^2=0.45 at periods of 50-55 days. We also demonstrate that the 20-30 day zonal wind stress variability is coherent with that of SST in he Sulawesi Sea with r^2 = 0.5. This dominant period band of the zonal wind stress does not exhibit eastward propagation, dissociating it from MJO forcing.

2.5.2. Discussion

The intraseasonal SST response in the Banda and Timor Seas to MJO surface flux is amplified during DJF and attenuated during JJA. The slab ocean model reveals the role of the mixed layer on the relationship of intraseasonal SST seasonal variability to surface

heat flux. During DJF in the Banda and Timor Seas, a larger air-sea net heat flux coupled with reduced wind and greater rainfall, results in more buoyant mixed layer depth that isolates the surface water from the cooler subsurface stratum inhibiting the role of ocean process in governing the mixed layer heat content variability.

The signature of the surface heat flux-induced intraseasonal SST in the Banda and Timor Seas displays variation not only at the seasonal timescale but also that at interannual timescale. The surface heat flux imprint on SST tends to be greater during neutral and La Niña years, when the mixed layer is more buoyant, with weaker SST response to surface heat flux during El Niño. The ENSO signal may indicate a response to the reduced rainfall during El Niño when the mixed layer is denser, increasing the role of ocean processes in regulating the mixed layer heat budget variability at intraseasonal timescales.

The role of ocean process is likely to be larger in the Banda Sea than in the Timor Sea as surface heat flux explains smaller fraction of intraseasonal SST variability within the Banda Sea. Major ocean processes that may contribute to SST variations in the Banda Sea are Ekman-driven upwelling and downwelling at seasonal and interannual timescales. Gordon and Susanto (2001) reported that coldest (warmest) SST in the Banda Sea occurs in JJA (DJF). The period of colder (warmer) SST is driven by stronger upwelling (downwelling). The JJA mixed layer is denser than the DJF mixed layer. A more buoyant mixed layer in DJF and during La Niña within the Banda Sea explains the atmospheric heat flux dominance in forcing intraseasonal SST in the Banda Sea during DJF and La Niña, when the ocean process's effect on SST is reduced.

We find that MJO surface heat flux accounts for significant variance of the

coherent intraseasonal SST in the Banda and Timor Seas. The characteristics of OLR, precipitation, and zonal winds stress at intraseasonal timescales over the Banda and Timor Seas are similar to that of SST and correspond to MJO characteristics (Zhang and Dong 2004; Zhang 2005).

The slab ocean model is relatively simple, and it does not resolve the impact of the sub-monthly surface mixed layer depth variability on intraseasonal SST because we applied monthly climatology in our computation. Our results, however, suggest that the model approximately reproduces observation delineating the dominant role of intraseasonal surface heat flux in forcing intraseasonal SST, particularly during DJF in the Banda and Timor Seas. Through applying a similar approach, Vialard et al. (2013) found that the slab model provides a good estimate of 79% SST variability at periods of 30-110 days in the NWAB. Moreover, Duvel et al. (2004); Duvel and Vialard (2007); Drushka et al. (2012) concluded that net surface heat flux anomalies dominate the overall mixed layer heat budget of the Indo-Pacific at intraseasonal timescales. We suggest oceanic heat flux significantly contributes to SST during the JJA and El Niño periods within the Banda and Timor Seas. To quantify the oceanic heat flux contribution, we would need to examine oceanic parameter measurements such as ocean currents and mixing rates, which are rather limited or non-existent in our study area.

We have shown that intraseasonal SST in the Banda and Timor Seas is responsive to the MJO, and the response displays interannual variation in which warmer (colder) background SST attributed to La Niña (El Niño) corresponds with stronger (weaker) projection of MJO in SST. Does warmer sea surface during La Niña in the Banda and Timor Seas provide positive feedback to strengthen the MJO signature as it propagates

over the maritime continent from the Indian Ocean to the Western Pacific Ocean? Future studies will explore this important issue.

Acknowledgments

The constructive comments from three anonymous reviewers are greatly appreciated. This research was funded in part under the Cooperative Institute for Climate Application Research (CICAR) Award NA08OAR4320754 from the National Oceanic and Atmospheric Administration, U.S. Department of Commerce. The statements, findings, conclusions, and recommendations are those of the authors and do not necessarily reflect the views of NOAA or the Department of Commerce. The TMI data are produced by Remote Sensing Systems and sponsored by the NASA Earth Science MEaSUREs DISCOVER Project.

(The data are available at www.remss.com. The RMM and Niño-3.4 SST index can be obtained from

http://cawcr.gov.au/staff/mwheeler/maproom/RMM/RMM1RMM2.74toRealtime.txt and

http://www.esrl.noaa.gov/psd/gcos_wgsp/Timeseries/Data/nino34.long.anom.data,

respectively.)

Chapter 3

Oceanic Responses and Feedbacks to the Eastward Propagation of the Madden-Julian Oscillation in the Maritime Continent

To be submitted as: Napitu, A. M., Gordon, A. L. and Pujiana., K. Oceanic Responses and Feedbacks to the Eastward Propagation of the Madden-Julian Oscillation in the Maritime Continent , Geophysical Research Letters.

Abstract The role of sea surface temperature [SST] in influencing eastward propagation of Madden-Julian Oscillation [MJO] events over the maritime continent [MC] is investigated using satellite and reanalysis data over the period of 1980 – 2012, during which there are 86 MJO events over the Indian Ocean, 51 of which traversed the MC into the western Pacific. The SST in the Indonesian Seas during the suppressed phase of these 51 MJO events is warmer by 0.5 °C than that associated with the MJO events that do not propagate over the MC. We argue that the warmer SST, which corresponds to increased surface turbulent air-sea heat flux, low-level moisture, and diurnal SST activity, serves as a favorable precondition for the MJO convection to propagate across the MC. During the MJO active phase, the SST-MJO coupling at El Niño Southern Oscillation [ENSO] timescale in the Indonesian Seas is sensitive to the thermocline depth and demonstrates stronger coupling during La Niña when the thermocline is deeper than during El Niño.

3.1. Introduction

Discerning behavior of Madden-Julian Oscillation [MJO] events traversing the maritime continent [MC] is key for improving the predictability in general circulation models [GCMs]. Earlier studies, aimed to describe the MJO propagation, identify the MC as a barrier to eastward propagation of the MJO events, as the MJO convection is substantially weakened over the MC and then strengthened over the western pacific warm pool (Salby and Hendon, 1994; Maloney and Hartmann, 1998).

A complete description of physical processes controlling the behavior of the MJO over the MC remains elusive, but it has garnered increased attention. Inness and Slingo (2006) suggested that the mountainous orography of Sumatra island, one of the larger islands composing the Indonesian archipelago, caused a blocking effect to the eastward propagation of the MJO via reducing the low-level convergence to the east of the MJO convection. More recent studies have shown competing interactions between diurnal precipitation and the larger-scale MJO convective envelope as the primary cause attenuating the signature of the MJO propagation over the MC. Enhanced diurnal precipitations over the Indonesian main islands, sustained by increased frictional moisture convergence, disrupts the convective signal of the MJO (Peatman et al., 2014; Hagos et al., 2016). Land-air interactions thus have been put forward as the primary mechanism controlling the eastward propagation of the MJO over the MC, while the roles of air-sea interactions have not been fully considered.

Eastward propagation is likely determined by zonal gradient of moist static energy (MSE) (Sobel and Maloney, 2012), as the MJO convective system requires a MSE source to the east of the convective phase to produce an eastward propagation

(Sobel and Maloney, 2013). Kim et al. (2014) suggested that column-integrated MSE budget is required to be maximum over the eastern Indian Ocean and minimum over the Western Pacific, setting up a precondition for an MJO event to traverse over the MC. They argued that advective moistening is the main component of the MSE budget, not air-sea surface fluxes.

The MJO is an atmosphere-ocean coupled system that causes substantial impacts on the dynamics and thermodynamics of the upper ocean, and it is sensitive to surface heat fluxes partially controlled by the sea surface temperature (SST). Over the open seas, imbalances between downward diurnal shortwave radiation and upward latent and sensible heat fluxes warm the surface mixed layer characterize the MJO suppressed phase. This suppressed phase is subsequently followed by the MJO active phase, during which upward net surface heat flux and downward turbulent heat flux across the surface mixed layer predominantly cools the SST by up to 0.5 – 1.5 °C (Moum et al., 2014; Pujiana et al., 2015).

Turbulent cooling may last longer during a strong MJO and continue to cool the ocean mixed layer, sustained by shear instability at the base of the mixed layer, and thereby retard the SST recovery during the subsequent MJO suppressed phase despite intense downward shortwave radiation (Pujiana et al., 2017). Colder SST decreases surface latent and sensible heat fluxes, which may affect the available moist static energy for the following MJO event (Moum et al., 2016). Upper ocean heat content thereby could contribute to control the strength of the MJO, and the role of the Indonesian Seas in modulating total surface heat fluxes may be important for the maintenance of the MJO eastward propagation over the MC.

The SST over the Indonesian Seas, particularly in Banda and Timor Seas, is significantly affected by the MJO. Napitu et al., (2015) show that intraseasonal SST variability in Banda and Timor Seas displays a strong coupling with MJO surface heat fluxes, where a passage of the MJO can modulate the SST by up to 1° C. They suggested that the coupling shows seasonal and interannual variations, stronger during boreal winter and during La Niña, and attributed the weaker coupling through boreal summer and an El Niño period to increased influence of ocean processes to regulate upper ocean heat content and SST. Wilson et al. (2013) demonstrated that more events of MJO propagation over the Indian Ocean are documented during negative IOD phases, where the eastern Indian Ocean is anomalously warmer. It is thus intuitively appealing to investigate whether warmer SST over the Indonesian Seas, such as during La Niña, could set up zonal MSE gradient favorable for more eastward MJO propagation events. Moreover, what are the impacts of diurnal SST variations on the behavior of the MJO over the MC?

Upper ocean heat content variability is closely linked to freshwater variability in the surface mixed layer. Rainfall-induced freshwater lenses may increase the strength of salinity stratification over thermal stratification that leads to the formation of a barrier layer within the surface mixed layer, acting to prohibit transfer of heat, salt, and momentum from the surface to deeper depth or vice versa (Chi et al., 2014; Pujiana et al., 2017). The presence of the barrier layer could enhance the rate of SST increase during the MJO suppressed phase, trapping downward shortwave radiation within the low salinity surface layer. By contrast, the barrier layer could minimize downward heat flux during the MJO active phase, which may lead to larger available heat content than is typically observed when the barrier layer is absent.

This study aims to investigate whether SST and its respective surface turbulent fluxes, latent and sensible heat fluxes, across the Indonesian Seas affect the eastward MJO propagation over the MC. The SST condition across the Indonesian Seas through the suppressed MJO phase for all MJO events registered during our observational period that demonstrate smooth eastward propagation over the MC is evaluated. The SST condition is then contrasted to that attributed to MJO events showing no eastward propagation over the MC. In addition to evaluating SST role in governing the MJO propagation across the MC, we also examine the SST response to the MJO. The focus is to explore the primary causes of non-uniform SST response to the MJO, particularly the role of interannual variability of the ocean to the response.

3.2. Data and Method

3.2.1. Reanalysis Data

To evaluate surface turbulent flux and temperature across the Indonesian Seas over as many MJO events as possible, we analyze daily latent and sensible heat fluxes as well as SST data from a suite of reanalysis TropFlux products [Kumar et al., 2012] that extend from 1980 to 2012. The data have a spatial resolution of 1° x 1° and demonstrate a good agreement with those gathered from equatorial moorings in the Indian and Pacific Oceans (De Szoeke et al., 2014). Moreover, the data reasonably reflect MJO events and explain intraseasonal SST variation across the Indonesian Seas (Napitu et al., 2015).

3.2.2. Diurnal variability estimates

To assess the strength of diurnal variability in modulating the overall SST variation, high frequency SST measurements in are required. Such measurements in the Indonesian Seas are not available. Diurnal SST cycle is then indirectly estimated using reanalysis shortwave radiation and wind speed data using the following formula:

$\boldsymbol{T_{predicted} = \alpha_1 SWR + \alpha_2 SWR + \alpha_3 V + \alpha_4}$ (Matthews et al., 2014),

where SWR is shortwave radiation, V is surface wind speed, α_1 = -2.16 x 10^{-4},°C m s W^{-1}, α_2 = -2.08 x 10^{-3} °C m^2 W^{-1}, α_3 = 1.52 x 10^{-2} °C s m^{-1}, α_4 = -1.82 x 10^{-1} °C. The formula was derived by regressing high-resolution in-situ measurements to the reanalysis data in the central equatorial Indian Ocean (Matthews et al., 2014) and has been applied to yield reasonable diurnal SST estimates in other regions (Baranowski et al., 2016).

3.2.3. MJO index and identification of MJO eastward propagation

The daily Wheeler and Hendon Real-time Multivariate MJO index (RMM; Wheeler and Hendon, 2004) is utilized to identify MJO events over the Indian Ocean and or the MC. A significant MJO convective activity occurs when the RMM index amplitude is greater than 1. To identify eastward propagation of the MJO, the RMM index is mapped into its phase space consisting eight sections (Wheeler and Hendon, 2004). A continuous eastward propagation of the MJO across the Indian Ocean and the MC would manifest as a counterclockwise arc in the phase space from phase 2 to phase 6. MJO events that do not propagate over the MC would demonstrate a trajectory in the phase space that lasts only until phase 3.

3.3. Results

3.3.1. MJO events

Using the method described above, we identify 86 MJO events generated over the Indian Ocean over a period of 32 years between 1980 and 2012. Of which, 35 MJO events do not survive passage over the MC, whereas, 51 events reach the west Pacific warm pool. The ratio of the number of MJO events propagating over the MC to the total number of MJO events is thus about 60%. Kerns and Chen (2016), applying a different method of tracking the MJO trajectory and datasets extending for a shorter period, found a similar ratio. The MJO events propagating over the MC are hereafter called eastward propagating [EP] MJO case, while those propagating over the Indian Ocean but do not survive the MC are assigned as non-propagating [NP] MJO case. The strength of the EP MJO does not differ from that of the NP MJO. Analyses of RMM amplitudes at phase 3 for the 86 MJO events indicate that the averaged value of RMM amplitude for both the EP and NP MJO is consistently near 1.8. This indicates that the initial strength of an MJO event over the Indian Ocean neither control nor determine its propagation over the MC.

Eleven El Niño and 9 La Niña events occur during 1980 – 2012. The number of MJO propagating across the MC during La Niña is 2.5 times as many as during El Niño (Table 3.1). More occurrences of EP MJO events during La Niña than El Niño were also documented in Kerns and Chen (2016). As for the MJO during the Indian Ocean Dipole (IOD) years, 10 MJO events are observed during negative IOD years, of which 8 events propagate from the Indian Ocean to the western Pacific (Table 3.1). The positive IOD years, on the other hand, document fewer number of MJO events traversing the MC. This is consistent with the finding of Wilson et al. (2013) suggesting that MJO convective

activity over the MC is enhanced during negative IOD. It hence appears that eastward MJO propagation over the MC occurs more frequently during La Niña and – IOD.

Table 3.1. The number of MJO events propagating over the MC vs over the Indian Ocean only observed during El Niño, La Niña, + IOD, - IOD phases over the period of 1980 – 2012.

	Propagating MJO	Non-propagating MJO
El Niño	8	10
La Niña	14	4
+ IOD	7	9
- IOD	8	2

After identifying the MJO events, including grouping those events into EP MJO and NP MJO categories, the next step is to analyze the SST, surface turbulent heat flux, low-level specific humidity conditions across the Indonesian Seas during the suppressed phase for each MJO category. The analyses results would provide insights into the contrast between the EP and NP MJO cases, useful to assess the role of the Indonesian Seas to regulate the MJO propagation over the MC. The results are presented in the following sections.

3.3.2. SST during MJO suppressed phase

Prior to the arrival of a MJO active (convective) phase over the MC, the MJO suppressed phase, the SST is warmer for the EP case than for NP case (Fig.3.1). The average SST across the Indonesian Seas attributed to 51 EP MJO events is warmer than that attributed to 35 NP MJO events (Fig.3.1). Warmer average SST is particularly evident in Java, Banda, and Timor Seas, where the MJO demonstrates its strongest

signature over the Indonesian Seas. The SST off the west coast of Sumatra is notably colder for the NP case, while the SST in Sulawesi Sea does not exhibit a notable contrast between the two cases. Napitu et al. (2015) reported that the MJO exerts its strongest influence on the SST in Banda and Timor Seas.

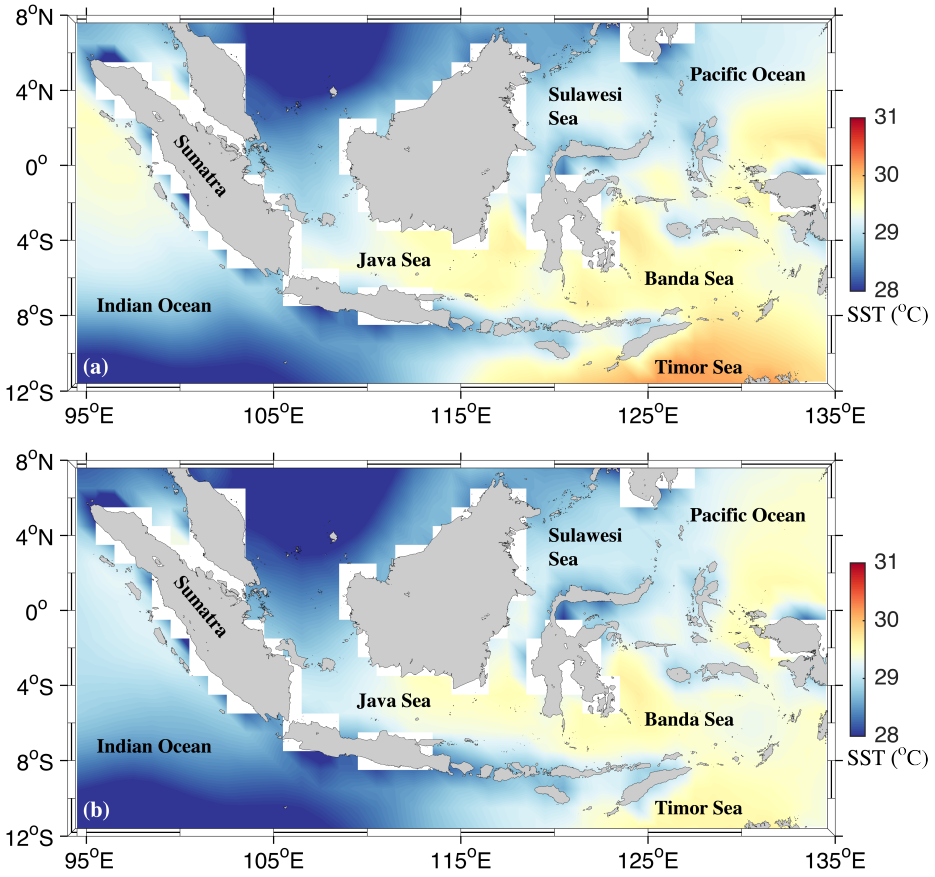

Figure 3.1. Average SST across the Indonesian Seas during the suppressed phase of MJO events observed over the course of 1980 – 2012. (a) The average SST for 51 MJO passages propagating over the MC [EP]. (b) The average SST for 35 MJO passages that do not propagate over the MC [NP].

The average suppressed phase SST in Java, Banda, and Timor Seas (from SST data observed within a 2°x2° box centered at 5°S 110°E for Java Sea, 6°S 126°E for Banda Sea, and at 12°S 123°E for Timor Sea) during the EP MJO event is 0.5 - 1°C warmer than during the NP MJO event. More occurrences of SST > 30°C across the Indonesian Seas are registered for the EP case (Fig.3.2). A Kolmogorov-Smirnov method is used to test whether the SST data observed during the EP MJO case differs from that during the NP case. The result distinctively distinguishes the SST distribution attributed to the propagating MJO from the non-propagating MJO.

The warmer SST condition prior to the passages of propagating MJO events over the MC also corresponds with increased surface turbulent fluxes. Upward turbulent fluxes, both latent and sensible heat fluxes, across Java, Banda, and Timor Seas prior to the EP MJO case significantly differ from those prior to the NP MJO case (Fig.3.3). The difference varies between 5 – 20 W/m^2 attributable to the latent heat flux and 2 – 3 W/m^2 for the sensible heat flux (Fig.3.3). Radiative fluxes attributed to both cases are not substantially different, although wind stress is slightly more energetic over the MC for the EP MJO case (not shown).

Enhanced surface turbulent fluxes act to destabilize the atmosphere, fostering shallow convection. Low level specific humidity over the course of the suppressed phase over Java, Banda and Timor Seas attributed to the propagating MJO case is slightly larger than the non-propagating MJO case (Fig.3.3). The lower troposphere moistens by 2 g kg^{-1} over the Java Sea and by a smaller amount over the Banda and Timor Seas prior to the MJO approach for the propagating over the MC case. Low-level moisture buildup to the

east of a MJO convective system over the central Pacific has been reported (Kiladis et al., 2009).

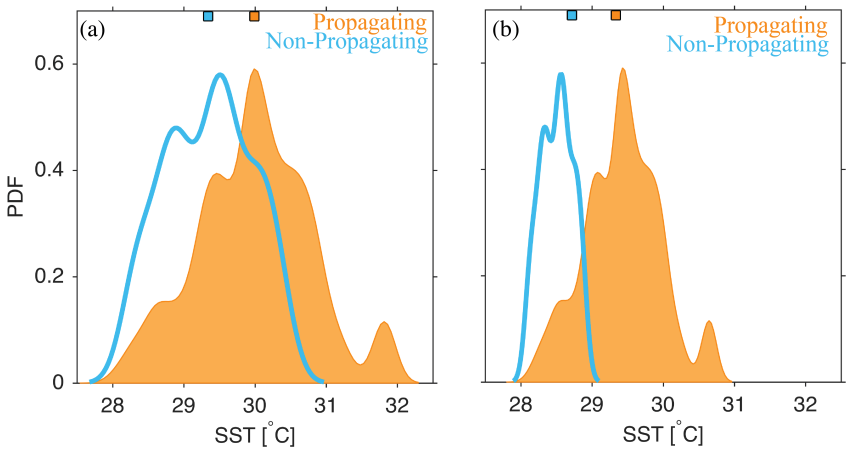

Figure 3.2. Probability distribution functions of SST in (a) Banda and Timor Seas and (b) Java Sea observed during the suppressed phase of 86 MJO events occurring between 1980 - 2012. The orange curve illustrates the SST distribution for MJO events that propagate over the MC, while the cyan curve indicates the SST distribution for MJO events that propagate over the Indian Ocean only.

A wide-array of ocean processes on various timescales contribute to regulate the SST. One of the fundamental timescales strongly influencing SST variability is the diurnal timescale. The imbalance between accumulated daytime heating and accumulated nighttime cooling may result in increased SST. The warmer average SST set up across Java, Banda and Timor Seas for the EP MJO event may relate to increased diurnal SST activity. Comparing variances of diurnal SST in the Indonesian Seas for both EP and NP MJO events, it is apparent that SST in Java, Banda and Timor Seas exhibits larger

variance, about 75% larger, during the suppressed phase of the EP MJO event than NP MJO event (Fig.3.4). It is also noticeable that diurnal SST variance is smaller in Java Sea than in Banda and Timor Seas (Fig.3.4). The relatively shallow Java Sea may explain the subdued diurnal SST variance. The nature of diurnal SST variation during the suppressed phase of an MJO event is thought to play a significant role to determine the strength of the MJO convective system. Li et al. (2013) surmised that solar radiation-controlled diurnal SST variability effects intraseasonal SST variability through non-linear rectification and modifies surface turbulent heat fluxes, important for the MJO initiation and evolution.

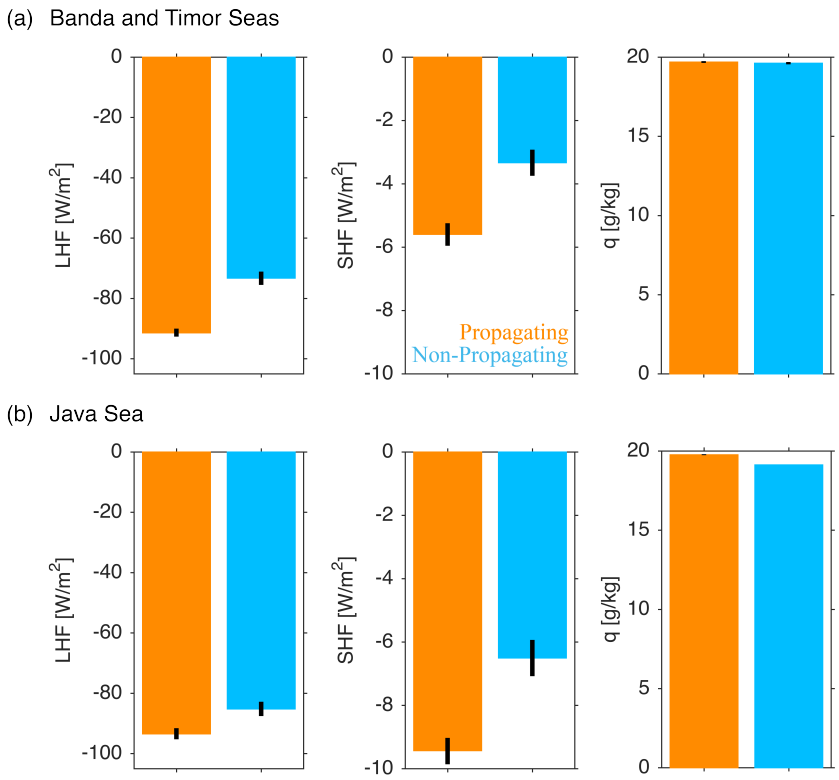

Figure 3.3 Average latent heat flux [LHF; left], sensible heat flux [SHF; middle], and specific humidity [q; right] at 2 m above the surface in (a) Banda and Timor Seas and (b) Java Sea observed during the suppressed phase of 86 MJO events occurring between 1980 - 2012. The orange bar indicates the average heat flux for MJO events that propagate over the MC, while the bar curve indicates the SST distribution for MJO events that propagate over the Indian Ocean only. The error bars denote 95% bootstrap confidence limits.

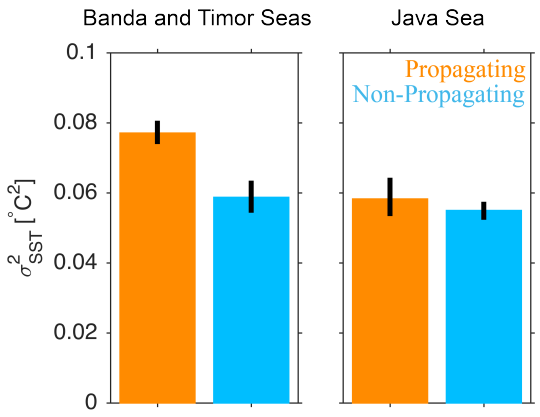

Figure 3.4. Average variance of diurnal SST in Banda and Timor Seas (left) and Java Sea (right) observed during the suppressed phase of 86 MJO events occurring between 1980 - 2012. The orange bar indicates the average heat flux for MJO events that propagate over the MC, while the bar curve indicates the SST distribution for MJO events that propagate over the Indian Ocean only. The error bars denote 95% bootstrapped confidence limits.

3.3.3. SST response to eastward propagation of the MJO

We have shown that SST, upward surface turbulent flux, and low-level specific humidity tend to be larger for Java, Banda and Timor Seas prior to the EP MJO events that traverse the MC. Increased activity of diurnal SST may account for the warmer SST observed in the Indonesian Seas prior to the events of eastward propagation of the MJO over the MC. Warmer SST in the Indonesian Seas during La Niña is also favorable for more eastward MJO propagation events over the MC. How does the SST in the Indonesian Seas respond to the MJO propagating aloft?

Primary characteristics of the SST responses to the MJO in the Indonesian Seas have been studied by Napitu et al. (2015). They reported that MJO surface heat fluxes, in

general, control the rate of change of SST in the Indonesian Seas on intraseasonal time scales. About 70% of intraseasonal SST variances in the Indonesian Seas are attributable to the MJO surface fluxes. We here will discuss the contrast of the SST response to the MJO between during El Niño and during La Niña.

A composite of band-passed surface net heat flux (NHF) along longitude of 80º-140ºE averaged across 4º-7ºS, encompassing Java and Banda Seas, during the suppressed and active phases of MJO events observed during El Niño years is similar to that observed during La Niña years. Nevertheless, the composite of band-passed SST within the demonstrates a contrast between El Niño and La Niña, that indicates that the SST response to the MJO in the Indonesian Seas during La Niña appears stronger than during El Niño (Fig.3.5). Although NHF during the suppressed phase of the MJO over Java and Banda Seas does not show variation with El Niño and La Niña, the SST anomalies increase more than 0.5º C during La Niña, compared to < 0.2º C during El Niño. Larger SST response is also evident during the active phase, over which the SST anomalies during La Niña and El Niño decrease by more than 0.5º C and by less than 0.5º C respectively despite both La Niña and El Niño demonstrate a similar magnitude of upward surface net heat flux. The discrepancy in SST response is apparent during both El Niño and La Niña phases independent of the MJO events with an average RMM amplitude of 2, indicative of a similar strength. Thus, SST across Java and Banda Seas appear to be more coupled to the MJO during La Niña.

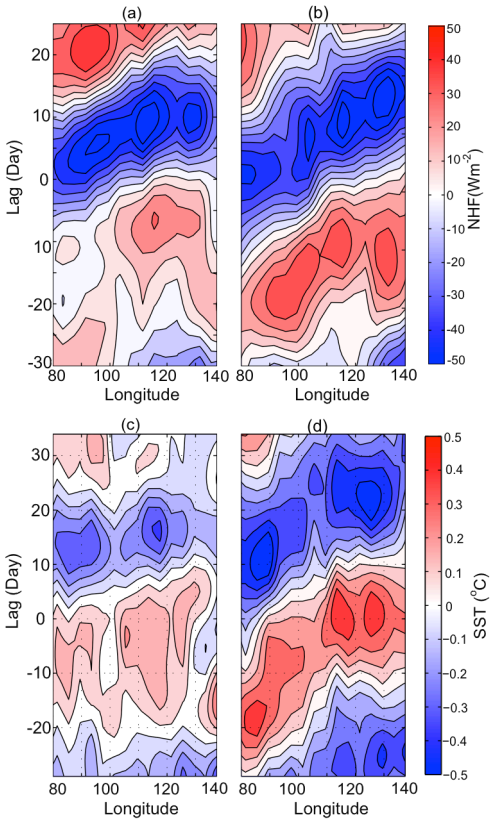

Figure 3.5. Composites of band-passed surface NHF (a, b) and SST (c, d) along longitude of 80º – 140ºE averaged across 4º - 7ºS observed during the MJO events between 1980 – 2012. The composites when El Niño prevails are shown in (a) and (c), while those attributed to La Niña are illustrated in (b) and (d).

Given the MJO strength does not vary on El Niño-Southern Oscillation [ENSO] time scale, the discrepancy in the SST response to the MJO might be due to various factors from thickness of the surface mixed layer to the depth of the thermocline. Larger (smaller) SST response during La Niña (El Niño) may correspond with deeper (shallower) thermocline. A deeper thermocline would be less favorable for heat exchange between the thermocline and surface mixed layer, and vice versa. Reduced heat exchange

between the thermocline and the mixed layer would result in stronger the SST-MJO heat flux coupling. Gordon and Susanto (2001) show that the thermocline depth in Banda Sea is deeper during La Niña than El Niño and is is likely not controlled by Ekman dynamics but rather by western tropical Pacific stratification advected into the MC by the Indonesian Throughflow (ITF).

3.4. Summary and Discussion

The role of Indonesian Seas SST in the eastward propagation of the MJO over the MC is investigated using satellite and reanalysis data over the period of 1980-2012. During this particular period, there are 86 MJO events documented over the Indian Ocean, of which 51 events (59%) manage to traverse the MC into the western Pacific. MJO propagation over the MC is sensitive to ENSO, with more propagation events during La Niña than El Niño.

We find that warmer SST over the Indonesian Seas, particularly in Java, Banda and Timor Seas, is a favorable precondition for the MJO to propagate over the MC. The SST in those particular seas is 0.5 - 1°C on average warmer prior to the EP MJO events. In addition to the warmer SST, increased surface turbulent heat fluxes and low-level specific humidity are also observed. Warmer SST in Java, Banda, and Timor Seas during the suppressed phase of the MJO might be related to increased activity of diurnal SST, which are 70% larger during the suppressed phase preceding to the MJO event propagating over the MC. Furthermore, regional SST over the Indonesian Seas are warmer by near 1°C during La Niña than El Niño.

We propose that increased moisture content in the atmospheric boundary layer over MC, due to the warmer SST, plays an important role in determining the MJO propagation to the western Pacific. Increased low level specific humidity over the MC could strengthen zonal gradient of moist static energy between the Indian Ocean and the Pacific Ocean, key for allowing a MJO propagation over the MC.

Analyses of SST responses to the MJO events over the MC reveal that SST is coupled to the MJO more during La Niña than El Niño. The peak-to-peak amplitude of the SST response (∂SST) is observed as large as 1°C during La Niña, compared to 0.5°C during El Niño despite of under the influence a similar MJO strength. It appears that the MJO-SST coupling is influenced by the thermocline depth, where deeper (shallower) thermocline strengthen (weaken) the coupling.

Acknowledgments, Samples, and Data

AMN acknowledges the Schlumberger Foundation, for the Faculty for the Future award. This research was funded by the National Oceanic and Atmospheric Administration (NOAA), Division of Climate Observations, U.S. Department of Commerce via grant UCAR Z15-17551. The statements, findings, conclusions, and recommendations are those of the authors and do not necessarily reflect the views of NOAA or the Department of Commerce. Lamont-Doherty Earth Observatory contribution number xxxx.

Chapter 4

Intraseasonal Relaxation of the Indonesian Throughflow

Submitted as: Napitu, A. M., Pujiana., K and Gordon, A. L. Intraseasonal Relaxation of the Indonesian Throughflow, Journal Of Physical Oceanography

Abstract The intraseasonal dynamics of the Indonesian Throughflow (ITF) are investigated using long-term observations of ITF variability in Makassar Strait in 2004 - August 2011 and August 2013 - August 2015. The ITF within Makassar Strait relaxes its mean southward flow mainly within the surface (< 80 m) layer. Seasonal and intraseasonal motions dominate the ITF relaxation in the surface layer, while semiannual and intraseasonal variations characterize the pycnocline layer. In the surface layer, the southward ITF attains its minima during boreal winter in response to the monsoon and the Madden-Julian Oscillation (MJO). Northward along-strait pressure gradient along with the vertical divergence between wind stress and turbulent stress at the base of the surface layer act to reduce or even reverse the southward ITF during strong MJO events. The maximum southward ITF resumes in boreal summer following the strengthening of southward pressure gradient.

4.1 Introduction

The Indonesian Throughflow (ITF), the flow of the Pacific water into the Indian Ocean via the Indonesian Seas, governs the exchange of heat and freshwater fluxes between these two basins, and hence plays of a substantial role to modulate the regional and global climate variability (Gordon, 2005; Sprintall et al., 2014). Observations at the ITF main passages in the Indonesian Seas indicate that the ITF variation demonstrates a broad-spectrum, encompassing timescales from intraseasonal to interannual (Gordon et al., 2003, 2012; Susanto et al. 2012; Sprintall and Revelard, 2014). On seasonal timescale, Indo-Australia monsoon affects the ITF that exhibits minimum (maximum) transport through boreal winter (summer). During the boreal winter monsoon months of December-February, northwesterly winds are dominant and drive buoyant South-China Sea (SCS) surface layer water into the Indonesia Seas, acting as a plug for the ITF transport within the upper 100 m of the water column (Gordon et al., 2012). In contrast, the opposite southeasterly winds prevailing over the course of the boreal summer monsoon (June-August) remove the plug. This seasonal variation of the ITF is sensitive to long-term, background conditions of regional climate such as El Niño Southern Oscillation (ENSO). Under an El Niño condition, more buoyant SCS water is flushed into the Indonesian Seas, strengthening the buoyant plug that further weakens the ITF (Gordon et al., 2012).

In addition to the seasonal signal, the ITF has significant intraseasonal (<90 days) variability (Pujiana et al., 2009; Drushka et al., 2012; Pujiana et al., 2013). Topographically trapped Kelvin waves, initially generated as equatorial Kelvin waves in the Indian Ocean, force 2-3 months variability at the outflow ITF passages such as

Lombok and Ombai Straits as well as in Makassar Strait, the ITF main inflow passage that accounts for 11 to 12 Sv of the total ITF of 15 Sv (Gordon et al., 2010). Shear-instability at the ITF core depth in the pycnocline, perturbed by planetary waves originating from the Western Pacific warm pool, generates the 1-month variability observed in Makassar Strait (Pujiana et al., 2012). Remote forcing also exerts influence on the sea surface variability at intraseasonal timescales in the broader Indonesian Seas. Madden Julian Oscillation (MJO; Zhang, 2013), a convective intraseasonal disturbance initiated in the tropical Indian Ocean and propagates eastward along the equator to circumnavigate the globe at an average speed of 3-9 m/s, dominates upper ocean processes on intraseasonal timescales in the Indonesian Seas as it traverses over the Maritime Continent (MC). Napitu et al. (2015) reported that the MJO exhibits seasonal variation over the MC, stronger (weaker) through boreal winter (summer). They also argued that MJO air-sea heat fluxes account for a significant fraction of intraseasonal sea surface temperature variances (SST) in the Indonesian Seas.

Despite MJO's ubiquitous imprint on SST over the Indonesian Seas, its impacts on the ITF variability have been less studied. The underlying processes dictating the ITF within the upper ocean over boreal winter, during which the MJO exhibits its strongest signature over the Indonesian Seas, are not completely addressed. In general, the dynamics regulating the ITF variability across the water column are still less understood. We, here, aim to describe the direct impact of the boreal winter MJO on the ITF within Makassar Strait, recurring synchronously with the occurrence of seasonal low-salinity SCS water to modulate the ITF transport within the upper layer.

The paper is organized as follows. Specifications of data used in this study are given in section 2. An overview of the ITF depth profiles and variations as well as the MJO over the MC is given in section 3. Section 4 describes physical processes pertinent to the ITF variability, particularly its attenuation or reversal, including an assessment of momentum budget in the upper layer to estimate the impact of the MJO on the ITF. Summary and discussion are given in section 5.

4.2. Data

We use the ITF time series of a mooring located at the main inflow pathway of the ITF in Makassar Strait (Fig.4.1), gathered during two observational programs: the International Nusantara Stratification and Transport (INSTANT) program from 2004-2006 and the Monitoring of the ITF (MITF) program spanning between 2007 - August 2011 and August 2013 - July 2015. Two moorings were deployed in Makassar Strait during INSTANT, but only the west mooring has remained operational under MITF (Fig.4.1). The scientific reason for maintaining a single mooring to monitor long-term variability of the ITF in Makassar Strait is because ~80% of the ITF transport is through Makassar Strait, and the two moorings deployed during the INSTANT program show that the ITF variability from those moorings are significantly correlated (Gordon et al., 2008, 2010). The reader is referred to Gordon et al. (2008, 2010) and Susanto et al. (2012) for detailed mooring configurations used during INSTANT and MITF.

We analyze current velocity data from a set of moored Acoustic Doppler Current Profilers (ADCPs), resolving zonal (u) and meridional (v) current velocity variability within the upper 450 m and through a period of 2004 - August 2011 and August 2013 -

August 2015. The data are gridded into a 25 m interval with depth and 1 hour resolution in time and subsequently low-pass filtered with a cut off frequency of 0.5 cycle day^{-1}, to remove tidal variation from the data. These filtered current vectors are then utilized to calculate the along channel (v*) and across channel (u*) flows. The along axis of Makassar Strait (y*) is oriented along 10^{o} relative from the true north.

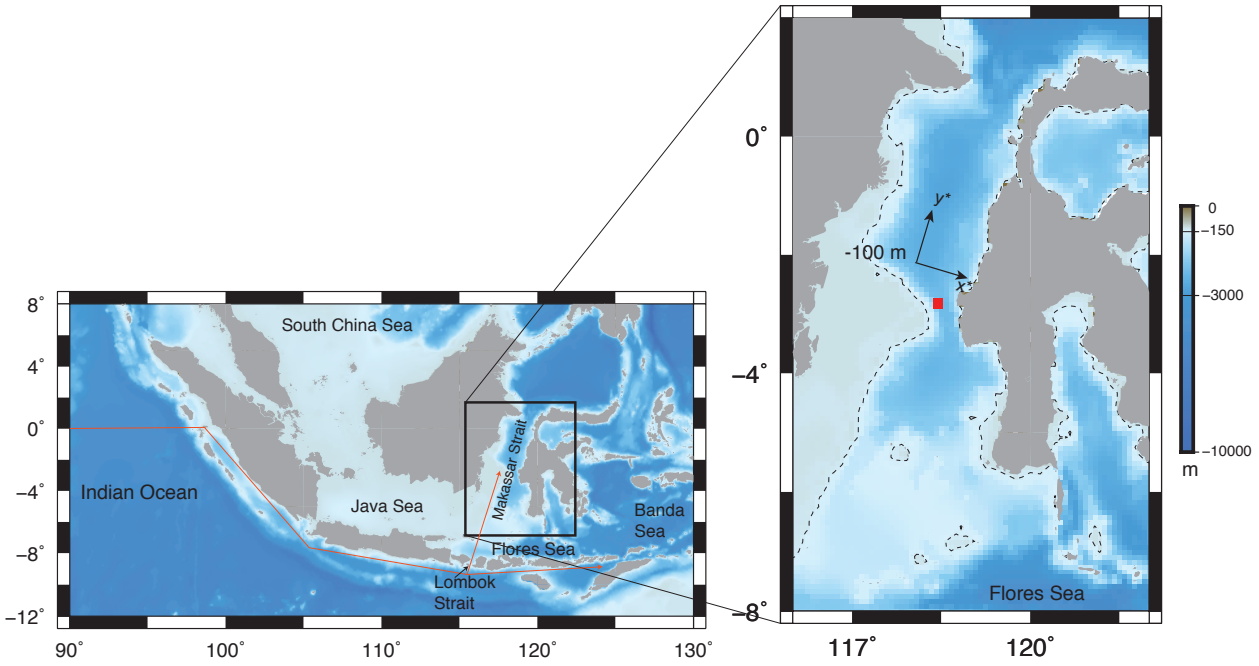

Figure 4.1. (Left panel) A map of Makassar Strait and the adjacent seas in the Indonesian maritime continent. Orange lines indicate the waveguide for a Kelvin wave propagating from the equatorial Indian Ocean to Makassar Strait. (Right panel) an enlarged version of the Makassar Strait map. Red rectangle indicates the INSTANT and MITF mooring location. Dashed contours indicate the 100 m isobaths. The along strait axis, y*, makes an angle of 10^{o} relative to the true north.

Remotely sensed and reanalysis data are also examined in this study. Altimeter satellite-derived sea surface height (SSH) data, a product of Archiving, Validation, and Interpretation of Satellite Oceanographic Data (AVISO) are examined (Ducet et al. 2000). The SSH data have a horizontal resolution of 0.25^o x 0.25^o and a temporal resolution of 7 days. In addition to the SSH, we use monthly average data of sea surface salinity (SSS) with a spatial resolution of 1^o x 1^o from the Level 3 Version 2 Aquarius Combined Active-Passive (CAP) product. As for the reanalysis data, we utilize TropFlux products (Kumar et al., 2012), consisting of gridded surface heat fluxes and wind stress data over the MC from 2004 to August 2015 with daily time resolution and a spatial resolution of 1^o x 1^o. We identify fundamental characteristics of the MJO over the Indonesian Seas, specifically in Makassar Strait, using wind stress and surface heat fluxes data. The SSH data are mainly used to explore the effects of the MJO on the ITF, while the SSS data are utilized to illustrate the seasonal signature of the monsoon and its influence on the ITF.

4.3. The Indonesian Throughflow

In this section, we will present mean and variations of the ITF in Makassar Strait, with a focus on the reduced (relaxed) ITF transport events due to seasonal and intraseasonal forcing. The ITF seasonal variability will be briefly discussed, extending previous studies of Gordon et al. (2008, 2012) and Susanto et al. (2012), by employing additional data observed in Makassar Strait between 2009 - 2011 and 2013 - 2015, which these studies did not analyze. Since the bulk of the ITF transport is in the along-strait

flow, we henceforth will focus our analysis to identify the reduced ITF events on the v^* component of the observed currents.

4.3.1 Seasonal Variability

The ~10 year long measurement of currents in the upper 500 m from a single sub-surface mooring in Makassar Strait reveals the ITF variability across a wide band of timescales. Vertical profiles of time-average v^* show that the southward throughflow attains its maximum at 100 m (Fig.4.2a), consistent with the result reported by Gordon et al. (2008) and Susanto et al. (2012). Seasonal variation of the ITF, maximum during boreal summer (June-July-August [JJA]) and minimum during boreal winter (December-January-February [DJF]), is also well resolved although our observations capture a weaker ITF during boreal winter in the upper 100 m compared to that documented by Susanto et al. (2012) (.2a). This attenuated ITF during boreal winter, weaker than what has been previously presented, is likely due to anomalously strong northward flow in the surface layer through December 2010 - February 2011 and December 2014 - February 2015 (Fig.4.2d).

Given the intricate depth structure of the ITF, we analyze the ITF variability based on three depth regimes (1) surface layer (< 80 m), where monsoon winds cause a strong influence; (2) energetic southward ITF layer between 80 and 150 m, defined as the depth with southward v^* of < - 0.6 ms^{-1}; (3) lower pycnocline layer (>150 m). The pycnocline depth in Makassar Strait extends between 80 - 450 m. The mean base of the surface layer is about 80 m, and is estimated from the local Ekman depth (d) at our

mooring location, defined as $d = 0.4(\frac{\tau}{\rho})^{0.5}/f$ $\mathrm{d} = 0.4\frac{(\tau/\rho)^{0.5}}{\mathrm{f}}$, where τ is wind stress (Fig.4.2c), ρ is seawater density, f is the local Coriolis acceleration.

Time-series of v^* averaged in the upper 80 m demonstrates that the surface layer ITF is on average directed to the south with a mean velocity of -0.53 ± 0.14 ms^{-1} (Fig.4.2d). The surface southward ITF is reduced during boreal winter, responding to the monsoon winds (Figs.4.2c, d). Northwest monsoon wind stresses (positive zonal wind stress τ_x and negative meridional wind stress τ_y) during boreal winter drive less salty, more buoyant SCS water via the Java Sea into the Flores Sea, resulting in a northward pressure gradient in the surface layer within Makassar Strait (Gordon et al., 2003, 2012). In contrast, the ITF registers maximum southward velocity in the surface layer during boreal summer in response to the prevailing southeast monsoon winds removing the northward pressure gradient (Figs.4.2c, d). This seasonal pattern is well demonstrated by the climatological mean of v^*, obtained from daily averages over the course of 2004 - 2011 and 2013 - 2015 (Fig.4.2d).

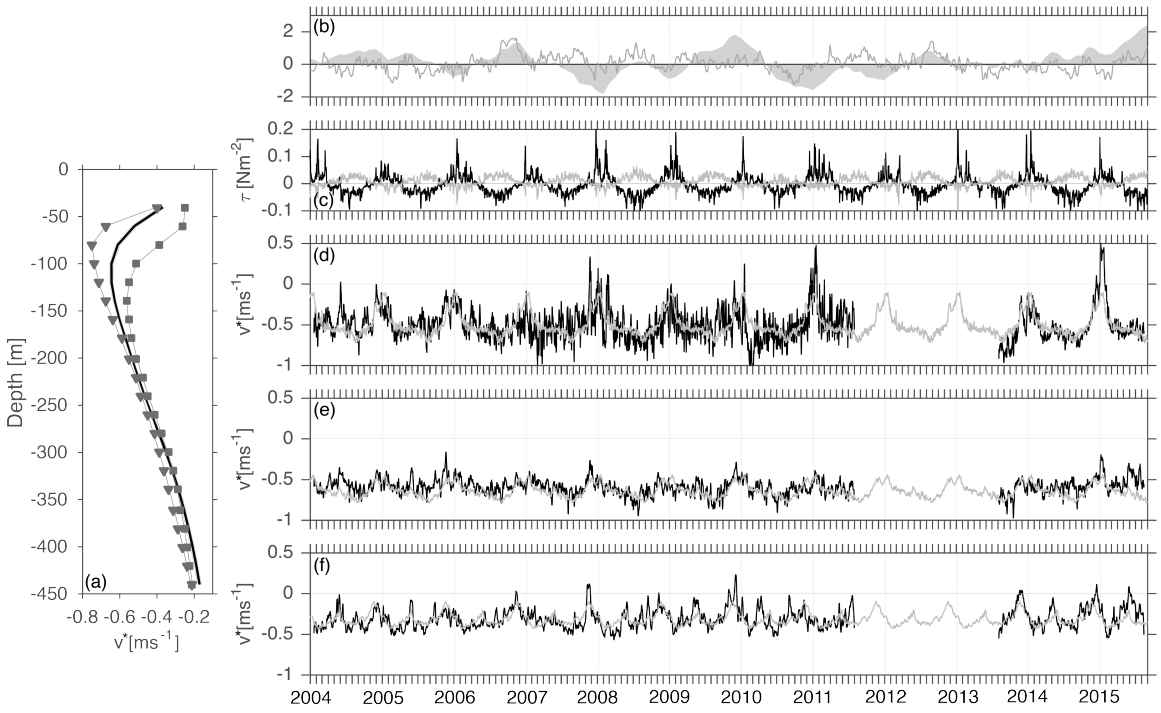

Figure 4.2. (a) Time-average of v^* time series for DJF (rectangle), JJA (triangle) and all months (solid line) observed in Makassar Strait between 2004 - August 2015. (b) Nino3.4 (shaded) and dipole mode (gray curve). (c) τ_x (black) and τ_y (gray). Positive τ_x (τ_y) indicates eastward (northward) wind stress. Depth - average of v^* averaged between (d) the surface and 100 m, (e) 100 - 250 m, and (f) 250 - 450 m. Positive v^* indicates northward along-strait velocity. Gray curves in (d), (e) and (f) indicate the climatological mean consisting of daily averages extending through the whole period of observation for each respective figure.

Recent satellite-derived SSS, SST and SSH data clearly illustrate the relation between the monsoon and seasonal variation of the ITF. The SSH data demonstrate that southward along-strait pressure gradient in Makassar Strait is reduced during the northwest monsoon/DJF and elevated during the southeast monsoon/JJA (Fig.4.3a). Consistent with the result of Gordon et al. (2003), the reduced southward pressure gradient in DJF is linked to buoyancy gain observed in the southern Makassar Strait following fluxes of less buoyant SCS water (Fig.4.3b). Figure 3b shows that SSS in Java Sea and southern Makassar Strait is fresher during DJF than JJA. SST in the southern Makassar Strait also shows seasonal variation favorable for reduced southward pressure gradient in Makassar Strait, warmer during DJF than JJA (Fig.4.3c). This combined influx of less buoyant and warm water into the southern Makassar Strait reduces the along-strait southward pressure gradient and thus weakens the throughflow.

The Makassar Strait v^* time series shows that surface layer variability of the ITF responds not only to seasonal forcing but also to interannual and intraseasonal forcing. On interannual timescale, Gordon et al. (2012) and Sprintall et al. (2014) argued that the southward ITF in Makassar Strait is enhanced (reduced) during La Niña (El Niño). Pronounced El Niño events occurred in late 2006, 2009, and in 2015, which were subsequently followed by strong La Niña events (Fig.4.2b). Milder El Niño events were observed in 2004 and 2014. Over the Indian Ocean, a positive (negative) dipole mode events in late 2006 (2010), coinciding with a strong El Niño (La Niña), occurred during our observational time frame. We reckon that the impact of intraseasonal variability is more pronounced than the interannual variation on the ITF within the surface layer in Makassar Strait. The importance of intraseasonal variation can be identifiable from the

discrepancy between the climatological mean and observed velocity, demonstrating that monthly variation enhances the effect of seasonal forcing to weaken the southward ITF during boreal winter (Fig.4.2d).

Unlike the surface layer, time-series of v^* in the lower pycnocline layer does not reveal seasonal variation. It instead exhibits semiannual variation characterized by the southward ITF minima in May and November, during which the observed v^* differs from the climatological mean the most (Fig.4.2f). In addition to the semiannual variation, the lower pycnocline ITF variability is also marked with intraseasonal variation, 1-3 month fluctuations (Fig.4.2f). Both the semiannual and intraseasonal variations reduce the southward ITF in the lower pycnocline layer, and the variations are attributed to Kelvin waves penetrating from the Indian Ocean into Makassar Strait (Sprintall et al., 2000; Pujiana et al., 2013). Sprintall et al. (2000), using Makassar Strait data observed between 1996 -1998, suggested that the Kelvin wave's influence to weaken the southward ITF in the lower pycnocline is more apparent during an El Niño phase. Our longer measurements reveal that substantial reduction of the southward ITF due to Kelvin waves can occur during either a strong El Niño phase or a significant La Niña episode. For example, the southward mean flow in the lower thermocline was turned northward by a Kelvin wave in late 2007, coinciding with a strong La Niña phase. The details of these intraseasonal and semiannual variations will be discussed below.

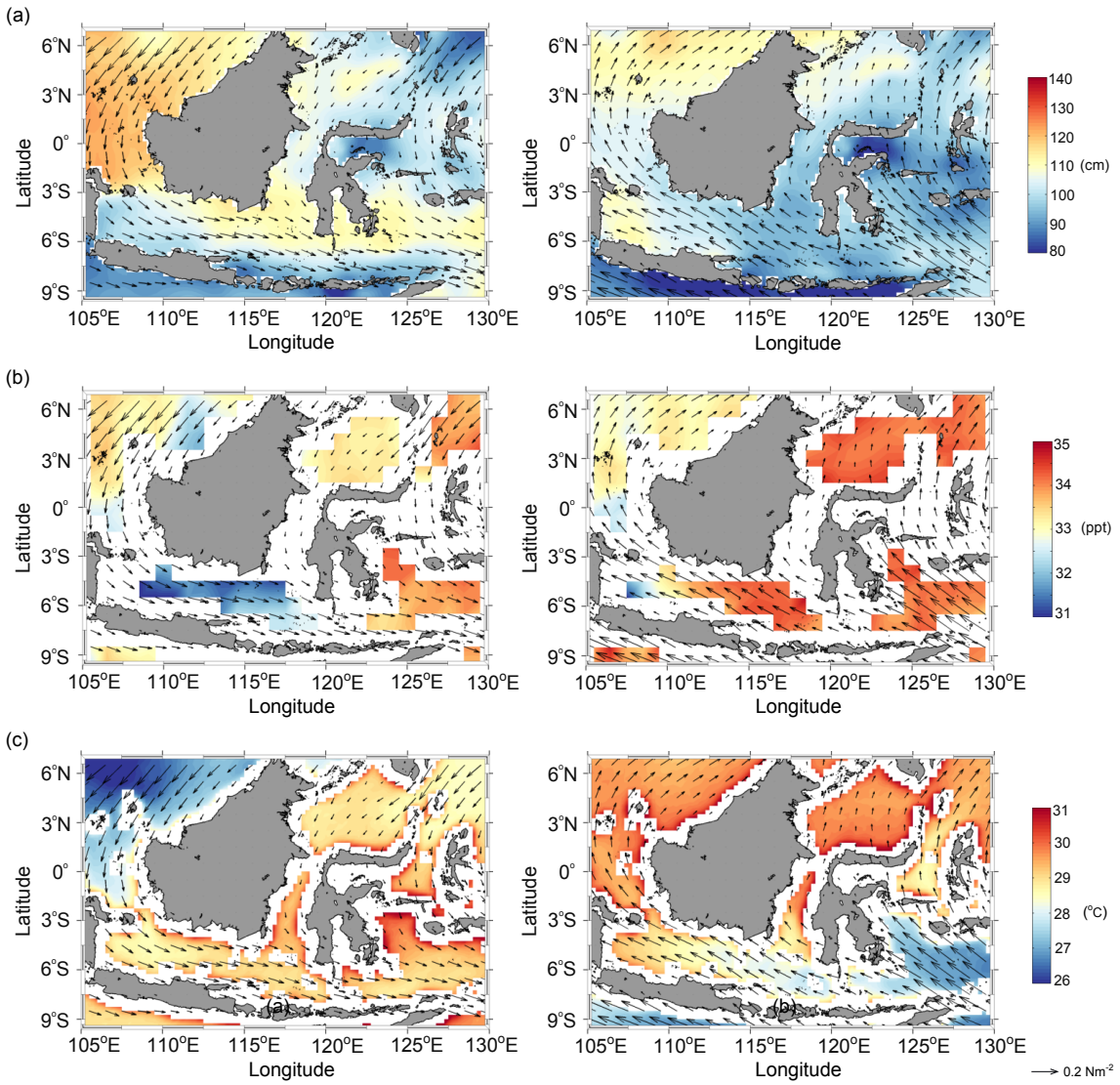

Figure 4.3. (a) Sea surface height [SSH] averaged during boreal winter (left panel) and summer (right panel). (b) Sea surface salinity [SSS] averaged during boreal winter (left panel) and summer (right panel) (c) Sea surface temperature [SST] averaged during boreal winter (left panel) and summer (right panel). Arrows denote wind stress.

4.3.2 Non-Seasonal Variability

4.3.2.1 Surface ITF Variability

We have shown that the southward ITF within the Makassar Strait surface layer displays a seasonal cycle. The ITF attains its minimum southward velocity during boreal winter. Furthermore, the seasonal relaxation is strongly modulated by intraseasonal forcing which acts to further weaken the southward ITF or reverse the throughflow northward. Napitu et al. (2015) reported that the MJO exhibits its strongest signature on sea surface winds over the Indonesian Seas during boreal winter. Zhou and Murtugudde (2010); Pujiana et al. (2013) argued that the MJO over the Indian Ocean affects the ITF variability only in the lower pycnocline layer, away from the surface. We here will show that boreal winter MJO events passing over the MC directly influence the ITF within the Makassar Strait surface layer.

There are 16 MJO events passing over the MC registered in the boreal winter months through our observational period as indicated by significant real-time multivariate index (>1) (Fig.4.4a). Each MJO event is characterized by suppressed and active phases. The active phase of each of these MJO events is marked with reduced net surface heat flux, J_q^0 (< 0) and strong westerly winds, τ_x (> 0.1 Nm^{-2}) (Figs.4.4b, c). These MJO wind bursts are concurrent with the background northwesterly monsoon winds (Fig.4.4c). Note that the MJO is not as evident in τ_y, as is in τ_x. As a response to the MJO westerly wind bursts, the surface southward ITF is attenuated and even turned northward on some occasions (Fig.4.4d). For example, seasonally weakened southward ITF during December 2007 - February 2008 (D07F08), appears to be further reduced and then turned northward by three MJO events (Fig.4.4d). Nevertheless, our observations also suggest that

significant MJO passages do not always translate into notable modification of the surface ITF variability. The minimal impact of a significant MJO event on the ITF is evident in December 2004 - February 2005 (D04JF05), during which the surface v^* variability in Makassar Strait does not differ substantially from its annual mean (Fig.4.4d). It appears that the D04JF05 event does not induce pronounced westerly peaks strong enough to cause northward flow in the surface layer, distinguishable from seasonally-driven northward flow (Figs.4.4c, d).

To provide a statistical estimate of the link between the MJO and the surface ITF variability, we analyze the degree of coherence between τ_x and v^* averaged in the upper 80 m. Our analyses show that both τ_x and v^* are significantly coherent on intraseasonal timescales particularly during boreal winter, indicating the MJO westerly wind burst might account for the observed reduced surface layer ITF (Fig.4.4e). Figure 4e illustrates that significant coherence between τ_x and v^* mostly occurs in DJF and on timescales of 1-3 months. For example, v^* associated with events of reduced southward ITF during D07JF08 shows a significant coherence with strong westerly winds attributed to MJO events on timescales of 2 months (Fig.4.4e).

As discussed above, a strong MJO event does not always coincide with weakened southward surface layer transport. The average westerly wind stress attributed to the D07JF08 MJO event (RMM = 1.6), $\tau_x = 0.05$ Nm^{-2}, is twice as strong as that associated with the December 2014 - February 2015 (D14JF15) MJO event (RMM = 1.2). Nevertheless, the surface layer ITF response to the D07JF08 MJO event is less energetic than that to the D14JF15 MJO event. This may imply that a linear relationship between

the strength of a MJO event and the surface layer ITF response does not hold and exemplify other ocean processes governing the near surface ITF variability.

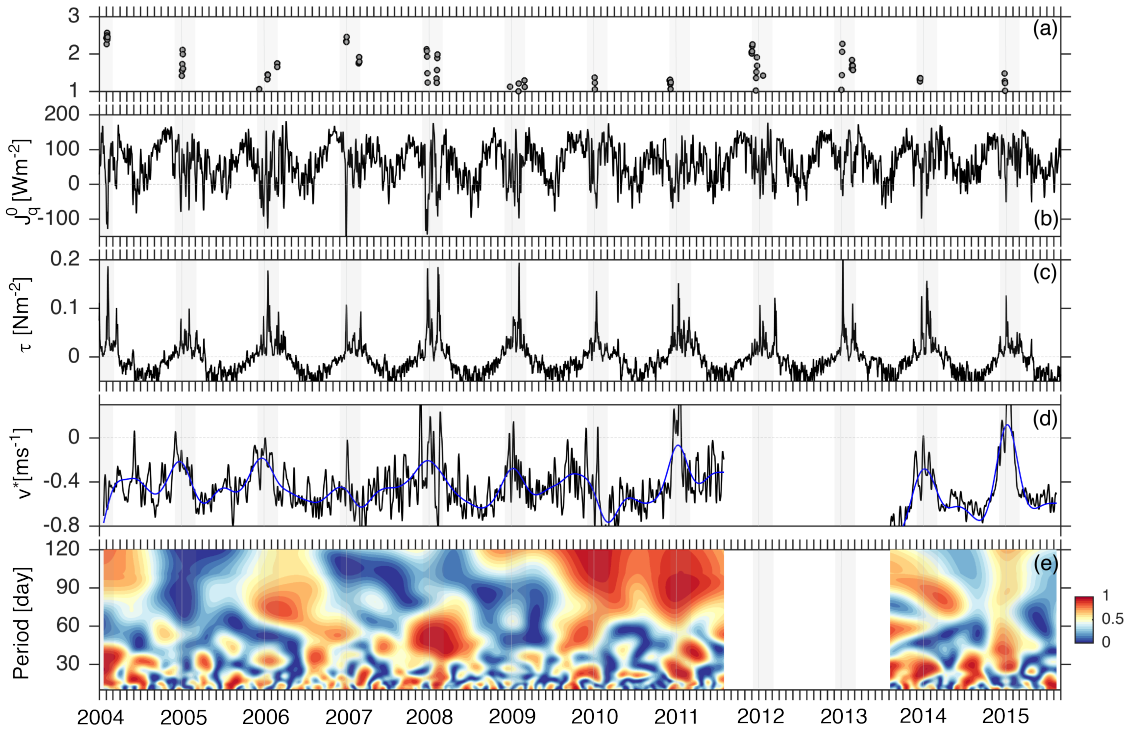

Figure 4.4. (a) Real-time multivariate indices at phase 4 indicating the strength of the MJO over the western-central MC. (b) J_q^0. (c) τ_x (black) and τ_y(gray). Positive τ_x (τ_y) indicates eastward (northward) wind stress. (d) v^* averaged between the sea surface and 100 m. Black curve demonstrates the 3-day low passed v^*, while blue curve shows the 120-day low passed v^*. Positive v^* indicates northward along-strait velocity. (e) Amplitude of wavelet coherence between (c) and (d). Gray shaded vertical bars mark the boreal winter months.

To further illustrate oceanic response in the Makassar Strait surface layer to MJO events, we compute composites of v^*, J_q^0, and τ_x measured within the upper 100 m for some select strong MJO events (RMM >1.6). Of 16 MJO events recorded during our observational period, there are 10 events with RMM >1.6. The composites of v^*, J_q^0 , and τ_x, attributed to these strong MJO events, indicate that the active phase of the MJO in Makassar Strait is marked with J_q^0 that becomes negative, the ocean loses heat into the atmosphere, and rapid strengthening of westerly wind stress in a way that the wind stress attains its strongest magnitude at the same time as the surface heat flux reaches its minimum (Figs.4.5a, b). It takes about ~10 days for both J_q^0 and τ_x of the MJO to reach their peak values over the Makassar Strait (Figs.4.5a, b). The surface layer response to the acceleration of the westerly wind stress is the formation of v^* directed northward within the upper ~80 m, flowing against the background southward ITF at deeper depth (Fig.4.5c). The maximum northward flow near the surface lagged the strongest westerly wind stress by a few days such that it occurs over a period when the wind stress is substantially reduced and surface heat flux resumes to be positive (Figs.4.5a-c).

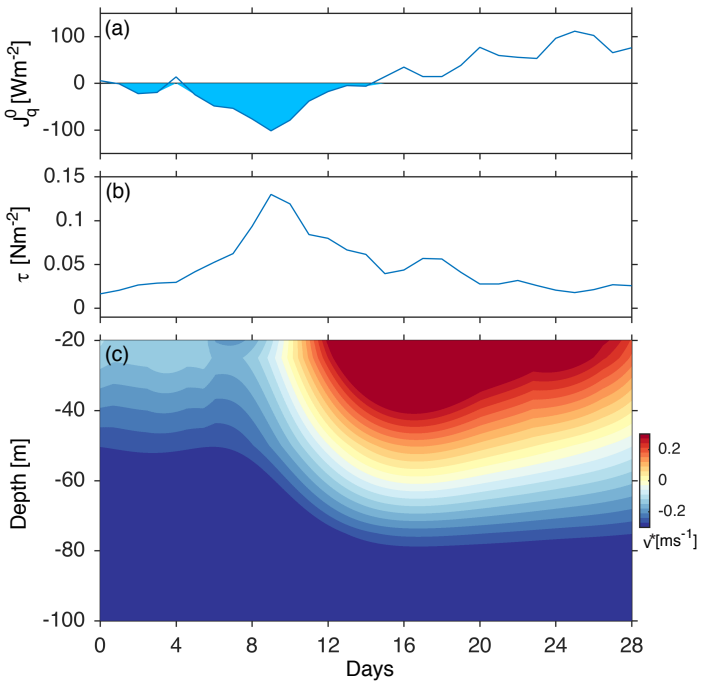

Figure 4.5. Composites of (a) J_q^0, (b) τ_x, and (c) v^* for 10 MJO events with RMM amplitude >1.6 observed during boreal winter of 2004 - 2015. Positive τ_x indicates eastward wind stress. Positive v^* indicates northward along-strait velocity.

Other evidence supporting the connection between the MJO and the relaxation of the ITF in Makassar Strait during boreal winter is that the surface layer ITF variability displays larger variance in DJF than in JJA. Distributions of the variance of the surface layer v^* anomalies, relative to the climatological mean, indicate that large variance of the surface layer v^* anomalies occurs more frequently in boreal winter than in boreal summer (Fig.4.6). This seasonal contrast is consistent with the MJO signature over the MC, more energetic in boreal winter than in boreal summer (Napitu et al. 2015).

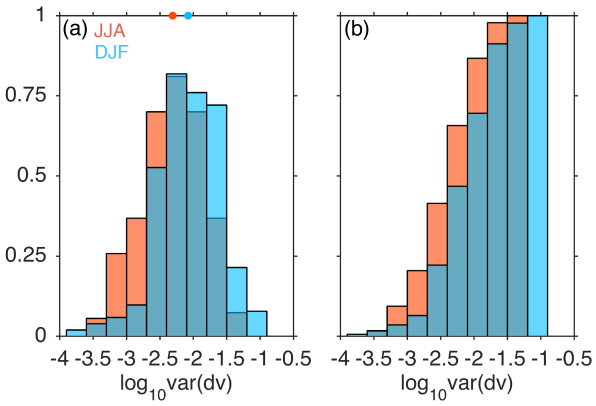

Figure 4.6. Probability distribution function (a) and cumulative distribution function (b) of variance of the difference between observed v^* and its climatological mean obtained from daily averages through 2004 - 2011 and 2013 - 2015.

4.3.2.2 Deep ITF Variability

As in the surface layer, the ITF variability within the lower pycnocline layer is generally directed southward but displays frequent changes in speed (Figs.4.7a, b). The magnitude of the southward background flow in the lower pycnocline layer varies on average in a range of -0.23 ± 0.15 ms^{-1}, and it is reduced on time scales ranging between 1 - 3 months to semiannual (Fig.4.7c). Over the course of the Makassar Strait time series (2004 - August 2015), we document 41 events during which the observed southward ITF in the lower pycnocline layer is weakened by 0.2 - 0.5 ms^{-1}, relative to its average magnitude. Its recurrence is energetic particularly in the months of May and November (Fig.4.7). Moreover, the ITF regularly turns northward in these months over the developing period of a strong 2015 El Niño (Figs.4.7a, b, and 2b).

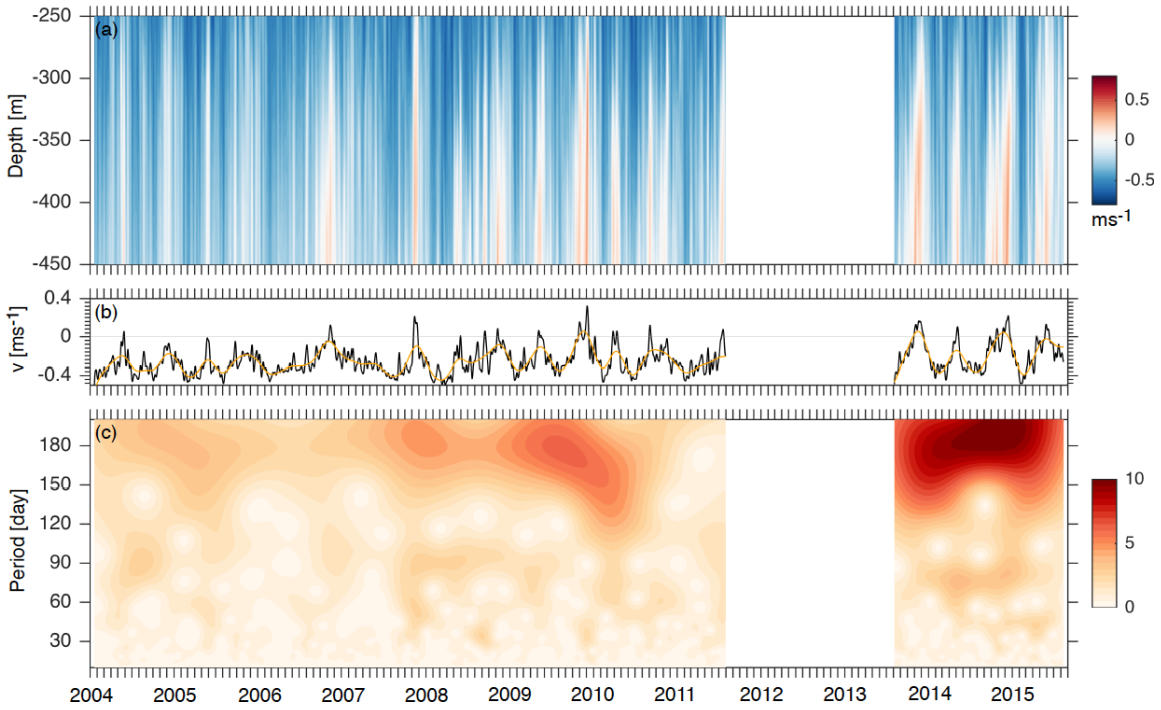

Figure 4.7. (a) Time-depth plot of v^* time series observed in Makassar Strait between 250 - 450 m between 2004 - August 2015. (b) Time series of depth-average of (a). Positive sign indicates northward along-strait flow. Orange curve shows the low-passed time series with a cut off frequency of 0.0067 cycle day^{-1}. (c) The local wavelet power spectrum of (b) using the Morlet wavelet.

Composites of v^* attributed to the ITF relaxation in May and November on semiannual timescales show a tendency of upward phase propagation, with a phase speed of 10 - 25 m day^{-1} (Fig.4.8). It appears that the May and November composites are asymmetric, as the November events tend to be more energetic at a slower vertical phase propagation speed than those in May. Notable contribution of intraseasonal variability to modulate the ITF is also evident (Fig.4.7b). It, along with the semiannual, reduces or

reverses the southward ITF across the lower pycnocline. Weakened southward ITF events on intraseasonal timescales occur through the time series, but most frequently in May and September (Fig.4.9). Seasonally, boreal summer monsoon registers more reduced southward ITF events than boreal winter monsoon.

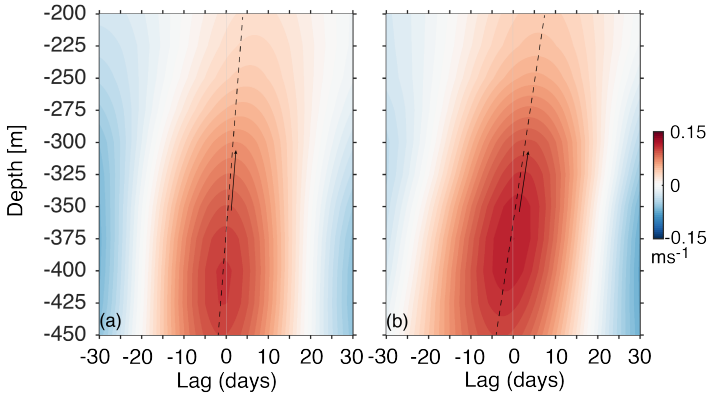

Figure 4.8. Composites of band-passed v^* observed in May (a) and November (b) between 250 - 450 m between 2005 - August 2015 in Makassar Strait. A band pass filter with cut off frequencies of 0.0042 cycle day-1 and 0.0083 cycle day^{-1} is applied. Dashed lines and arrows indicate a tendency of upward phase propagation. Positive v^* indicates northward along-strait flow, while negative v^* indicate southward along-strait flow.

Composites of v^* attributed to the intraseasonal events demonstrate a more intricate vertical structure than that associated with the semiannual events. Unlike the semiannual events that show continuous upward tilt across the lower pycnocline, the intraseasonal ones generally exhibit upward phase propagation between 250 - 450 m and a tendency of downward phase propagation at depth shallower than 250 m (Fig.4.10). Moreover, the phase tilt attributed to the intraseasonal events indicates faster upward propagation speed (particularly in May), varying between 70 - 110 m day^{-1}, about 5 times faster than the vertical propagation speed of the semiannual events (Fig.4.10).

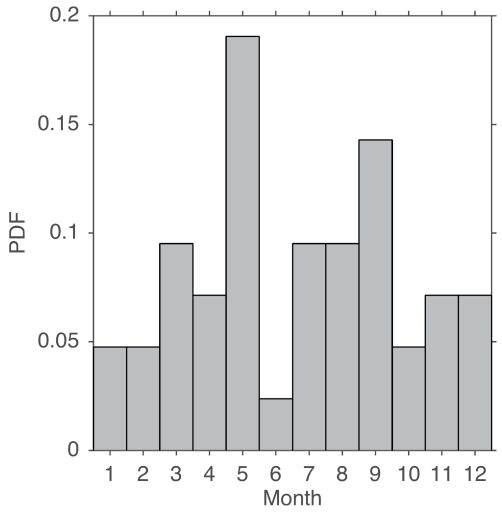

Figure 4.9. Probability distribution function of the month attributed to the ITF relaxation events inferred from v^* on intraseasonal timescales averaged between 250 - 450 m in Makassar Strait

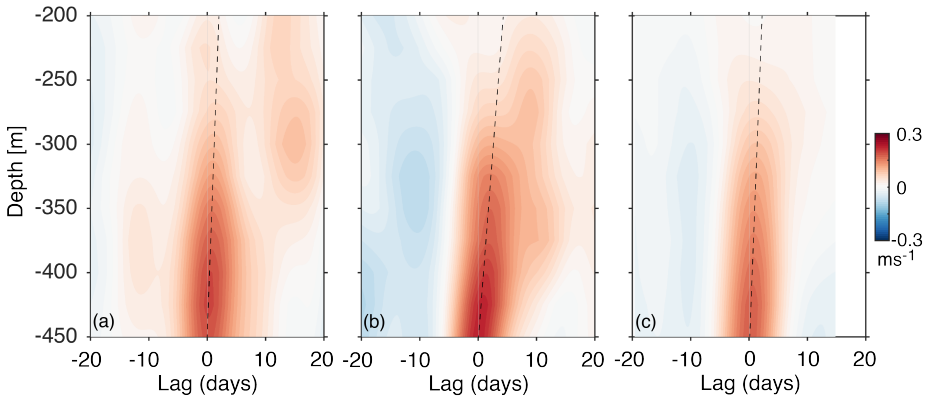

Figure 4.10. Composites of band-passed *v** observed in May (a) September (b), and in other months across 250 - 450 m between 2004 - August 2015 in Makassar Strait. A band pass filter with cut off frequencies of 0.1 cycle day^{-1} and 0.0083 cycle day^{-1} is applied. Dashed lines indicate a tendency of upward phase propagation. Positive *v** indicates northward along-strait flow, while negative *v** indicates southward along-strait flow.

4.4. Dynamics of the ITF on intraseasonal variations

a. Momentum budget in the surface layer

To estimate the role of non-seasonal forcing to regulate the ITF relaxation within the surface layer, we analyze the along-strait momentum budget using a simplified equation for horizontal momentum conservation integrated between two depths, h_1 and h_2. The equation is given as follows:

$$\frac{\partial \overline{v^*}}{\partial t} = -\beta \Delta y \overline{u^*} - g\frac{\partial \eta}{\partial y^*} + \frac{\tau_x sin\gamma + \tau_y cos\gamma}{\rho\,(h_2 - h_1)} - \frac{k_z}{\rho\,(h_2 - h_1)}\frac{\partial v^*}{\partial z} + R, \qquad (1)$$

where $\overline{v^*}$ is vertically averaged along-strait flow, $\overline{u^*}$ is vertically averaged across-strait current, β is the variation of Coriolis parameter with latitude, Δy is the meridional

distance from the equator of the mooring, g is gravity acceleration, η is sea level anomaly, γ is the angle between the true north and the along-strait axis, τ_x is zonal wind stress, τ_y is meridional stress, k_z is vertical diffusivity, and ρ is the background density set equal to 1023 kg m^{-3}. We assign a canonical value of 10^{-4} m^2s^{-1} for the vertical diffusivity. The first term on the right-hand side of (1) expresses the Coriolis force. The second term denotes momentum component due to the along-strait pressure gradient, the third represents momentum transferred from the along-strait wind stress, and the fourth indicates momentum associated with the Reynolds stress at the base of the surface layer. R contains terms that our measurements do not resolve including advection of sheared along-strait flow and errors associated with the measurements. Low-pass filtered data (tidal oscillations are removed) are used to examine momentum budget within the surface layer, and the examination is focused on three distinct periods: typical DJF with insignificant MJO, DJF with strong MJO, and JJA.

For the typical winter months with no MJO case, surface layer momentum budget indicates that momentum from wind stress counteracts southward pressure gradient to yield northward along-strait acceleration (Fig.4.11a). The residual term substantially contributes to accelerate the mean surface layer flow northward since the southward momentum transfer from the pressure gradient force exceeds that from the northward along-strait wind stress. The northward surface layer acceleration over the MJO-less DJF period is in contrast to the southward surface layer acceleration in JJA (Figs.4.11a, c). The southward acceleration observed in the surface layer during boreal summer is mainly driven by the along-strait pressure gradient, whose southward momentum transfer is over the northward momentum input from the wind by a factor of 2. Further contrasting the

momentum budget in DJF and JJA, we reckon that momentum input due to the along-strait pressure gradient in JJA is about three times more energetic than in DJF (Figs.4.11a, c). This suggests that the southward pressure gradient is maximum in JJA and significantly reduced in DJF. Our quantitative result confirms previous studies that qualitatively relate the reduced southward pressure gradient, due to monsoon-driven buoyancy input, to weakened southward ITF in the surface layer during boreal winter.

Momentum balance for the MJO case illustrates that northward momentum from wind stress and pressure gradient exceeds southward momentum due to the residual and subsurface turbulence which thereby accelerates the surface layer northward (Fig.4.11b). The surface layer is accelerated northward over strong MJO events during DJF at a rate twice the northward acceleration rate observed during the DJF with no MJO period (Figs 11a, b). In contrast to the southward acceleration observed in the DJF with no MJO period, along-strait pressure gradient under the influence of the MJO causes northward acceleration in the surface layer. Furthermore, wind stress transfers more momentum to accelerate the surface layer northward during strong MJO periods. Note that the contribution of subsurface turbulence to decelerate northward along-strait flow in the surface layer is also increased during strong MJO periods.

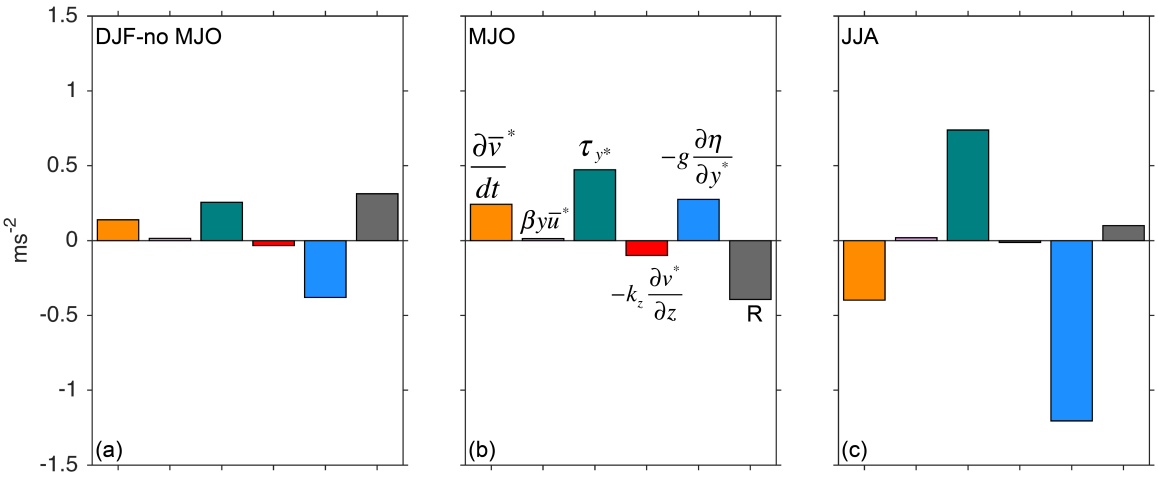

Figure 4.11. The mean magnitude of each term of momentum equation constituting momentum budget within the upper 80 m in Makassar Strait averaged over (a) DJF with no MJO, (b) significant MJO events during DJF, and (c) JJA observed during 2004 - 2015. Orange bars indicate along-strait acceleration, magenta bars denote Coriolis force, green bars express momentum transferred from along-strait wind stress, red bars indicate momentum transfer due to Reynolds stress at 80 m, blue bars show momentum input from along-strait pressure gradient force, and grey bars account for the residual. Positive (negative) values indicate northward (southward) along-strait acceleration.

4.5 Summary and Discussion

We have identified and analyzed physical process regulating the relaxation of the ITF, inferred from observations within Makassar Strait between January 2004 - August 2011 and August 2013 - August 2015. Long-term observations in Makassar Strait allow identification of the climatological mean of the ITF within the surface and pycnocline layers. They confirm earlier research based on shorter time series (Gordon et al. 2003; Susanto et al. 2012; Pujiana et al. 2012): The seasonal signal is dominant from the surface to the upper pycnocline, marked with maximum (relaxed) southward ITF during boreal summer (winter). A simple quantitative assessment of momentum balance in the surface layer demonstrates that the evolution of the southward ITF from its peak during boreal summer to its minima during boreal winter is predominantly controlled by the strength of the southward along-strait pressure gradient, which is substantially weakened during boreal winter. In the lower pycnocline layer, semiannual oscillation is evident, characterized by the southward ITF minima in May and November. The observations also reveal the impact of intraseasonal oscillations on the reduced southward ITF:

- Surface Layer: Weakened southward-directed ITF in the upper 80 m of Makassar Strait during boreal winter displays impact of the MJO on 1-3 months timescales. The MJO weakens or reverses the southward along-strait pressure gradient during boreal winter and increases northward momentum transfer from wind stress. The northward acceleration yields substantial reduction of the surface layer southward transport on many occasions inducing the ITF total transport northward. Increased turbulent stress at the base of the surface layer acts to decelerate the anomalous

northward ITF during MJO events. This result provides a new insight into the direct impact of the MJO on the relaxation of the ITF during boreal winter.

- The dynamic response of the surface layer ITF to the MJO has been investigated with a numerical experiment between fall 2010 and spring 2011 (Shinoda et al., 2016). They suggest that the surface layer in Makassar Strait responds to a MJO forcing by generating northeastward current, which contributes to the reduction of the southward along-strait flow in Makassar Strait. Although a quantitative assessment on factors controlling the northeastward current was not presented in their analyses, their results are in agreement with ours. Our momentum balance computation indicates that the residual term may play an important role in dictating the surface layer dynamic under the MJO. In the equatorial Indian Ocean, the upper ocean responds to a passage of the MJO through the formation of a strong eastward current, and the dynamic of the eastward jet is mainly controlled by wind stress, subsurface turbulence, and advection of momentum (Pujiana et al., 2017). As in the equator, the role of Coriolis to regulate motions in the surface layer appears to be negligible in Makassar Strait as well. Thus, nonlinear terms such as along-strait advection of momentum might form the residual component of the surface layer response to the MJO in Makassar Strait. A more extensive approach, involving a coupled ocean-atmosphere general circulation model, is required to quantitatively examine how each term of the

equation of motion regulates the surface layer response to the MJO in Makassar Strait.

- In addition to reducing the southward throughflow, the MJO-driven current also substantially alters the meridional SST gradient along the Makassar Strait. Shinoda et al. (2016) indicated that a meridional SST gradient is set up along the Makassar Strait following through the MJO cycle, where the southern Makassar Strait was observed colder than its northern part. Colder SST in the southern Makassar Strait and Flores Sea might, however, be a product of more intense MJO air-sea interaction in that particular area than over the northern Makassar Strait. Napitu et al. (2015) showed that upward net surface heat flux attributed to the MJO wind during boreal winter cools the SST in the Indonesian Seas, particularly those located in the southern hemisphere. It is also possible that subsurface turbulent mixing, triggered by increased instability due to northward flow near the surface overlying southward flow at deeper depth, might promote downward heat transfer leading to colder SST in Makassar Strait.
- Quantifying competing processes, from advection to subsurface turbulent mixing to air-sea heat flux, that regulates SST along the ITF pathways or the Indonesian Seas in general during the MJO is an open question. Nevertheless, we suspect that colder and smaller transport into the Indian Ocean might be the net effect of the MJO on the ITF. Our Reynolds stress estimate, function of a canonical value of vertical diffusivity and vertical

shear of observed currents, at the base of the surface layer indeed indicates that subsurface mixing is enhanced during MJO. The vertical diffusivity constant, $k_z = 10^{-4}$ m^2s^{-1}, we choose for estimating the subsurface turbulent stress is based on an indirect estimate reported in Ffield and Gordon (1996). Ongoing moored mixing measurement is currently in place to document long-term mixing data in Makassar Strait, and we will use the mixing data to validate our present estimates and report the results for a future work.

Acknowledgements We are grateful for continuing support from the Ministry of Marine Affairs and Fisheries of the Republic of Indonesia to maintain and service the Makassar Strait mooring. AMN acknowledges the Schlumberger Foundation, for the Faculty for the Future award. This research was funded by the National Oceanic and Atmospheric Administration (NOAA), Division of Climate Observations, U.S. Department of Commerce via grant UCAR Z15-17551. The statements, findings, conclusions, and recommendations are those of the authors and do not necessarily reflect the views of NOAA or the Department of Commerce. Lamont-Doherty Earth Observatory contribution number xxxx.

Chapter 5

Summary and Future Work

My dissertation discusses the impacts of the Madden-Julian Oscillation [MJO], a prominent atmospheric forcing at intraseasonal timescales originating from the Indian Ocean, on the dynamics of the Indonesian Seas from the surface to the ocean interior. Using satellite, reanalysis and mooring data, I have identified and described major MJO impacts on variability in the Indonesia Seas. The sea surface temperature (SST) of the Indonesian Seas, particularly of Banda and Timor Seas, demonstrates a clear coupling with the MJO convective system when passing the Maritime Continent [MC]. The MJO influences the SST both directly through air-sea fluxes and indirectly by modifying oceanic process.

In this study, I also attempt to understand whether the Indonesian Seas act as a passive component in the MJO air – sea interactions or could actively provide feedbacks to the atmospheric boundary layer affecting the MJO propagation over the MC. To explore plausible contributions of the Indonesian Seas SST to set a favorable precondition for the MJO to propagate over the MC, I analyze satellite-derived SST and reanalysis surface heat fluxes data in the Indonesian Seas during the suppressed phase for all MJO convective events in the Indian Ocean documented between 1980 - 2012. Although the dynamical explanation remains elusive, it appears that warmer SST across the Indonesian Seas promotes more eastward propagation events of the MJO over the MC.

One of the most important features effecting the Indonesia Seas dynamics is the Indonesian Throughflow (ITF), the transfer of the Pacific water to the Indian Ocean. The ITF is an important component that regulates the heat and freshwater budgets of the Pacific and Indian Oceans such that it is fundamental to fully understand its variability. Analyses of the ITF variability in Makassar Strait, the most important ITF inflow passage in the Indonesian Seas, indicate that the MJO plays an important role to modulate seasonal variation of the ITF.

The main results of this study are summarized as follows.

- The intraseasonal variability accounts for 18% of the total SST variations in the Indonesian Seas, and the intraseasonal SST variances are observed largest in Banda, Timor and Sulawesi Seas. Energy peaks centered at 35 days, 25 days, and 56 days characterize intraseasonal SST in Banda, Timor, and Sulawesi Sea respectively.
- The intraseasonal SST signals in Banda and Timor Seas show seasonal variation, stronger during the northern hemisphere winter months (December-January-February/DJF) and weaker in the summer months (June-July-August/JJA). No seasonal variation is identifiable from intraseasonal SST in Sulawesi Sea.
- MJO air-sea heat fluxes account for 75% of the intraseasonal SST variability in Banda and Timor Seas as indicated by a slab ocean model.
- The MJO footprint on the SST is evident in Banda and Timor Seas over the period of MJO propagation over the MC. Through the MJO suppressed phase, the SST build up is evident in response to intense solar radiation characterizing this particular MJO phase. When the active convective system sets in, the SST rapidly

decreases following the imbalance between reduced solar radiation and increased latent heat transfer to the atmosphere in response westerly wind bursts.

- Despite its significant variance, intraseasonal SST in Sulawesi sea is independent from the MJO and exhibits different characteristics from that observed in Banda and Timor Seas. It shows no significant correlation with MJO air-sea heat fluxes and seasonal variability. Eddies and local winds predominantly control intraseasonal SST variability in Sulawesi Sea.

- Over the course of 1980 - 2012, 51 of 86 MJO events manage to make a complete eastward propagation, from the Indian Ocean into the Pacific Ocean, while 35 events discontinue in the eastern Indian Ocean, or show no propagation (NP) over the MC. Eastward propagation (EP) MJO events occur more frequently during La Niña years than during El Niño years.

- Analysis of SST across the Indonesian Seas, when the MJO suppressed phase prevails over the region that precedes the EP and NP MJO events over the MC, illustrates that the mean SST in Java, Banda, and Timor Seas for the EP events is warmer by 0.5^{o}C than the NP events. Warmer SST prior to the EP MJO events is commensurate with enhanced surface latent and sensible heat fluxes as well as low level moisture in the atmospheric boundary layer. More intense diurnal activity accounts for the warmer SST.

- The SST response in the Indonesian Seas to various MJO events with similar strength reveals interannual variability is stronger during La Niña than during El Niño. The response is influenced by the thermocline depth, where deeper

thermocline in the Indonesian Seas during La Niña limits the heat exchange between the warm surface layer and the cold that in turn a stronger coupling between SST and MJO air-sea heat fluxes.

- The direct impact of the MJO is not only evident on the surface but also in the interior of the Indonesian Seas. The MJO effects the ITF in Makassar Strait, especially in the upper 80 m, during the boreal winter months, by reducing the ITF transport into the Indian Ocean. This provides a new insight into our understanding of the ITF, in which the canonical view of the ITF variability has suggested that the ITF transport is reduced during boreal winter chiefly in response to the monsoon-driven buoyant water movement across the Indonesian Seas.
- A simple quantitate assessment of momentum balance in Makassar Strait illustrates that the MJO weakens or even reverses the southward along-strait pressure gradient as well as increase northward momentum transfer from wind stress, that result in substantially reduced southward ITF transport into the Indian Ocean.

A full understanding of the physical processes governing the MJO remains a challenge. Open questions such as fundamental factors dictating the MJO evolution and strength as well as the ocean's role to alter the MJO behavior are still not fully addressed. Most of coupled atmosphere-ocean general circulation models have shown unsatisfactory predictive skills in simulating the MJO processes. The common thread to the poor performance of the couple GCMs in predicting the MJO is the paucity of observations. Recently, an extensive observational campaign targeted physical processes in the atmospheric-oceanic boundary layers at the MJO initiation region in the Indian Ocean. This observational campaign provides new insights into our understanding of the MJO

processes, particularly the MJO initiation, in Indian Ocean. For example, the recently observed extensive data suggest that the ocean feedbacks to the atmosphere and plays a role to determine the MJO magnitude or strength, which contrast the traditional view of the MJO initiation that emphasizes on the role of internal atmospheric processes.

Despite new revelations of the MJO characteristics in the Indian Ocean, the MJO processes over the MC are still relatively unknown. The complex topography of the Indonesian archipelago, together with the complex bathymetry of the Indonesian Seas and Straits, constituting the MC causes a substantial number of unusual MJO behaviors when traversing the region. A commonly known MJO feature such as a smooth eastward propagation over the Indian Ocean does not always hold over the MC. Thus, some MJO theories applicable over the Indian Ocean may not be totally applicable over the MC. This study provides some preliminary understanding of the MJO processes over the Indonesian MC. Through this study, I can identify and describe essential features of the MJO across the MC, particularly its signatures in the Indonesian Seas, but more questions are still open for discussion. Some research questions that we need to tackle in future studies as follows:

- What are the processes prohibiting MJO to propagate over the MC?
- How big is the MJO-induced northward ITF transport during boreal winter?
- What is the role of the Indonesian Seas to amplify/weakens the MJO:
    - Can the ocean barrier layer reduce the effect of the active MJO to cool down the SST?

- How is the mechanism of diurnal variability in Java, Banda and Timor Seas to foster the MJO to propagate across the MC?
- How extensive can ocean mixing regulate the dynamics of coupled atmosphere-ocean process during MJO events?

To answer these questions, more in-situ observations are required. For example, high frequency SST data in the Indonesia Seas do not exist. The high frequency SST data are needed for discerning the role of diurnal SST variation in dictating the build-up of surface layer heat content over the suppressed phase period of the MJO, instrumental to govern the strength of the MJO. Long-term, high frequency surface heat fluxes data across the Indonesian Seas are also absent. In-situ surface heat flux measurements would not only complement but also improve the reliability of the reanalysis products, such as TropFlux. Mixed layer depth and barrier layer data, two very crucial oceanic components of the MJO studies, are also not available in the Indonesian Seas region due to the non-existence of long-term observations of temperature and salinity profiles. Future deployments of Argo profilers to measure temperature and salinity profiles in Banda Sea are being planned. Furthermore, subsurface turbulence data, crucial to understand how strong ocean mixing can influence the MJO processes in the Indonesian Seas, are not available. Temperature microstructure sensors have been operational in Makassar Strait as part of the ITF monitoring program since August 2015. This mixing measurement, once recovered later this year, will provide the first long-term mixing measurement in Makassar Strait, useful not only for ITF studies but also for MJO studies. I will compare my indirect estimate of turbulent momentum flux with the estimate from this mixing measurement for my future research.

In addition making more data available, using numerical modelling is also crucial to give a better illustration in completing this study, especially in answering questions raised in chapters 3 and 4. Simulations of coupled atmospheric-oceanic processes in the ITF pathways may give us more insights into the dynamics of MJO in relaxing the ITF. Detailed contribution of all terms of the equation of motion that explains the southward ITF deceleration would be better represented in numerical experiments. This would allow us to quantify the contribution of the MJO to weaken or reverse the southward ITF.

Numerical modelling may also be useful to simulate interannual variation of the SST response the MJO. We may be able to see better the changes of the thermocline depths in Banda Sea in response to ENSO and relate the changes to stronger or weaker SST responses to the MJO.

Bibliography

Ardizzone, J., R. Atlas, R. N. Hoffman, J. C. Jusem, S. M. Leidner, and D. F. Moroni, 2009: New multiplatform ocean surface wind product available. Eos, Transactions American Geophysical Union, 90 (27), 231–231.

Baranowski DB, Flatau MK, Flatau PJ, Matthews AJ, 2016: Impact of atmospheric convectively coupled equatorial Kelvin waves on upper ocean variability, Journal of Geophysical Research: Atmospheres, 121, 2045-2059.

Bond, Nicholas A., and Gabriel A. Vecchi. "The influence of the Madden–Julian oscillation on precipitation in Oregon and Washington." Weather and Forecasting 18.4, 2003: 600-613.

Chi, Nan-Hsun, Ren-Chieh Lien, Eric A. D'Asaro and Barry B. Ma, 2014: The surface mixed layer heat budget from mooring observations in the Central Indian Ocean during Madden-Julian oscillation events. J. Geophys. Res. Oceans, 119, 4638–4652.

DeMott, C. A., N. P. Klingaman, and S. J. Woolnough, 2015: Atmosphere-ocean coupled processes in the Madden-Julian Oscillation. Reviews of Geophysics, 53 (4), 1099–1154, doi:10.1002/2014RG000478,

De Boyer Montegut, C., G. Madec, A. S. Fischer, A. Lazar, and D. Iudicone, 2004: Mixed layer depth over the global ocean: An examination of profile data and a profile-based climatology. Journal of Geophysical Research: Oceans (1978–2012), 109 (C12).

De Szoeke, S. P., J. B. Edson, J. R. Marion, and C. W. Fairall, 2014: The MJO and air-sea interaction in TOGA COARE and DYNAMO. J. Climate, 0.1175/JCLI-D-14-

00477.1.

Drushka, K., J. Sprintall, S. T. Gille, and I. Brodjonegoro, 2010: Vertical structure of Kelvin waves in the Indonesian Throughflow exit passages. Journal of Physical Oceanography, 40 (9), 1965–1987.

Drushka, K., J. Sprintall, S. T. Gille, and S. Wijffels, 2012: In situ observations of Madden-Julian Oscillation mixed layer dynamics in the Indian andWestern Pacific Oceans. Journal of Climate, (7), 2306–2328.

Ducet, N., P.-Y. Le Traon, and G. Reverdin, 2000: Global high-resolution mapping of ocean circulation from Topex/Poseidon and ERS-1 and-2. Journal of Geophysical Research: Oceans (1978–2012), 105 (C8), 19 477–19 498.

Duvel, J. P., R. Roca, and J. Vialard, 2004: Ocean mixed layer temperature variations induced by intraseasonal convective perturbations over the Indian Ocean. Journal of the atmospheric sciences, 61 (9), 1004–1023.

Duvel, J. P., and J. Vialard, 2007: Indo-Pacific sea surface temperature perturbations associated with intraseasonal oscillations of tropical convection. Journal of Climate, 20 (13), 3056–3082. Gordon, A. L., 2005: Oceanography of the Indonesian Seas. Oceanography, 18 (4), 14.

Ffield, A., and A. L. Gordon, 1996: Tidal Mixing Signatures in the Indonesian Seas, Journal of Physical Oceanography, 26, 1924-1937.

Ffield, Amy, and Arnold L. Gordon. "Vertical mixing in the Indonesian thermocline." Journal of Physical Oceanography 22.2, 1992: 184-195.

Gordon, A. L., B. A. Huber, E. J. Metzger, R. D. Susanto, H. E. Hurlburt, and T. R. Adi, 2012: South-China sea throughflow impact on the Indonesian throughflow,

Geophysical Research Letters, 39 (11).

Gordon, A., J. Sprintall, H. Van Aken, D. Susanto, S. Wijffels, R. Molcard, A. Ffield, W. Pranowo, and S. Wirasantosa, 2010: The Indonesian throughflow during 2004–2006 as observed by the instant program, Dynamics of Atmospheres and Oceans, 50(2), 115-128

Gordon, A., R. Susanto, A. Ffield, B. Huber, W. Pranowo, and S. Wirasantosa, 2008: Makassar Strait throughflow, 2004 to 2006, Geophysical Research Letters, 35(24).

Gordon, A. L. , 2005: Oceanography of the Indonesian Seas, Oceanography, 18 (4), 14.

Gordon, A. L., R. D. Susanto, and K. Vranes, 2003: Cool Indonesian throughflow as a consequence of restricted surface layer flow, Nature, 425 (6960), 824–828.

Gordon, A. L., and R. D. Susanto, 2001: Banda Sea surface-layer divergence. Ocean Dynamics, 52 (1), 2–10.

Gordon, Arnold L., R. Dwi Susanto, and Amy Ffield., 1999: Throughflow within Makassar Strait, Geophysical Research Letters 26.21, 3325-3328.

Gottschalck, Jon, et al., 2013: Large-scale atmospheric and oceanic conditions during the 2011–12 DYNAMO field campaign, Monthly Weather Review 141.12, 4173-4196.

Grinsted, A., J. C. Moore, and S. Jevrejeva, 2004: Application of the cross wavelet transform and wavelet coherence to geophysical time series. Nonlinear processes in geophysics, 11 (5/6), 561–566.

Hagos, S. M., C. Zhang, Z. Geng, C.D. Burleyson, C. De Mott, B. Kerns, J. J. Benedict, and M. N. Martini, 2016: The impact of the diurnal cycle on the propagation of Madden-Julian Oscillation convection across the Maritime Continent, J. Adv. Model. Earth Syst., 8, 1552-1564.

Halkides, D., T. Lee, and S. Kida, 2011: Mechanisms controlling the seasonal mixed-layer temperature and salinity of the Indonesian Seas. Ocean Dynamics, 61 (4), 481–495.

Ham, S., S.-Y. Hong, and S. Park, 2014: A study on air-sea interaction on the simulated seasonal climate in an ocean-atmosphere coupled model, Clim. Dyn., 42, 1175–1187.

Hidayat, Rahmat, and Shoichi Kizu. "Influence of the Madden–Julian Oscillation on Indonesian rainfall variability in austral summer." International Journal of Climatology 30.12, 2010: 1816-1825.

Inness, P. M. and J. M. Slingo, 2006: The interaction of the Madden-Julian Oscillation with the Maritime Continent in a GCM, Q. J. R. Meteorol. Soc., 132, 1645-1667.

Jayakumar, A., et al. "Processes controlling the surface temperature signature of the Madden–Julian Oscillation in the thermocline ridge of the Indian Ocean." Climate dynamics 37.11-12, 2011: 2217-2234.

Joseph, S., A. J. Wallcraft, T. G. Jensen, M. Ravichandran, S. S. C. Shenoi, and S. Nayak, 2012: Weakening of spring Wyrtki jets in the Indian Ocean during 2006–2011, J. Geophys. Res., 117, C04012, doi:10.1029/2011JC007581.

Kessler, W. S., 2001: EOF representations of the Madden-Julian Oscillation and its connection with ENSO. Journal of Climate, 14 (13), 3055–3061.

Kiladis, G. N., M. C. Wheeler, P. T. Haertel, K. H. Straub, and P. E. Roundy, 2009: Convectively coupled equatorial waves. Rev. Geophys., 47, RG2003,

Kida, S., and K. J. Richards, 2009: Seasonal sea surface temperature variability in the Indonesian Seas. Journal of Geophysical Research: Oceans, 114,

doi:10.1029/2008JC005150.

Koch-Larrouy, Ariane, et al. "Water mass transformation along the Indonesian throughflow in an OGCM." Ocean Dynamics 58.3-4, 2008: 289-309.

Kumar, P. B., J. Vialard, M. Lengaigne, V. Murty, and M. McPhaden, 2012: Tropflux: air-sea fluxes for the global tropical ocean - description and evaluation, Climate Dynamics, 38 (7-8), 1521–1543.

Lee, S.-K., W. Park, M. O. Baringer, A. L. Gordon, B. Huber, and Y. Liu, 2015: Pacific origin of the abrupt increase in Indian ocean heat content during the warming hiatus, Nature Geoscience, 8 (6), 445–449.

Liebmann, B., 1996: Description of a complete (interpolated) outgoing longwave radiation dataset. Bull. Amer. Meteor. Soc., 77, 1275–1277.

Madden, R. A., and P. R. Julian, 1994: Observations of the 40-50-day tropical oscillation-a review. Monthly Weather Review, 122 (5), 814–837.

Maloney, E. D., and D. L. Hartman, 1998: Frictional moisture convergence in a composite life cycle of the Madden-Julian Oscillation, J. Clim., 11, 2387 – 2403.

Masumoto, Y., T. Kagimoto, M. Yoshida, M. Fukuda, N. Hirose, and T. Yamagata, 2001: Intraseasonal eddies in the Sulawesi Sea simulated in an ocean general circulation model. Geophysical research letters, 28 (8), 1631–1634.

Matthews, A. J., D. B. Baranowski, K. J. Heywood, P. J. Flatau, and S. Schmidtko, 2014: The surface diurnal warm layer in the Indian Ocean during DYNAMO. J. Climate, 27, 9101–9122.

McBride, J. L., M. R. Haylock, and N. Nicholls, 2003: Relationships between the Maritime Continent heat source and the El Nin˜o-Southern Oscillation phenomenon.

Journal of climate, 16 (17), 2905–2914.

Meehl, G. A., 1987: The annual cycle and interannual variability in the tropical Pacific and Indian ocean regions. Monthly Weather Review, 115 (1), 27–50.

Moum, J. N., K. Pujiana, Ren-Chieh Lien, and W. D. Smyth, 2016: Ocean feedback to pulses of the Madden–Julian oscillation in the equatorial Indian ocean. Nat. Commun. 7, 13203.

Moum, J. N., and Coauthors, 2014: Air–sea interactions from westerly wind bursts during the November 2011 MJO in the Indian Ocean. Bull. Amer. Meteor. Soc.,95, 1185–1199

Murtugudde, Ragu, Antonio J. Busalacchi, and James Beauchamp., 1998: Seasonal to interannual effects of the Indonesian throughflow on the tropical Indo Pacific Basin." Journal of Geophysical Research: Oceans 103.C10, 21425-21441.

Napitu, A. M., A. L. Gordon, and K. Pujiana, 2015: Intraseasonal sea surface temperature variability across the Indonesian Seas, Journal of Climate, 28 (22), 8710–8727.

Peatman, S.C., A. J. Matthews, and D. P. Stevens, 2014: Propagation of the Madden-Julian Oscillation through the Maritime Continent and scale interaction with the diurnal cycle of precipitation, Q. J. R. Meteorol. Soc., 140, 814-825.

Praveen Kumar, B., J. Vialard, M. Lengaigne, V. Murty, and M. McPhaden, 2012: Tropflux: air sea fluxes for the global tropical ocean - description and evaluation. Climate dynamics, 38 (7-8), 1521–1543.

Pujiana, K., A. L. Gordon, J. Sprintall, and R. D. Susanto, 2009: Intraseasonal variability in the Makassar Strait thermocline. Journal of Marine Research, 67 (6), 757–777.

Pujiana, K., A. L. Gordon, E. J. Metzger, and A. L. Ffield, 2012: The Makassar Strait

pycnocline variability at 20–40 days. Dynamics of Atmospheres and Oceans, 53, 17–35.

Pujiana, K., A. L. Gordon, and J. Sprintall, 2013: Intraseasonal Kelvin wave in Makassar Strait. Journal of Geophysical Research: Oceans, 118 (4), 2023–2034.

Pujiana, K., J. N. Moum, W. D. Smyth, and S. J. Warner, 2015: Distinguishing ichthyogenic turbulence from geophysical turbulence. J. Geophys. Res. Oceans, 120, 3792–3804, doi: 10.1002/2014JC010659.

Pujiana, K., J. N. Moum, and W. D. Smyth, The role of subsurface turbulence in redistributing upper ocean heat, freshwater and momentum in response to the Madden-Julian Oscillation in the equatorial Indian Ocean, Journal of Physical Oceanography (submitted).

Qiu, B., M. Mao, and Y. Kashino, 1999: Intraseasonal variability in the Indo-Pacific throughflow and the regions surrounding the Indonesian Seas. Journal of physical oceanography, 29 (7), 1599–1618.

Qu, T., Y. Du, J. Strachan, G. Meyers, and J. Slingo, 2005: Sea surface temperature and its variability. Oceanography, 18 (4), 50.

Rothstein, L. M., D. W. Moore, and J. P. McCreary, 1985: Interior reflections of a periodically forced equatorial Kelvin wave, Journal of physical oceanography, 15 (7), 985–996.

Salby, M. L., and H. H. Hendon, 1994: Intraseasonal behavior of clouds, temperature, and motion in the tropics. Journal of the Atmospheric Sciences, 51 (15), 2207–2224.

Schiller, Andreas, et al., 2010: Pathways of intraseasonal variability in the Indonesian Throughflow region, Dynamics of atmospheres and oceans 50.2, 174-200.

Seo, H., A. C. Subramanian, A. J. Miller, and N. R. Cavanaugh, 2014: Coupled impacts of the diurnal cycle of sea surface temperature on the Madden-Julian oscillation, J. Clim., 27, 8422–8443.

Shinoda, T., W. Han, T. G. Jensen, L. Zamudio, E. J. Metzger, and R.-C. Lien, 2016: Impact of the Madden–Julian oscillation on the Indonesian throughflow in the Makassar Strait during the CINDY/DYNAMO field campaign, Journal of Climate, 29 (17), 6085–6108, doi:10.1175/JCLI-D-15-0711.1.

Shinoda, T., H. H. Hendon, and J. Glick, 1998a: Intraseasonal variability of surface fluxes and sea surface temperature in the tropical Western Pacific and Indian Oceans. Journal of climate, 11 (7), 1685–1702.

Shinoda, T., H. H. Hendon, and J. Glick, 1998b: Intraseasonal variability of surface fluxes and sea surface temperature in the tropical Western Pacific and Indian Oceans. Journal of climate, 11 (7), 1685–1702.

Sobel, A. H., and E. D. Maloney, 2012: An idealized semi-empirical framework for modeling the Madden–Julian oscillation. J. Atmos. Sci., 69, 1691–1705.

Sobel, A. H., and E. D. Maloney, 2013: Moisture modes and the eastward propagation of the MJO. J. Atmos. Sci., 70, 187–192.

Sprintall, J., and A. Révelard, 2014: The Indonesian throughflow response to Indo-Pacific climate variability, Journal of Geophysical Research: Oceans, 119 (2), 1161–1175.

Sprintall, J., A. L. Gordon, A. Koch-Larrouy, T. Lee, J. T. Potemra, K. Pujiana, and S. E. Wijffels, 2014: The indonesian seas and their role in the coupled ocean-climate system. Nature Geoscience.

Sprintall, J., A. L. Gordon, R. Murtugudde, and R. D. Susanto, 2000: A semiannual

Indian Ocean forced Kelvin wave observed in the Indonesian seas in May 1997, Journal of Geophysical Research: Oceans, 105 (C7), 17,217–17,230.

Susanto, R. D., A. Ffield, A. L. Gordon, and T. R. Adi, 2012: Variability of Indonesian throughflow within Makassar Strait, 2004–2009, Journal of Geophysical Research: Oceans, 117 (C9).

Tanaka, M., 1994: The onset and retreat dates of the austral summer monsoon over Indonesia, Australia and New Guinea. Journal of the Meteorological Society of Japan, 72 (2), 255–267.

Tillinger, D., and A. L. Gordon., 2010, Transport weighted temperature and internal energy transport of the Indonesian throughflow, Dynamics of Atmospheres and Oceans 50.2, 224-232.

Torrence, C., and G. P. Compo, 1998: A practical guide to wavelet analysis. Bulletin of the American Meteorological society, 79 (1), 61–78.

Vialard, J., K. Drushka, H. Bellenger, M. Lengaigne, S. Pous, and J.-P. Duvel, 2013: Understanding Madden-Julian-induced sea surface temperature variations in the North Western Australian basin. Climate dynamics, 41 (11-12), 3203–3218.

Vialard, J., G. Foltz, M. McPhaden, J.-P. Duvel, and C. de Boyer Monte´gut, 2008: Strong Indian Ocean sea surface temperature signals associated with the Madden-Julian Oscillation in late 2007 and early 2008. Geophysical Research Letters, 35 (19).

Waliser, D. E., C. Jones, J.-K. E. Schemm, and N. E. Graham, 1999: A statistical extended-range tropical forecast model based on the slow evolution of the Madden-Julian oscillation. Journal of climate, 12 (7), 1918–1939.

Wang, W., and M. J. McPhaden, 1999: The surface-layer heat balance in the equatorial

Pacific Ocean. Part 1: Mean seasonal cycle. Journal of physical oceanography, 29 (8), 1812–1831.

Wentz, F. J., C. Gentemann, D. Smith, and D. Chelton, 2000: Satellite measurements of sea surface temperature through clouds. Science, 288 (5467), 847–850.

Wheeler, M. C., and J. L. McBride, 2005: Australian-Indonesian monsoon intraseasonal variability in the atmosphere ocean climate system, pp. 125–173, Springer, Praxis.

Wheeler, M. C., and H. H. Hendon, 2004: An all-season real-time multivariate MJO index: Development of an index for monitoring and prediction. Monthly Weather Review, 132 (8), 1917-1932.

Wijffels, S., and G. Meyers, 2004: An intersection of oceanic waveguides: Variability in the Indonesian Throughflow region. Journal of Physical Oceanography, 34 (5), 1232–1253.

Wilson, E. A., A. L. Gordon, and D. Kim, 2013: Observations of the Madden Julian oscillation during Indian Ocean dipole events, J. Geophys. Res. Atmos., 118, 2588–2599.

Yoneyama, K., C. Zhang, and C. N. Long, 2013: Tracking pulses of the Madden-Julian Oscillation. Bulletin of the American Meteorological Society, 94 (12), 1871–1891.

Zhang, C., (2013), Madden-Julian Oscillation Bridging Weather and Climate, Bulletin of The American Meteorological Society, 94 (12), 1849–1870.

Zhang, C., 2005: Madden-Julian Oscillation. Reviews of Geophysics, 43 (2).

Zhang, C., and M. Dong, 2004: Seasonality in the Madden-Julian Oscillation. Journal of climate, 17 (16), 3169–3180.

Zhou, L., and R. Murtugudde, 2010: Influences of Madden–Julian oscillations on the

eastern Indian Ocean and the maritime continent, Dynamics of Atmospheres and Oceans, 50 (2), 257–274